

2023

The effects of fragmentation on temperate forests in the northeastern United States: measuring the extent and impacts on forest growth and structure

<https://hdl.handle.net/2144/49218>

Downloaded from DSpace Repository, DSpace Institution's institutional repository

BOSTON UNIVERSITY
GRADUATE SCHOOL OF ARTS AND SCIENCES

Dissertation

**THE EFFECTS OF FRAGMENTATION ON TEMPERATE FORESTS IN THE
NORTHEASTERN UNITED STATES: MEASURING THE EXTENT AND
IMPACTS ON FOREST GROWTH AND STRUCTURE**

by

LUCA LLOYD MORREALE

B.S., Cornell University, 2013

Submitted in partial fulfillment of the
requirements for the degree of
Doctor of Philosophy

2023

© 2023 by
LUCA LLOYD MORREALE
All rights reserved, except for chapter 2
which is © 2021 by Springer Nature.

Approved by

First Reader

Lucy R. Hutyra, Ph.D.
Professor of Earth & Environment

Second Reader

Jonathan Thompson, Ph.D.
Senior Ecologist
Harvard University, Harvard Forest

Third Reader

Mark Friedl, Ph.D.
Professor of Earth & Environment

Fourth Reader

Kevin Lane, Ph.D.
Assistant Professor of Environmental Health

DEDICATION

I dedicate this work to my parents, Rebecca and Steve, who imbued me with a deep appreciation for science and inspire me daily with their tireless work ethic, appetite for learning and, most of all, their dedication to kindness; to my brother and best friend, Jonah, who lightened my heaviest moments in graduate school with his love, quick wit and willingness to engage in pedantic debates when I most needed a distraction; and my partner, Sarah, who was with me every step of the way and who taught me that the best part of science and life is having someone to share it with.

ACKNOWLEDGMENTS

I must first acknowledge my primary advisor, Lucy Hutyra, whose invaluable support, guidance and mentorship has shaped my research and helped me grow immensely as a scientist. I would like to thank my secondary advisor Jonathan Thompson for introducing me to the fields of landscape and forest ecology and for his mentorship and unwavering support during my time at Harvard Forest and then throughout my PhD. I thank my committee members, Mark Friedl and Kevin Lane, for their positive encouragement and critical scientific insights. Science is truly a collaborative effort, and I thank the many additional colleagues I have had during my PhD: my co-authors Xiaojing Tang, Andrew Reinmann, and Valerie Pasquarella for their invaluable contributions and feedback to my dissertation research, as well as Danelle Laflower, Karen Harper, Alexey Kalinin, and Jonathan Holt for their research assistance and guidance; members of the Hutyra and Thompson Labs for their constant positive feedback, friendship and comradery, including Hristiana Stoyanova, Taylor Jones, Ian Smith, Leeza Moldavchuk, Joy Winbourne, Conor Gately, Laura Schifman, Josh Plisinsiki, Meghan Blumstein, Matthew Duvenceck, Meg MacLean, Joe Tumber-Dávila, Lucy Lee, Kirsten Johnson, Lauren Cabrera, and Wiley Hundertmark.

I would like to thank the Frederick S. Pardee Center, the Rafiki B. Hariri Institute and the BU URBAN program for financial support, community, and invaluable opportunities to gain experiences outside of my core dissertation research. Additional thanks to the Town of Arlington, MA and Ken Pruitt for inviting me to conduct my

URBAN internship there and providing mentorship throughout. My work was additionally supported and funded by the United States Department of Agriculture National Institute of Food and Agriculture (USDA NIFA), the National Science Foundation through the Harvard Forest Long Term Ecological Research site, the BU Biogeosciences program, and the U.S. Carbon Leadership Program. I owe much to the departmental administrators of Earth & Environment and URBAN, especially Alissa Beideck Landry, Frederick George III, Evan Kuras, Matthew Dicintio and Lauren Consalvo, for their tireless support and aid with many issues over the years. I must thank my fellow scientists and graduate students who I was so lucky to share my PhD experiences with: Alia Al-Haj, John Foster, Tess McCabe, Ana Reboredo Segovia, Kathryn Wheeler, Emily Schottenfels, Andrew Christ, Nick Ray, James Garner, Valentina Pivotti, Sam Levy, and many others. A special thanks to my original officemates Julia Marrs and Andrew Trlica who helped guide me through the early years and supported me long beyond. I could not have done this without the support and love of my family and friends both within and beyond graduate school. Lastly I thank Sarah Garvey, with whom I've shared every moment of PhD life since the very first day. Through all the highs and the lows of the PhD, I remained grateful to graduate school for introducing me to my partner in science and in life.

**THE EFFECTS OF FRAGMENTATION ON TEMPERATE FORESTS IN THE
NORTHEASTERN UNITED STATES: MEASURING THE EXTENT AND
IMPACTS ON FOREST GROWTH AND STRUCTURE**

LUCA LLOYD MORREALE

Boston University Graduate School of Arts and Sciences, 2023

Major Professor: Lucy R. Hutyra, Professor of Earth & Environment

ABSTRACT

Forest fragmentation is a pervasive consequence of human land use that creates novel forest boundaries in place of contiguous, intact forest. Boundary forests, or edges, experience environmental conditions distinct from the forest interior driven by lateral exposure to adjacent non-forest land cover. Forest edges tend to be hotter, drier and experience increased wind turbulence and atmospheric deposition with significant consequences for ecosystem processes and biogeochemical cycling. Much of what we know about forest edge structure and function derives from tropical forest research, despite prolific fragmentation in temperate forests. Building on recent field studies of temperate forest edges in the northeastern United States (US), I combine measurements from the US national forest inventory (NFI) with remotely-sensed maps of forest area to characterize broad patterns in the extent and impacts of fragmentation on temperate forest ecology. Using the US NFI to identify forest edges across a 20-state region, I report increased biomass and growth of edge forests compared their interior counterparts. I then compare the prevalence of forest edges in the US NFI and commonly-used forest maps to

very-high-resolution land-cover maps, and I demonstrate that conventional methods of forest characterization systematically undercount and exclude forest edge area. Finally, I synthesize these findings to quantify aboveground carbon (C) cycling in New England using a novel approach that partitions forest C fluxes into forest edge and interior categories. I find that forest edges are disproportionately vulnerable to land-use conversion and are a critical component of both forest C uptake and emissions. Accounting for elevated growth rates in forest edges increases estimates of the net forest C sink in New England by 8.6% (4.36 Tg C). My dissertation research demonstrates the need to better understand the extent and effects of fragmentation in temperate forests, provides support for the treatment of forest edges as a distinct system, and highlights the need to include forest edges in current and future C accounting.

TABLE OF CONTENTS

| | |
|---|------|
| DEDICATION | iv |
| ACKNOWLEDGMENTS | v |
| ABSTRACT | vii |
| TABLE OF CONTENTS..... | ix |
| LIST OF TABLES | xiii |
| LIST OF FIGURES | xiv |
| LIST OF ABBREVIATIONS..... | xvii |
| CHAPTER ONE: INTRODUCTION..... | 1 |
| CHAPTER TWO: ELEVATED GROWTH AND BIOMASS ALONG TEMPERATE FOREST EDGES..... | 8 |
| Abstract | 8 |
| Introduction..... | 9 |
| Results and Discussion | 10 |
| Distinct characteristics of forest edges | 10 |
| Estimating the regional impact of enhanced growth..... | 14 |
| The global extent of forest fragmentation..... | 16 |
| Methods..... | 18 |
| Overview..... | 18 |
| Study area..... | 19 |
| Identifying edges in forest inventory data | 19 |

| | |
|--|----|
| Isolating the effect of edges on growth..... | 23 |
| Abiotic controls..... | 23 |
| Forest composition..... | 23 |
| Matching, GLM regressions, and model selection | 24 |
| Mortality and timber harvest..... | 26 |
| Scaling edge effects on forest growth across the Northeast | 27 |
| Quantifying fragmentation..... | 27 |
| Ecoregion edge impacts | 28 |
| Quantifying global forest fragmentation..... | 29 |
| Acknowledgements..... | 30 |
| CHAPTER THREE: EDGE CASES — FRAGMENTATION IN TEMPERATE | |
| FOREST LANDSCAPES..... | 36 |
| Abstract..... | 36 |
| Introduction..... | 36 |
| Processes at the edge..... | 38 |
| Linking pattern and process | 40 |
| Underestimations in forest area and forest edge..... | 42 |
| Edges as a distinct class | 45 |
| Making edges count | 46 |
| Panel: The consequences of underrepresenting forest area and edges for carbon accounting..... | 48 |

| | |
|--|----|
| Acknowledgements..... | 49 |
| CHAPTER FOUR: THE ROLE OF FOREST EDGES IN TEMPERATE FOREST | |
| CARBON CYCLING..... | 54 |
| Abstract..... | 54 |
| Introduction..... | 55 |
| Material and methods..... | 58 |
| Study area..... | 58 |
| Mapping forest area and forest change | 59 |
| Creating forest edge and interior classes | 61 |
| County-level forest growth rates..... | 62 |
| Forest C accounting | 64 |
| Results..... | 65 |
| Change in forest area and pattern..... | 65 |
| Forest carbon fluxes..... | 67 |
| Discussion..... | 68 |
| A changing forest landscape | 68 |
| C fluxes in New England forests | 70 |
| Conclusions..... | 72 |
| Acknowledgements..... | 73 |
| CHAPTER FIVE: CONCLUSIONS | 81 |
| APPENDIX A: SUPPLEMENTARY FIGURES..... | 85 |

| | |
|---------------------------------------|-----|
| APPENDIX B: SUPPLEMENTARY TABLES..... | 96 |
| BIBLIOGRAPHY..... | 104 |
| CURRICULUM VITAE..... | 118 |

LIST OF TABLES

| | |
|---|-----|
| Supplementary Table 2.1. Definition of forest type groups with sample size used in final analyses. | 96 |
| Supplementary Table 2.2. Model forms and fits from GLMs with BA and BAI as response variables. | 97 |
| Supplementary Table 2.3. Predicted mean marginal effects for each forest type and edge group. | 99 |
| Supplementary Table 2.4. Pre- and post-matching covariate distributions for all edges. | 101 |
| Supplementary Table 2.5. Pre- and post-matching covariate distributions for anthropogenic edges..... | 102 |
| Supplementary Table 3.1. Condensing individual land cover map legends to a simplified 3-class (Forest, Developed, Agriculture) legend for forest area intercomparison.. | 103 |

LIST OF FIGURES

| | |
|--|----|
| Figure 2.1. Forest edges have elevated growth and basal area. | 32 |
| Figure 2.2. Temperate forest edges have higher mean stem density than the forest interior but exhibit no difference in mean tree diameter. | 33 |
| Figure 2.3. Edges increase productivity in temperate forests. | 34 |
| Figure 2.4. Temperate forests are nearly 1.5 times more fragmented than tropical forests. | 35 |
| Figure 3.1. Example of resolution effects on estimates of forest area and forest edge area. | 50 |
| Figure 3.2. Underestimates of forest edge percent increases with decreasing forest cover. | 51 |
| Figure 3.3. Development leads to higher amounts of forest edge than agriculture. | 52 |
| Figure 3.4. Undercounting forest edges significantly changes estimates of aboveground forest carbon..... | 53 |
| Figure 4.1. Maps of study area — the New England region of the northeastern United States. | 74 |
| Figure 4.2. Examples of forest disturbance and loss. | 75 |
| Figure 4.3. Total annual change in forest area by state and year of change. | 76 |
| Figure 4.4. Percent (%) of annual forest loss and forest area in forest edge category..... | 77 |
| Figure 4.5. C fluxes across our study region from 2010 to 2020..... | 78 |
| Figure 4.6. Net C flux by county from 2010 to 2020. | 79 |

| | |
|---|----|
| Figure 4.7. Difference in estimates of net C flux for each county when accounting for forest edges.. | 80 |
| Supplementary Figure 2.1. Study region and approximate locations of edge and interior FIA plots. | 85 |
| Supplementary Figure 2.2. Sensitivity of basal area estimates to subplot area. | 86 |
| Supplementary Figure 2.3. Mortality differences between edge, interior, and anthropogenic edges. | 87 |
| Supplementary Figure 2.4. Gridded abiotic predictors of forest productivity. | 88 |
| Supplementary Figure 2.5. Increases in total ecoregion BAI ($\text{m}^2 \text{yr}^{-1}$) associated with elevated growth at the forest edge. | 89 |
| Supplementary Figure 2.6. Edge and interior forest cover designated from the 2016 National Land Cover Database | 90 |
| Supplementary Figure 2.7. Results from the robustness test of % forest cover threshold for estimates of temperate and tropical fragmentation using a 30% forest cover minimum definition of forest. | 91 |
| Supplementary Figure 2.8. Percent edge forest of 247 ecoregions located in the Northeast US derived from Hansen Global Forest Change (v1.7) 16 dataset versus from NLCD land cover map 13. | 92 |
| Supplementary Figure 3.1. Study area (in red) spanning the Chesapeake Bay Watershed and the Commonwealth of Massachusetts in the northeastern United States. | 93 |

| | |
|--|----|
| Supplementary Figure 3.2. The increase per county in total aboveground carbon across the Chesapeake Watershed portion of our analysis. | 94 |
| Supplementary Figure 3.3. Accuracy assessment of Mass Audubon’s Losing Ground 6 land cover product..... | 95 |

LIST OF ABBREVIATIONS

| | |
|-----------------|---|
| # | number |
| % | percent |
| ° | degree |
| ABG | aboveground biomass |
| AIC | Akaike information criterion |
| BA | basal area |
| BAI | basal area increment |
| BDFFP | Biological Dynamics of Forest Fragments Project |
| BU | Boston University |
| C | carbon |
| CI | confidence interval |
| cm | centimeters |
| CO ₂ | carbon dioxide |
| dbh | diameter at breast height |
| <i>e.g.</i> | <i>exempli gratia</i> ; for example |
| EPA | Environmental Protection Agency |
| FIA | US Forest Inventory and Analysis Program |
| GEE | Google Earth Engine |
| GHG | greenhouse gas |
| GLM | generalized linear model |

| | |
|-------------|--|
| GPP | gross primary productivity |
| ha | hectare |
| HF | Harvard Forest |
| <i>i.e.</i> | id est; that is |
| IGBP | International Geosphere Biosphere Programme |
| km | kilometer |
| LCMAP | Land Change Monitoring, Assessment, and Projection |
| ILTER | Long-Term Ecological Research program |
| LULCC | land use and land cover change |
| m | meter |
| Mg | megagrams |
| MODIS | Moderate Resolution Imaging Spectroradiometer |
| <i>n</i> | number |
| N | nitrogen |
| NADP | National Atmospheric Deposition Program |
| NFI | national forest inventory |
| NRT | National Research Traineeship |
| NLCD | National Land Cover Database |
| NPP | net primary productivity |
| NSF | National Science Foundation |
| Pg | petagrams |

| | |
|-------|---|
| R^2 | coefficient of determination |
| RMSE | root mean square error |
| T_0 | initial year, 2010 |
| T_L | year of loss |
| Tg | tera-grams |
| US | United States |
| USDA | United States Department of Agriculture |
| USFS | US Forest Service |
| VHR | very high resolution |
| yr | year |

CHAPTER ONE: INTRODUCTION

The modern era, referred to as the Anthropocene, is shaped by human alterations of the global climate system, biogeochemical cycles, and almost all terrestrial and aquatic ecosystems. In this era, forests constitute the dominant terrestrial ecosystem: they cover 31% of Earth's land surface and harbor the majority of terrestrial biodiversity, while simultaneously playing large roles in biogeochemical cycling (Pan et al., 2013; *The State of the World's Forests 2022*, 2022). Moreover, human society is inextricably intertwined with forests. Over 95% of the world's non-urban population (approximately 4.17 billion people) lives within 1 km of a forest, and a similar amount is estimated to rely on non-timber forest products for their livelihoods and/or personal use (*The State of the World's Forests 2022*, 2022).

Forests also serve a key role in offsetting anthropogenic emissions of carbon dioxide (CO₂), removing CO₂ from the atmosphere through photosynthesis (*i.e.*, gross primary production; GPP) and then storing that carbon (C) in their woody biomass. Through the storage of C in tree biomass (*i.e.*, net primary production; NPP), forests globally are estimated to uptake 4.21 ± 49 Pg C from the atmosphere each year (Harris et al., 2021). Forests also release C back into the atmosphere through natural processes and disturbances (*e.g.*, decomposition and wildfires), as well as human-induced mortality through deforestation. Even when accounting for emissions from both natural and anthropogenic sources, forests function as a net sink of 2.05 ± 49 Pg C, or roughly 1.5 times the amount of C emitted by the United States each year (Harris et al., 2021). While tropical forests contribute 55% of gross forest C uptake, due to substantial forest C

emissions this biome is only 30% of the net forest C sink. Instead, temperate forests are the largest contributor to the global net forest C sink, constituting 48% of net forest C uptake from the atmosphere. Given its importance in slowing the rate of climate change, there is ongoing pressure to constrain estimates of the forest C sink (Grassi et al., 2017). Despite concerted efforts to improve understanding of forest C cycling, large uncertainties remain in the estimates of forest C fluxes in general and in temperate forests in particular (Grassi et al., 2018; Harris et al., 2021).

Although our species relies on forests for their critical ecosystem services, human alterations to the biosphere (hereafter, global change drivers) pose the biggest threat to forest ecosystems' overall health and continued function as a C sink (Prävälíe, 2018; Trumbore et al., 2015). The central questions underpinning modern forest science revolve around understanding how global change drivers such as rising temperatures, shifts in precipitation, increased atmospheric CO₂ concentrations, and land-use change, will affect current and future forests (Prävälíe, 2018). While some aspects of global change like CO₂ fertilization and rising temperatures in cooler regions are expected to increase forest ecosystem GPP, the majority are expected to inhibit tree growth, increase tree mortality and decrease forest NPP (McDowell et al., 2020).

Land-use change, *i.e.*, alteration of the natural landscape through human activities, is recognized as the largest perturbation of forest ecosystems through the Anthropocene to this point (Foley et al., 2005). Human use of forest lands ranges both in spatial scale and severity of the impacts, from local subsistence agroforestry to region-wide deforestation. The effects of land-use on forest ecological processes extend beyond

direct perturbations from anthropogenic disturbance. Patterns of forest area and land-use additionally mediate forest structure, composition, and function (Turner, 1989a).

Deforestation, resulting in a conversion from a forested ecosystem to a non-forest land cover, is frequently the focus of research on the effects of land-use on forest dynamics. Notably, in forest C accounting across large regions, C fluxes associated with land-use change are often synonymous with emissions resulting from forest clearing. However, the persistent conversion of forest land to other land cover modifies landscape pattern and has further consequences for the forests that remain. Forest loss usually results in the division of the remaining ecosystems into smaller areas of contiguous forest, or fragments, set within a matrix of other human land cover. Fragmentation results in rapid proliferation of forest edges, forest area that is exposed and affected by non-forest land cover (Fischer et al., 2021). Moreover, fragmentation is ubiquitous throughout forest ecosystems as over 70% of the world's forests is within 1 km of a forest edge (Haddad et al., 2015). Studies of land use and forest function often overlook the resulting changes in forest pattern, as landscapes previously characterized by wide stretches of intact forest are transformed into many smaller forest fragments with large amounts of edge area.

Forest edges are physically distinct from interior, intact forests primarily due to their lateral exposure to adjacent, non-forest land cover resulting in biophysical gradients from the forest edge to the interior (Matlack, 1993). Increased solar radiation at the forest edge is associated with elevated air temperatures and increased aridity in addition to greater light availability (Schmidt et al., 2017). The non-forest-forest boundary also creates an abrupt vertical transition that disturbs the wind profile and results in increased

atmospheric deposition of airborne nutrients and pollutants in edge forests (Remy et al., 2016; Weathers et al., 2001; Wuyts et al., 2008). Abrupt disturbance in the wind profile, combined with increased wind speeds over the less-resistant non-forest area, can increase turbulence and exert strong lateral-shear on trees at the forest edge (Laurance & Curran, 2008).

Forest edges are further altered by ongoing human activities on the adjacent non-forest land use. When forest abuts agricultural or residential lands, it can experience increased loading of nitrogen and phosphorus through lateral exposure to fertilizer applications (Decina et al., 2017; Pocewicz et al., 2007b). Nearby human use of pesticides, road-deicers, and even pet waste can also drive the addition of cations, heavy metals, and other pollutants that are absent from the forest interior (Allen et al., 2020; Bryson & Barker, 2002; Zehetner et al., 2009). Impervious surface run-off and irrigation may lead to large pulses of hydrological inputs increasing variability in soil moisture compared to the interior forest. Heat island effects from developed land uses and pavement may further exacerbate increased temperatures in edge forests.

The existence of edge-to-interior gradients of microclimate, nutrient inputs, and pollutant concentrations has been well documented (Laurance & Yensen, 1991; Matlack, 1993; Meeussen et al., 2021; Schmidt et al., 2017; Smith et al., 2018). The myriad consequences of forest edge exposure represent significant perturbations to fundamental environmental constraints on forest ecosystems. However, understanding the overall effects of these concurrent changes on forest structure and function poses challenges (Franklin et al., 2021; Harper et al., 2005). Lack of a universal definition of forest edge

and consistent delineation of the depth of forest edge influence has hindered efforts to identify consistent edge to interior trends in forest processes (Cadenasso et al., 2003; Harper & Macdonald, 2011; Schmidt et al., 2017).

Heretofore, the prevailing narrative of the consequences of forest fragmentation has been dominated by research in tropical forests, specifically in the Brazilian Amazon (Laurance et al., 2007). The establishment of the Biological Dynamics of Forest Fragments Project (BDFFP) in central Amazonia, an experimental design of a replicated series of forest fragments, produced an initial baseline for understanding the structure and function of forest edges (Bierregaard, et al., 1992). Early results from this long-term ecological experiment reported that forest edges, especially new ones, experienced significantly higher tree mortality and damage than the forest interior, attributable to wind-throw and shifts in microclimate (Laurance et al., 1998). In later studies, researchers conclude that edge tree mortality decreased over time from high initial rates following edge creation, though edge mortality still remained elevated relative to the forest interior (Laurance et al., 2011a). They further reported that surviving trees exhibit suppressed growth rates, and they observed compositional shifts, described as degradation, from more structurally complex forests to fast-growing lianas and pioneer species. These findings were concurrent with growing emphasis on quantifying tropical deforestation and fragmentation, ultimately giving rise to the view of forest fragments and edges as degraded remnants.

However, results from observational field campaigns in temperate forests complicate this narrative. Contrary to the tropics, studies in the northeastern US and

southwestern Europe found that temperate forest edges may grow faster than the forest interior (Briber et al., 2015; Reinmann & Hutyra, 2017; Remy et al., 2016). These findings, though limited in geographic extent, report increased tree basal area (BA), faster growth, and higher overall aboveground C storage at the forest edge relative to the interior. Temperate forests are also highly fragmented, though not as a result of widespread, ongoing deforestation (Haddad et al., 2015). Rather, much of the temperate forest biome experienced landscape-wide deforestation centuries ago and has since regrown due to large shifts in land use (*i.e.* agricultural abandonment) (Foster, 1992; Mather, 1992). Modern temperate forests exist within a matrix of anthropogenic land covers, persisting as forest edges and fragments among roads, agriculture, and human settlements.

In this dissertation, I build upon previous site-based studies of temperate forest edges to characterize the extent and effects of temperate forest fragmentation in the northeastern US and beyond. My second chapter leverages the US national forest inventory (NFI) to investigate differences between forest edge and interior growth and biomass across the northeastern US. I also refine previous estimates of the extent of global fragmentation in both temperate and tropical forests. In the third chapter of my dissertation, I review the current understanding of fragmentation effects on ecological processes in temperate forests and quantify the ability of modern forest measurement techniques, *i.e.*, forest inventories and land-cover maps, to characterize fragmentation. I then recommend improvements to these techniques to better represent fragmented forests. In my final research chapter, I create a 10-year aboveground C budget for six states in the

northeastern US that partitions C fluxes into interior and edge forest categories to quantify the role of forest edges in the temperate forest C sink. I also assess changes in forest edge area across our study period. My research aims to elucidate the consequences of fragmentation for temperate forest structure and function and to bring greater attention to the fragmented reality of the modern temperate forest landscape.

CHAPTER TWO: ELEVATED GROWTH AND BIOMASS ALONG TEMPERATE FOREST EDGES

Morreale, L.L., J.R. Thompson, X. Tang, A.B. Reinmann, L.R. Huttyra, 2021.

Elevated growth and biomass along temperate forest edges. *Nature*

Communications 12, 1781. <https://doi.org/10.1038/s41467-021-27373-7>.

Abstract

Fragmentation transforms the environment along forest edges. The prevailing narrative, driven by research in tropical systems, suggests that edge environments increase tree mortality and structural degradation resulting in net decreases in ecosystem productivity. We show that, in contrast to tropical systems, temperate forest edges exhibit increased forest growth and biomass with no change in total mortality relative to the forest interior. We analyze > 48,000 forest inventory plots across the north-eastern US using a quasi-experimental matching design. At forest edges adjacent to anthropogenic land covers, we report increases of 36.3% and 24.1% in forest growth and biomass, respectively. Inclusion of edge impacts increases estimates of forest productivity by up to 23% in agriculture-dominated areas, 15% in the metropolitan coast, and +2% in the least-fragmented regions. We also quantify forest fragmentation globally, at 30-m resolution, showing that temperate forests contain 52% more edge forest area than tropical forests. Our analyses upend the conventional wisdom of forest edges as less productive than intact forest and call for a reassessment of the conservation value of forest fragments.

Introduction

Deforestation is a pervasive consequence of land-use change (Foley et al., 2005) and is impactful not just due to what is lost, but also due to its effects on the forest fragments that remain. Forest fragmentation is globally ubiquitous, with over 70% of forests located less than one kilometer from a non-forest edge (Haddad et al., 2015). Fundamental constraints on forest growth (Nemani et al., 2003; Wang & Houlton, 2009) and carbon cycling are altered near edges relative to interior forests (Harper et al., 2005; Smith et al., 2018), with increases in light availability, temperature, wind, and reactive nitrogen deposition, as well as altered water availability (Matlack, 1993; Wuyts et al., 2008). While fragmentation occurs across biomes, reported effects of these perturbations on higher-order dynamics in fragmented forests (i.e., structure, composition, function, and mortality) have largely focused on tropical ecosystems, where sharp increases in mortality and long-term forest degradation are reported at the forest edge (Chaplin-Kramer et al., 2015; Dantas de Paula et al., 2015; Laurance et al., 2011a; Ordway & Asner, 2020; Pütz et al., 2014). Expanded analyses suggest significant reductions in tropical ecosystem net carbon sequestration and, more broadly, the terrestrial carbon sink (Brinck et al., 2017; Chaplin-Kramer et al., 2015; Ordway & Asner, 2020). However, environmental controls on temperate forests differ from the tropics, and temperate forest fragmentation studies are both fewer and more limited in scale (c.f. Reinmann & Hutrya, 2017; Remy et al., 2017). Temperate forest edges have similar microclimatic differences, but contrasting biomass and productivity responses, emphasizing a need for a better

understanding of edge ecosystems in non-tropical biomes (Reinmann et al., 2020; Reinmann & Hutyra, 2017; Remy et al., 2016; Smith et al., 2018).

Here we offer a large-scale estimation of fragmentation impacts on temperate forest growth and structure along forest edges, with broader implications for global evaluation of fragmented forests. Hereafter, we use the term edge to refer to forest area bounded, in part, by a non-forest land cover and, conversely, interior as a designation of forest area bounded fully by forest. We report differences in tree basal area (BA; a metric of forest structure, strongly correlated with biomass), basal area increment (BAI; a measure of forest growth), tree mortality, and average stem density and diameter, between the forest edge (edge plots; <15 m from a non-forest land cover) and forest interior (interior plots; nonadjacent to non-forest land cover). We show that the temperate forest edges within our study area exhibit dramatically increased growth, tree stem density, and total basal area, with negligible changes in mortality. We then scale these results to estimate regional increases in forest growth attributable to the distinct forest edge environment. Finally, we place our results in context of global patterns of forest fragmentation.

Results and Discussion

Distinct characteristics of forest edges

To examine forest edges in the Northeastern US, we used inventory data from the US Department of Agriculture Forest Inventory and Analysis (FIA) program. The FIA program has established permanent, fixed-area (675 m²), forest plots in a hexagonal grid across the US (Bechtold & Patterson, 2005). This national forest inventory includes

measurements of tree size, growth, and land use; re-measuring every 5-7 years in our study area. Using >48,000 FIA plots distributed throughout 20 northeastern US states (Supplementary Figure 2.1), we compared structural and growth dynamics along temperate forest edges to those of interior forests. Individual tree measurements are collected within four fixed-radius subplots (168.7 m² area) with a fixed orientation; subplot characteristics are recorded even if the subplot contains partially forested or non-forest area. We leverage partially forested subplots to identify forest edges within the FIA database.

Using a quasi-experimental statistical matching framework followed by a generalized linear model (GLM) regression analysis, we compared BA, BAI, and tree mortality on FIA subplots that are adjacent to a non-forest land cover, to matched subplots within the forest interior. Matching approximates an experimental design where control plots (interior) were selected based on similarity to the treatment plots (edge) in relation to confounding predictors (light, water, temperature, nitrogen deposition, and forest type; Supplementary Figure 2.5) (Stuart, 2010). We report the results from GLM regression models as percent differences with significance derived from Wald tests on regression coefficients and we include Nagelkerke Pseudo-R² from the most parsimonious models as a goodness-of-fit metric (Nagelkerke, 1991). Detailed descriptions of plot filtering, statistical matching, GLM selection and analysis are provided in the Methods section.

Edges come in many forms. Natural edges exist as both transitions in growing conditions (*e.g.*, forest-grassland ecotones, wetlands) and sharp boundaries (*e.g.*, lakes,

rivers, geologic features) with variable effects on forest growth. In contrast, anthropogenic edges often exist as abrupt transitions in areas that were once fully forested (*e.g.*, agricultural fields, roads, and developments). Average BAI along anthropogenically formed edges is 36.3% greater ($p < 0.001$; $R^2 = 0.149$) than interior forest, while BAI along all edges (encompassing anthropogenic, natural and unspecified edges) is 24.1% greater ($p < 0.001$; $R^2 = 0.153$) than interior forest (Figure 2.1). BA exhibits smaller differences, but the same trend: anthropogenic edges have 21.0% greater ($p < 0.001$; $R^2 = 0.059$) BA and along all edges BA is 13.9% greater ($p < 0.001$; $R^2 = 0.069$) than the forest interior. Notably, our analyses exclude trees smaller than 12.7 cm in diameter. Given that densities of small diameter woody vegetation are typically higher along forest edges (Smith et al., 2018), it follows that the differences in BA and BAI between edge and interior forests observed here represent a conservative estimate.

There are just three pathways to increased basal area in edge forests: more trees, larger trees, or some combination thereof. We find no significant difference in the average tree diameter between the forest edge and interior, even when comparing with only anthropogenic edges. In contrast, by averaging individual tree measurements within each subplot, we find a mean increase of 58 trees per hectare ($p < .001$) across all edges as compared with the forest interior (Figure 2.2). Along anthropogenic edges, the difference increases to 82.6 additional trees per hectare ($p < .001$), which is consistent with the observed patterns of BA in all versus anthropogenic edges.

Along tropical edges, the primary driver of decreased productivity is heightened tree mortality, frequently attributed to increased impacts of wind, lianas, and more

frequent droughts (Laurance et al., 2011b). In contrast, we find no significant differences in biogenic mortality between edge and interior forests (Supplementary Figure 2.3b).

Within our study area, the largest cause of mortality in forests is anthropogenic removals (Thompson, Canham, et al., 2017). While we do find a statistically significant ($p < .001$) increase in anthropogenic removals in both edge groups compared to the interior (Supplementary Figure 2.3c), there is no difference in overall total mortality (Supplementary Figure 2.3a). Given the prevalence of forest management in this region, we performed a robustness test of our main result to quantify any potential impacts of harvesting. We withheld all plots that had a record of tree removal ($n = 3642$) within the FIA inventory and found no changes in the overall pattern between edge and interior in either BA or BAI.

Tree species composition mediates forest response to anthropogenic environmental perturbations (Anderson-Teixeira et al., 2013). Individual species responses to altered energy and biogeochemical inputs at the edge can vary due to climatic tolerance and successional characteristics (Laurance et al., 2006). Therefore, we quantified differences in structure and growth responses to edges by species composition groups (sensu Thompson, Canham, et al., 2017) (Figure 2.1). In most compositional groups, BAI increases significantly at all forest edges, but with varying magnitudes: Northern Pines - Hemlock forests exhibit the smallest increase in BAI, 16.9% ($p < 0.001$); Oak - Pine forests have the largest, 32.5% ($p < 0.001$). The effect size increases across almost all compositional groups when comparing BAI specifically along anthropogenic edges with forest interiors. Of the eight forest type groups, only the

Southern Conifers group has no statistically significant difference in BAI. The increase in BAI ranges from 25.5% ($p < 0.001$) in Northern Pines - Hemlock, to 67.7% in Spruce - Fir. The Oak – Hickory group exhibits 41.1% ($p < 0.001$) higher tree growth at anthropogenic edges than the forest interior, an effect $> 28\%$ larger than when all edges are pooled. Interior-to-edge enhancements of BA are smaller than BAI, but five compositional groups have significantly greater BA along edges: Oak – Hickory (16.5%; $p < 0.001$), Northern Hardwood (16.1%; $p < 0.001$), Northern Pines – Hemlock (15.1%; $p < 0.001$), Oak – Pine (18.5%; $p < 0.001$) and Bottomland Forests (12.5%; $p < 0.001$). When comparing anthropogenic edges with the interior, the effect is again stronger, and five compositional groups exhibit significant increases in edge BA. Of these groups, Aspen - Birch have the largest increase in BA (31.7%; $p < 0.001$); Northern Hardwoods have the smallest (19.5%; $p < 0.001$).

Estimating the regional impact of enhanced growth

To scale the edge impacts on growth across our study area, we coupled the results from the GLM regression analysis with a land-cover map (Jin et al., 2019) and a forest-type map (Ruefenacht et al., 2008). We aggregate our results to ecoregions, geographic areas that are ecologically and climatically similar, to account for mismatches in spatial resolution between our gridded inputs (Omernik & Griffith, 2014)³¹. For these analyses, we focused on the effects of anthropogenic edges. The increases in growth and biomass we observe at temperate forest edges are greatest adjacent to anthropogenic edges and are evidence of a largely unrecognized impact of the ongoing process of forest fragmentation. Large variability was observed in fragmentation patterns across our study

region. The proportion of forest area within 30 m of an edge varies across ecoregions from < 5 to 68% of all forest area, with an area-weighted average of 18.5% (Figure 2.3a). We quantified the expected difference between interior and edge forest based on ecoregion-specific forest composition (Figure 2.3b) and abiotic predictors, then combined the proportion of forest within 30 m of an edge with ecoregion BAI differences to quantify the effect of edges on overall forest productivity. We estimated the total increase in annual BAI within each ecoregion associated with increased growth at anthropogenic forest edges (Supplementary Figure 2.5). Estimates determined that elevated BAI found at anthropogenic forest edges represents a >6% increase in total forest growth across the entire region (Figure 2.3c). The BAI response varied across our study domain; increases in forest growth range from 23% increase in agricultural-dominated areas (region shown in Supplementary Figure 2.6b), a 2% increase in the least-fragmented northern regions (region shown in Supplementary Figure 2.6c), and a 15% increase within the metropolitan east coast (region shown in Supplementary Figure 2.6d).

Our findings contrast with the conventional narrative based on tropical forest studies, that forest edges decrease net forest productivity and, consequently, lower forest aboveground carbon storage. Temperate and tropical forests have distinct ecologies and climate; it follows that similar perturbations can have markedly different effects. The absence of any increase in tree mortality, as repeatedly observed in tropical forest edges, suggests that temperate forest edges are less wind-threatened and less sensitive to the elevated temperatures and water stress that occur along all forest edges. Rather, increases in radiation may release the most-limiting biogeochemical constraints on temperate

forests (temperature and light) (Nemani et al., 2003; Reinmann et al., 2020; Smith et al., 2018). The growth response is almost certainly related to greater light availability, which affects tree canopy architecture and can increase forest leaf area index and, in turn, stimulate productivity (Mourelle et al., 2001; Reinmann et al., 2020).

The global extent of forest fragmentation

Comparison of our results and those of previous tropical studies is complicated by differences in land-use history, specifically the time since edge creation. Forests in our study region and, more broadly, the temperate forest biome have undergone centuries of deforestation, forest transitions, and fragmentation. Some forest edges included in our study have existed for decades. However, research on newly created edges in this region has shown large growth increases in remaining trees, without associated increases in mortality, immediately following edge creation (Briber et al., 2015). Given that abrupt formation of edges can expose the previously intact forest to secondary disturbances, individual tree characteristics, including height, drought tolerance, and rooting depth, may determine whether the cascading perturbations induce mortality. Shorter, more wind-firm trees, prevalent in temperate forests, may not experience altered biogeochemical conditions only as negative perturbations and, instead, are more likely to be advantaged by increased resource availability. In contrast, the taller trees found in temperate forests of the Pacific Northwestern US, in which fragmentation patterns are characterized by deforestation and clear-cut timber harvests, might exhibit a similar initial mortality response to tropical forests (Chen et al., 1992). However, forestry research from the same US Pacific Northwest region also finds large increases in BAI in

surviving conifers adjacent to silvicultural treatments (Walter & Maguire, 2004), analogous to the edge enhancements in BAI that we report. Furthermore, a recent study on European temperate forests similarly found that temperate forest edges exhibit a 95% increase in aboveground carbon stock within 5 m of an edge (Meeussen et al., 2020). Together, these results suggest that the pattern of elevated growth along forest edges holds true across large portions of the temperate forest biome.

The implications of these findings on global estimates of tree growth and carbon storage are proportional to the amount of fragmentation within temperate and tropical forest biomes. We quantified forest fragmentation throughout both types of forests using a 30-meter resolution, global, forest-cover map (Hansen et al., 2013a)³¹ (Figure 2.4). Temperate forests have >50% more forest area within 30 m of a forest edge than tropical forests (217 million ha compared to 143 million ha, respectively) (Figure 2.4b). Europe has the highest percent of edge temperate forests (21.5%), while North America has the highest percent of edge tropical forests (29.1%) (Figure 2.4a). Fragmented forests are often perceived as degraded remnants. However, the prevalence of temperate forest edges and their distinctive ecosystem functions, demonstrated here, argue for a reassessment of forest edges and fragments. These are the forests that people interact with most, they are distinct from interior forests in ways that need to be better understood, and, in some functions, are of disproportional value. The large increases in growth near forest edges that we observe here have major implications for understanding how these ecosystems will respond to ongoing fragmentation and climate change.

Emphatically, this research does not argue for proactive forest fragmentation as a prescription to increase carbon sequestration. The increased carbon storage along the edges of fragmented remnants does not come close to offsetting the loss of terrestrial carbon stocks and future sequestration capacity associated with forest loss (Reinmann & Hutyra, 2017). Furthermore, there is evidence that the temperate edge responses are hindered by extreme heat, suggesting that rising global temperatures may exacerbate heat stress at temperate forest edges (Reinmann & Hutyra, 2017) and cause them to respond more similarly to tropical forest edges. Instead, this is a call to acknowledge the complexity of interactions between global change drivers across diverse ecosystems. Centuries of fragmentation have created a permanent shift in the microenvironment of a large and growing proportion of the global temperate forest area. With rising populations, expanding urban and agricultural areas, and ongoing deforestation, the critical need to understand fragmented forests as distinct ecosystems only grows. Any attempt to predict future forests must account for ongoing changes in the prevalence of forest edges and the potential contributions of fragments to terrestrial carbon storage.

Methods

Overview

We used data from the national forest inventory conducted by the US Department of Agriculture, Forest Service, Forest Inventory and Analysis (FIA) program to quantify tree biomass and growth along forest edges and within the forest interior. We estimated the causal impact of the forest edge environment on patterns of tree biomass and growth, while accounting for potentially confounding variables. We then used the regression

models to estimate the aggregate difference in growth attributable to forest edges throughout the northeastern US. Finally, to better understand the implications of our findings, we quantified the degree of forest fragmentation throughout temperate and tropical forest biomes world-wide, using a 30 m forest cover map.

Study area

Our analyses of edge impacts on forest biomass and growth were conducted throughout twenty-states (1.7 million km²) in the northeastern and upper mid-west of the US (Supplementary Figure 2.1). This region contains 765,000 km² of forest and encompasses gradients of dominant land-uses, climatic conditions, and forest composition while remaining within deciduous, coniferous, and mixed temperate forest ecosystems.

Identifying edges in forest inventory data

The FIA collects measurements of tree size, growth, and land-use within a nested plot design across the country (Bechtold & Patterson, 2005). Each FIA plot is composed of four individual subplots; within each subplot, the diameter at breast height (dbh) of every tree >12.7cm is measured during each measurement period. The re-measurement frequency for FIA plots in our study area is between 5 and 7 years, but this can differ between Forest Service regions. In addition to tree measurements, the database details land-use condition data that includes the proportion of the area that is forested and, on some plots, the land-cover class of the non-forest area (FIA User's Manual, Condition Table). FIA plots are considered forested if some portion of the plot includes a contiguous forest patch (including potentially outside of the plot area) of greater than

4047 m² that has more than 10% canopy cover. With a memorandum of understanding between the USFS and Harvard University, we had access to the true, unfuzzed plot coordinates, which are not publicly available. Evaluating >48,000 plots in the USFS Northern Region sampled from 2010 to 2020 and selecting the most recent measurement cycle for each plot, we identified subplots that contained both a forest & a non-forest condition and categorized these as edges (Supplementary Table 2.1). Only subplots that included a forest condition in both the most recent and previous measurement were included. Subplots where the mapped condition changed from forest to non-forest were excluded. Changes in the amount of mapped forest condition were included and are incorporated into the calculation of response variables using the most recent condition area. We identified FIA plots where all four subplots were fully forested as interior plots to be used for comparison. Subplots located within the same plot as an edge subplot (i.e. edge-proximate subplots) were excluded from this study due to limitations in our ability to quantify their distance from an edge. The spatial configuration of subplots is such that a fully forested subplot may be up to ~65 m away from an identified forest edge within another subplot. Studies suggest that the distance of edge influence in temperate forest does not extend more than 30 m into the forest interior (Meeussen et al., 2020; Reinmann & Hutyra, 2017). Since the FIA does not contain information about the geometry of non-forest conditions beyond the subplot boundary, we deemed that the large uncertainty in the relationship between these subplots to a non-forest edge precluded their inclusion in the study. The FIA plot configuration prevented quantification of the distance of edge

influence in our analysis; the exclusion of subplots adjacent to edge-subplots may limit direct comparisons with other fragmentation studies.

We used the FIA condition data to characterize the non-forest land use in edge subplots. Information on adjacent non-forest land cover is not collected on all FIA plots (4327 of 6607 edge subplots). We aggregated FIA land-cover classification to a binary anthropogenic or unknown edge type designation and present results from all edge subplots and the anthropogenic edge subset (FIA User's Manual Condition Table, Section 2.4.50).

For each subplot (168 m² in area), we calculated two primary response variables of interest: total live tree basal area (BA) and basal area increment (BAI). Notably, trees smaller than <12.7 cm diameter are only recorded within a small portion of the plot, called the microplot. Our study design prevented the inclusion of the microplot and therefore excludes trees beneath this diameter threshold. Trees that grew into the measurement size class between the previous and most recent measurement are included. The exclusion of small trees and saplings may result in a conservative estimate of the difference between edge and interior BA and BAI, as other studies have found a higher density of small-stemmed woody vegetation along forest edges (Ziter et al., 2014). BA is calculated from a single plot measurement, as the summed BA of all live adult trees (> 12.7 cm dbh) in m². BAI was calculated on a per-tree basis as the difference in radial growth of live adult trees between the most recent and previous measurements, and then divided by the number of years between measurements (m² yr⁻¹). Additionally, we

aggregated individual tree diameter measurements to calculate mean stem density (stems ha^{-1}) and mean tree diameter for each subplot (Fig 2).

We accounted for variable subplot area by normalizing both BA and BAI to a per-hectare of forested area basis, resulting in units of $\text{m}^2 \text{ha}^{-1}$ and $\text{m}^2 \text{ha}^{-1} \text{yr}^{-1}$, respectively. To account for potential small-area bias, we performed a sensitivity analysis on the relationship between basal area and subplot forested area (Supplementary Figure 2.2). We subsequently excluded 1284 subplots under 30 m^2 in area as the area to basal area relationship asymptotes relationship above this threshold. Finally, we accounted for errors in field dbh measurements, sometimes resulting in negative BAI values, by excluding the <2.5% and >97.5% quantiles of both BA and BAI distributions.

Given their spatial configuration, FIA subplots are not fully independent measurements, potentially introducing issues with pseudo-replication and spatial autocorrelation within our dataset. To test for spatial autocorrelation we examined the semivariance of model residuals (F. Dormann et al., 2007), and found that there was high correlation only at distances of less than 1 km. The spatial stratification of the FIA plot design minimizes issues of plot-plot proximity within our study. However, to account for autocorrelation between subplots, we filtered our pre-matched dataset to only including one subplot from each FIA plot. For plots containing multiple edge subplots, we selected the subplot with the largest forested area. For interior plots, we selected the central subplot and excluded all others.

Isolating the effect of edges on growth

Abiotic controls

To account for environmental controls on forest growth we included the most critical abiotic predictors of terrestrial vegetation productivity (light, water, temperature and nitrogen deposition) as covariates in the regression models (Supplementary Figure 2.4, Supplementary Table 2.2). Light, water, and temperature data were drawn from spatial raster maps (0.5° resolution) as unit-less indices of relative limitation on vegetation productivity, ranging from 0 to 1 (Nemani et al., 2003). Nitrogen data were drawn from the 2018 NADP gridded inorganic wet nitrogen deposition product (4 km spatial resolution; kg of N ha⁻¹) (Office, 2020). To interpolate across small gaps in the raster data (usually along water bodies), we used the Nibble tool from ArcGis Pro (ESRI Team). We then used FIA plot locations to extract values from each raster layer for all FIA subplots.

Forest composition

Tree species may vary in their responses to biogeochemical changes that occur on forest edges. Overall forest community response emerges from complex interactions between species. We used aggregations of tree species, termed forest composition groups (or forest types) (Eyre, 1980), to assess if species composition influenced the response to altered edge condition. Forest type classifications for each subplot are provided by the FIA (FIA User's Manual, Condition Table) and are defined in Appendix D therein. We aggregated the FIA forest types into eight broader species groups, following Thompson et al. (Thompson, Canham, et al., 2017), and defined in Supplementary Table 2.1.

Matching, GLM regressions, and model selection

All statistical analyses and most of the data processing were conducted in R, version 3.4 (R Team, 2019). Using a causal inference framework, we created a quasi-experimental statistical design that included pre-matching followed by a generalized linear model (GLM) regression analysis (Enderlein, 1987). Matching emulates an experimental design using observational data by identifying control groups of untreated (forest interior) plots that were as similar as possible to treated (forest edge) plots in terms of observable confounders. By capturing key differences in abiotic variables we control for the fundamental drivers of forest productivity, allowing for a direct estimation of the average treatment effect of edges. Similarity was defined by nearest-neighbor covariate matching determined by Mahalanobis distance, implemented in the MatchIt library in R (Ho et al., 2011), the simplest and best method when the dataset is robust enough to find a match for every treated plot (Stuart, 2010). This method excludes forest interior plots that are not matched with an edge plot. Given differences in sample size between the full edge dataset and the subset designated as anthropogenic edges, we performed matching separately on the two datasets. To assess the efficacy of matching on reducing the differences in covariate distributions, we used summary statistics calculated with the MatchIt library and report the pre- and post-matched covariate balance in Supplementary Table 2.4 and Supplementary Table 2.5 (*sensu* Schleicher et al., 2017). Matching was highly successful, largely eliminating differences in all covariate distributions in both datasets.

Our primary response variables of interest, BA and BAI, were right-skewed, non-normally distributed and violated the assumptions of normality necessary for ordinary least squares regression (Chambers et al., 1990). We therefore used a generalized linear model (GLM) to better fit the structure of our data. GLMs are an extension of linear regression that allow more freedom in the choice of probability distribution function through the use of a link function to model relationships between predictors and response variables (Guisan et al., 2016). The gamma probability distribution is frequently chosen to model BA, given its assumptions of positive, continuous values and flexible model form (Canham et al., 2013; Thompson, Canham, et al., 2017). We performed a series of GLM regressions on our post-matched datasets, using a gamma probability distribution with an inverse link function to model the relationship of BA and BAI with a suite of predictor variables, using the *glm* function as implemented in the R Core *stats* package (R Team, 2019). Due to differences in sample size between the all-edge dataset and the anthropogenic-edge subset, we modeled these two datasets separately for each of BA and BAI, resulting in four separate regression analyses. We used a model selection framework to identify the most parsimonious model within each of the model sets based on the Akaike Information Criterion (AIC) and residual deviance statistic (Akaike, 1998; Nelder & Wedderburn, 1972). We report the model-selection and model-fit results for each of our separate analyses, including model forms, AIC, Nagelkerke Pseudo- R^2 , and residual deviance in Supplementary Table 2.2. Across all four regression analyses, the best-performing model was one that included an interaction between the edge-status and

forest type categorical variables, as well as the variables of temperature-limitation, light-limitation, water-limitation, and nitrogen deposition.

We then used the best performing model from each analysis to compare the differences in BA and BAI between forest edge and interior across each forest type. We estimated the treatment effect of edge-state within each forest type using the *ggeffects* package (Lüdtke, 2018) to calculate marginal effects with the continuous predictors (temperature, light, water, and nitrogen deposition) held at their within-forest type regional means. The results of this analysis are displayed in Figure 2.1 and Supplementary Table 2.3; primary error bars on the interior point show the 95% confidence interval of the marginal effect from the full edge model, while secondary error bars show the CI from the anthropogenic edge model. Due to the smaller sample size in the anthropogenic model, estimates of the mean marginal effect of the interior plots vary slightly (though non-significantly) from those from the full dataset. The main text description reports outputs from both models, calculated from separate interior mean estimates. For visual clarity, we only display one set of interior means in Figure 2.1.

Mortality and timber harvest

In tropical forests, large reductions in productivity along edges are associated with increased tree mortality. (Laurance et al., 2011a) To assess differences in tree mortality across our study region, we applied a simplified GLM analysis, including edge-state as our only predictor variable. The FIA differentiates between mortality attributed to timber harvest and that attributed to other, non-harvest causes. The results of this analysis are presented as marginal effects of each edge category in Supplementary Figure 2.3. There

are no significant differences in biogenic mortality between edge groups and no difference in overall mortality (combined biogenic and anthropogenic); there is a small, but statistically significant ($p < .001$), increase in harvested BA within both all-edge and anthropogenic edges as compared with the forest interior. We note that the exclusion of small-diameter trees from our study could alter these results if there was differential mortality between edge and interior in smaller tree size classes.

Temperate forests are heavily impacted by forest management (M. L. Brown et al., 2018). We tested the robustness of the effect of edges on growth and biomass by withholding all subplots with a record of anthropogenic removals on the full FIA plot (*i.e.* management; $n = 3642$). We found no difference in the overall effect of edges nor meaningful differences within forest type groups.

Scaling edge effects on forest growth across the Northeast

Ecoregions are a widely-used geographic partitioning of ecosystems into coherent spatial units as defined by abiotic, biotic, and anthropogenic characteristics (Omernik & Griffith, 2014). EPA Level IV ecoregions are delineated by differences in environmental characteristics analogous to those that we used to model forest growth and thus are a comparable spatial unit to quantify the aggregated effects of fragmentation.

Quantifying fragmentation

To quantify anthropogenic forest edge area, we identify forest cover within 30 m of a road, development, or agricultural field (*sensu* Smith et al. (Smith et al., 2018)) using a 30 m resolution land-cover product from 2016 of the National Land Cover Database (NLCD) (Yang et al., 2018). Edge forest was defined as all forest pixels adjacent

(queen's rule) to a non-forest cultivated or developed pixel (Supplementary Figure 2.6a). Figure 2.3a shows the percentage of total forest area classified as edge within each ecoregion. We report that 18% of the total forest area in our study domain is adjacent to an anthropogenic edge. Differences from the reported 22% in Smith et al. are likely attributable to the use of a different NLCD product. Note that the definition of forest edge here may differ from that of the FIA analysis, given the constraints on quantification of the distance of edge influence and the spatial resolution of the land cover products.

Ecoregion edge impacts

To scale the effects as illustrated in Figure 2.3 we quantified ecoregion forest composition by: (1) Using a 250 m resolution USFS forest type map (Ruefenacht et al., 2008), we aggregated raw forest type values to the aggregated forest type groups included in our regression models (Figure 2.3b), (2) We calculated the total area of each forest type group within each ecoregion, then used the average temperature, light, water, and nitrogen deposition in each ecoregion as inputs to our GLM regression models to calculate the BAI of edge and interior forest for each forest type. With the proportional area of each forest type, we calculated an area-weighted mean and then differenced the estimated edge and interior BAI to produce an expected difference of forest growth (BAI $\text{m}^2 \text{ha}^{-1}$) between edge and interior within each ecoregion (Supplementary Figure 2.5). Finally, we combined the proportion of edge forest with the expected growth difference to quantify the estimated difference in percent increases in ecoregion BAI within each ecoregion attributable to increases of forest growth at the edge (Figure 2.3c).

Quantifying global forest fragmentation

We quantified the extent of forest fragmentation throughout temperate and tropical forests worldwide at the scale of ecoregions using the Hansen Global Forest Change (v1.7) (Hansen et al., 2013b) dataset on Google Earth Engine (GEE) (Gorelick et al., 2017). Tropical and temperate biomes were delineated in a global ecoregion map (Olson et al., 2001), analogous to the more detailed ecoregions described earlier. The tree canopy cover layer from the Hansen dataset provided estimates of percent tree canopy cover for the year 2000 at 30 m resolution globally produced by time series analysis of Landsat images (Hansen et al., 2013b). To calculate the percentage of edge forest in each ecoregion: (1) a 10% threshold (following the FIA definition of minimum forest cover (Bechtold & Patterson, 2005)) was applied to the tree canopy cover layer to separate forest and non-forest pixels, (2) each forest pixel adjacent (queen's rule) to a non-forest pixel was classified as edge forest on GEE, and (3) ArcGIS Zonal Statistics Tool was used to calculate the percentage of edge forest in each ecoregion. Definitions of forest cover via % canopy cover vary between studies, therefore we performed a robustness check on our results to the threshold definition of forest cover by re-analyzing with a 30% canopy threshold. While there were differences in the calculated raw area of forest edges, the ratio of area fragmented between temperate and tropical forests did not change meaningfully (Supplementary Figure 2.7). We then compared the Hansen-derived forest fragmentation to the 2016 NLCD-derived forest fragmentation used in our previous analysis to assess comparability of the two products. Supplementary Figure 2.8 shows the agreement between the percent edge forest values calculated based on the two forest

maps for the 247 ecoregions in the Northeast US. The agreement is strong especially in large and more forested ecoregions. The Hansen-derived percent edge forest explained 84.5% of the variance in NLCD-derived percent edge forest with RMSE of 6.1 (%) at ecoregion level. The spatial aggregation to ecoregion level largely reduced the uncertainty in the mapping of forest pixels in both products.

Acknowledgements

We thank the many colleagues who gave us friendly feedback throughout this research, in particular to C. Canham, S.C. Wofsy and D. Foster for their thoughtful suggestions, J. Holt and A. Kalinin for their statistical guidance. FIA plot location data was made available via Memorandum of Understanding 09MU11242305123 between the US Forest Service and Harvard University. Funding: This work was supported, in part, by the United States Department of Agriculture National Institute of Food and Agriculture Award 2017-67003-26487, the Harvard Forest LTER Program (NSF DEB 18-32210), the Rafiki B. Hariri Institute at Boston University and by a National Science Foundation Research Traineeship (NRT) grant to Boston University (DGE 1735087). The processed, post-matching FIA data generated in this study and used to generate Figures 2.1 and 2.2 have been deposited in the Harvard Forest Data Archive under accession code HF419. The spatially-aggregated estimates of BAI presented in Figure 2.3c and summaries of global forest edge area displayed in Figure 2.4a are available in the HF Data Archive under accession code HF419. The un-fuzzed FIA location data are protected and are not available due to data privacy laws. Unprocessed FIA inventory data is available at

<https://apps.fs.usda.gov/fia/datamart/>. The National Land Cover Database land cover layer is at <https://www.mrlc.gov/data>. The forest cover map we use for the global analysis is available on Google Earth Engine.

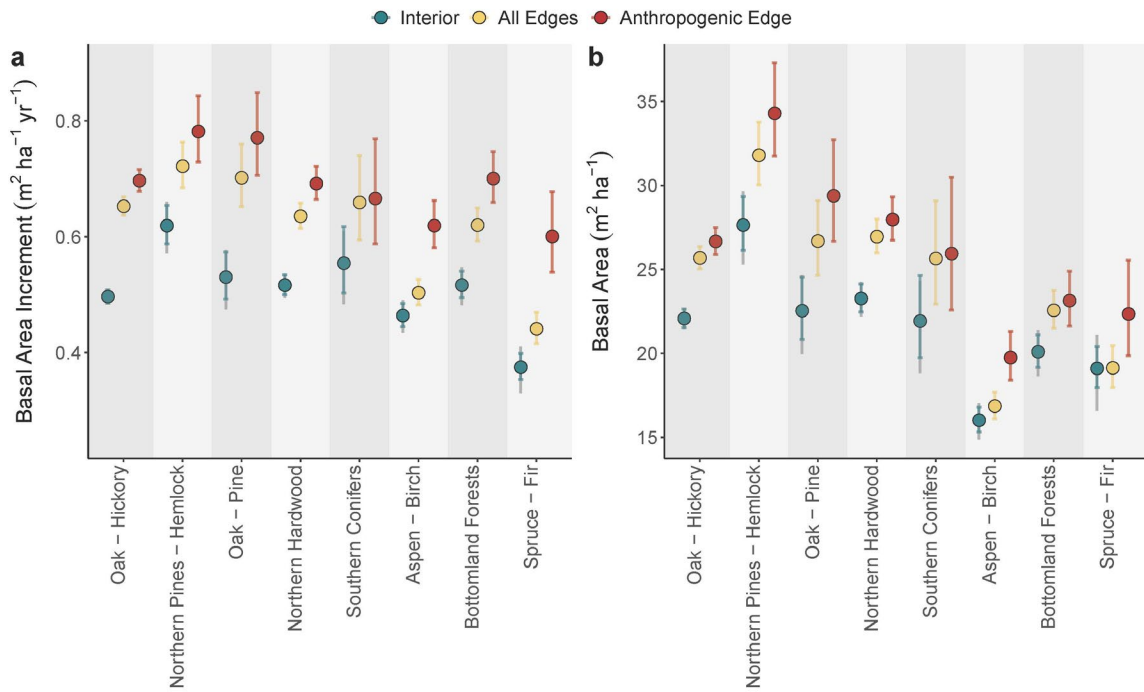


Figure 2.1. Forest edges have elevated growth and basal area.

BAI (a) and BA (b) show the average marginal effects of edge-class and forest-type from GLM outputs. Results are presented in Interior, All Edges, and Anthropogenic Edge groups and ordered by forest type abundance (Supplementary Figure 2.5). Interior and All Edge groups have $n = 6607$ independent subplots, Anthropogenic Edges have $n = 4327$ independent subplots. Data are presented as the mean marginal effects with inner error bars show 95% confidence intervals on the marginal effects; outer error bars on interior group are for comparison with anthropogenic edges.

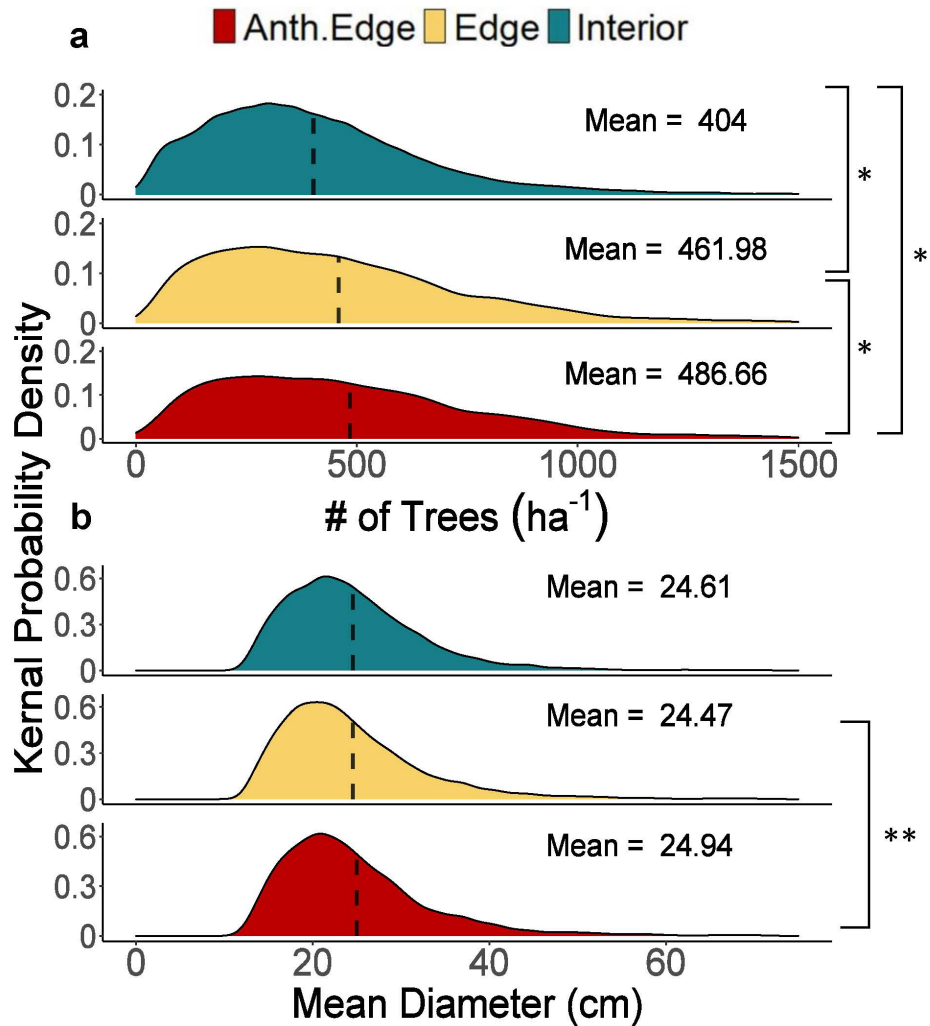


Figure 1.2. Temperate forest edges have higher mean stem density than the forest interior but exhibit no difference in mean tree diameter.

a) Distributions of mean subplot stem density (# of trees per hectare). b) Distributions of mean subplot tree diameter (diameter in centimeters). Dashed lines show mean values of all subplots within each edge class. Asterisks denote significance (*: $p < .00001$; **: $p = .0078$) as calculated with two-sided pairwise t-tests using a Bonferroni adjustment. Interior and All Edge groups have $n = 6607$ independent subplots, Anthropogenic Edges have $n = 4327$ independent subplots.

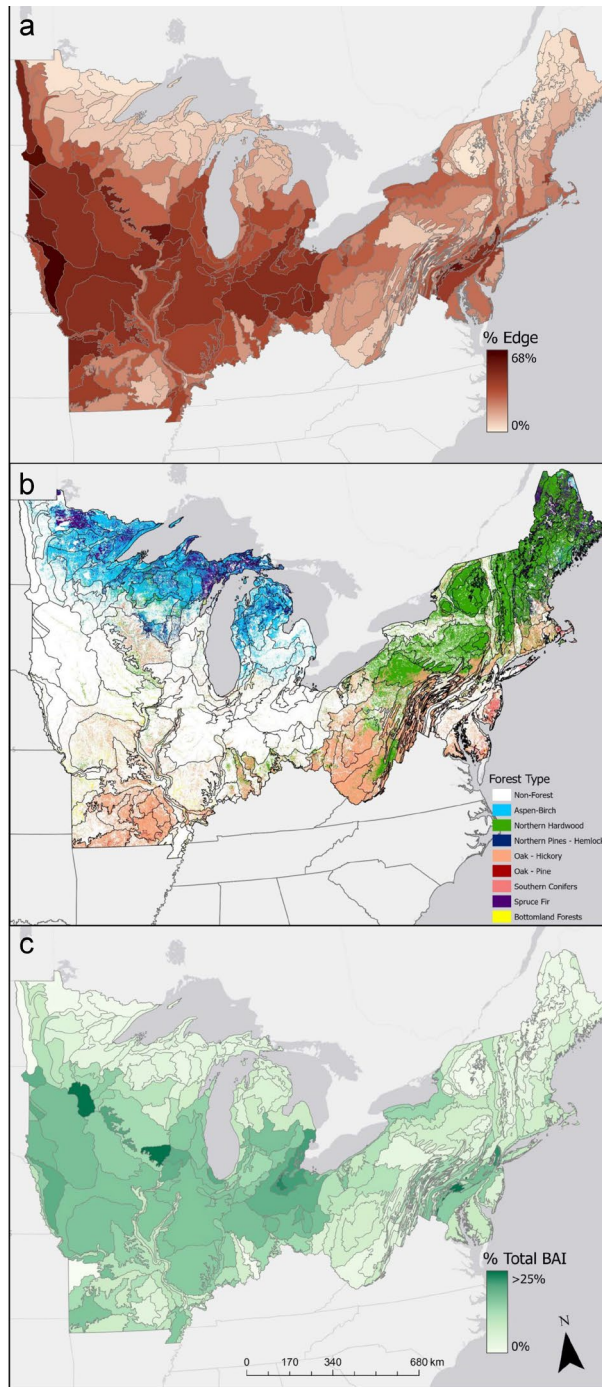


Figure 2.3. Edges increase productivity in temperate forests.

a) The percent of forest area within 30m of an anthropogenic edge within each ecoregion. b) Spatial distribution of aggregated forest types used in study. c) The percent increase in ecoregion total BAI attributable to elevated growth at anthropogenic edges.

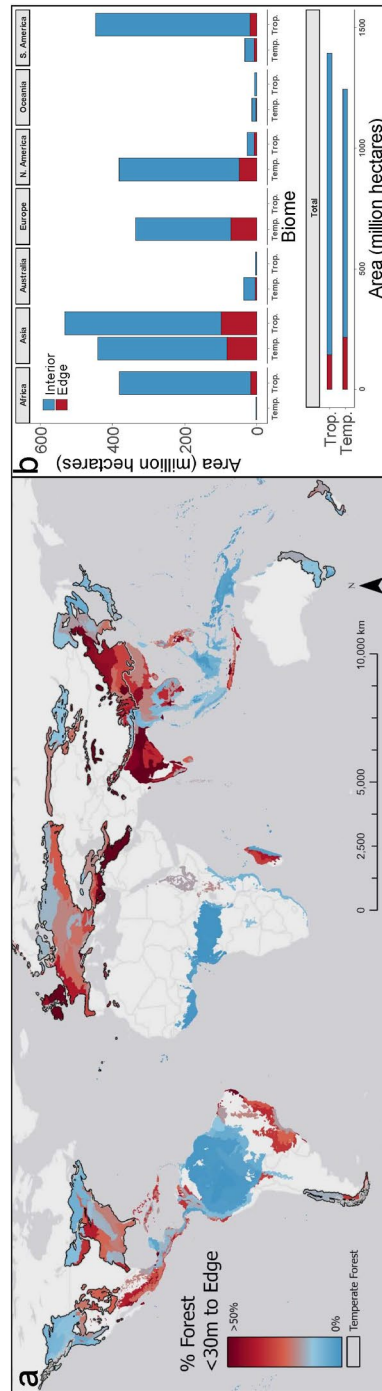


Figure 2.4. Temperate forests are nearly 1.5 times more fragmented than tropical forests.
 a) The percent of temperate and tropical forest area within 30 m of an anthropogenic edge within each global ecoregion. b) The area (in millions of hectares) of edge and interior forest, grouped by biome and continent.

CHAPTER THREE: EDGE CASES — FRAGMENTATION IN TEMPERATE FOREST LANDSCAPES

Morreale, L.L., J.R. Thompson, V.J. Pasquarella, L.R. Hutya, 2021.

Edge cases: Fragmentation in temperate forest landscapes. *Frontiers in Ecology & the Environment (In Review)*.

Abstract

Temperate forests are the most fragmented forest biome, yet current understanding of fragmentation effects on ecological processes, such as carbon cycling, is rooted in tropical forest research. We review the impacts of fragmentation on temperate forest ecology and quantify the extent to which the US national forest inventory and land-cover maps represent forest edge area. We report a systematic exclusion of forest edges across all methods. Compared with very high resolution (1 m) maps, conventional 30 m resolution forest cover maps underestimate forest edge area by 16.4%, on average. Accounting for all forest edge area and distinct edge ecology results in a 14.8% median increase in aboveground forest carbon estimates with 23.8% and 74.2% increases in agriculturally and urban dominated counties, respectively. We conclude by proposing improvements to forest inventories, maps, and models to better represent the fragmented temperate forest landscape.

Introduction

Global land-use change is driving deforestation and forest fragmentation, exacerbating biodiversity loss and climate change (Foley et al., 2005). It is well-established that landscape pattern influences ecological processes (Turner, 1989b), but

how patterns of forest fragmentation affect ecosystems remains understudied (Franklin et al., 2021).

While fragmentation affects all forest biomes, temperate forests are the most heavily fragmented, with approximately 17.5% (217 million hectares) of forested area located within 30 m of a non-forest edge (Morreale et al., 2021). Our limited understanding of fragmentation impacts on forest function is rooted in modern tropical deforestation (Laurance et al., 2011b), often evoking images of large swaths of intact forest being logged, burned, and converted to agriculture or development. In tropical forests such as the Brazilian Amazon, ongoing deforestation cleared over 11 million hectares of forest in 2021 (World Resources Institute, 2022). Temperate forests, however, have a long history of intense land use and a landscape ecology that is distinct from their tropical counterparts (Haddad et al., 2015). The modern mosaic of temperate fragmented forests has resulted from a mix of recent deforestation and legacy of Colonial-era agricultural clearing followed by partial reforestation, termed a forest transition (Mather, 1992). Given these differences in drivers, we should not assume that the patterns of fragmentation, and the consequences of it, are analogous across biomes.

Accounting for the impacts of fragmentation requires mechanistic understanding of fragmented forest ecosystems and accurate characterizations of the patterns themselves. Recent research has improved our ecological understanding of forest fragments (Franklin et al., 2021), but our ability to scale empirical measurements remains limited by our ability to quantify the affected area. Here, we review the state of knowledge on the impact of fragmentation on temperate forest structure, demography,

and carbon cycling. We then analyze how alternate delineations of fragmentation via forest maps and inventories influence our understanding of its scope and impacts. Finally, we offer a series of recommendations for better characterizing pattern and process in the modern temperate forest landscape.

Processes at the edge

Forests once covered vast geographic regions interrupted only by water bodies, environmental ecotones, geologic features, or natural disturbances. Through human land use, forests are cleared and converted to non-forest land. In addition to reducing the total forest area, once-contiguous forests are divided into smaller areas (hereafter fragments) by agriculture, roads and settlements. Landscape alteration into a configuration of many, smaller fragments results in a proliferation in the area of forest edges. Forest edges refer to the transitions or boundaries between forest and non-forest ecosystems. Here we focus on forest edge area—*i.e.*, the portion of forest directly altered by adjacent non-forest land cover, rather than on fragments as a whole.

Across biomes, anthropogenic edges are distinct from persistent natural forest boundaries as they do not arise from pre-existing environmental conditions (Franklin et al., 2021; Schmidt et al., 2017; Smith et al., 2018). Persistent anthropogenic edges tend to exist as hard boundaries, *i.e.*, abrupt ecological transitions to crops, pavement, or other abutting human land covers (Esseen et al., 2016). When compared with a closed-canopy forest interior, anthropogenic forest edges experience increases in light through lateral exposure to solar radiation. Consequently, edges are hotter and drier than the interior (Schmidt et al., 2017), while also experiencing greater wind exposure and altered

atmospheric deposition (Weathers et al., 2001). Management of the adjacent non-forest can further alter water and nutrient gradients—*e.g.*, fertilizer use can increase nitrogen and phosphorous inputs, and run-off from impervious surfaces and/or irrigation can increase hydrological inputs while also depositing salt and other chemicals into the forest (Pocewicz et al., 2007a).

While microclimatic and other physical gradients along abrupt forest edges have been well-documented and are generalizable across biomes, their resultant impact on ecological processes are more variable and less well-understood. In many tropical forests, forest edges exhibit elevated tree mortality and suppressed growth relative to the interior as a result of increased drought stress, elevated wind exposure, and liana invasions (Laurance et al., 2011b). Conversely, temperate forest edges are more productive than their interior counterparts (Meeussen et al., 2020; Morreale et al., 2021; Reinmann & Hutya, 2017). Increases in leaf area and stem density at the forest edge suggest increased light availability as the mechanism driving increases in biomass and productivity (Morreale et al., 2021; Reinmann et al., 2020). In other studies, elevated growth has been attributed to increased nitrogen deposition at the forest edge (Meeussen et al., 2020). With limited exception, these temperate studies have found no increase in tree mortality at the edges, even in montane regions that exhibit lower overall biomass at the forest edge (Morreale et al., 2021; Pöpperl & Seidl, 2021). The growing body of research suggests altered carbon cycling along temperate forest edges, especially when combined with recent findings on belowground carbon dynamics (Garvey et al., 2022; Meeussen et al., 2020; Reinmann et al., 2020). Observed differences in forest structure, biodiversity and

understory dynamics at the edge suggest that projected trajectories for forest composition may differ from traditional expectations of forest succession based on interior ecosystems (Bormann & Likens, 1979).

Linking pattern and process

Early attempts to establish a unified theoretical framework of ecological edges focused on defining the boundaries between ecosystems (Cadenasso et al., 2003). This framing, rooted in both landscape ecology and empirical observations, emphasized that ecological boundaries affect the adjacent systems (Laurance & Yensen, 1991; Weathers et al., 2001). Further research quantified the depth of edge influence on the abutting forest ecosystem (Harper et al., 2005). Due to high variability in edge influence and varying definitions of forest edges, conceptual frameworks have moved away from an emphasis on a single linear boundary and towards the idea of a transition zone between ecosystems (Erdős et al., 2011). (Schmidt et al., 2017)(2017) synthesized and adapted the transition zone concept into a framework for understanding biogeochemical cycling across fragmented ecosystems. They posit that a defining characteristic of forest edges is the existence of predictable gradients in microclimate and nutrient cycling. The flexibility of the transition zone framework allows for variable depths of edge influence, multiple definitions of both the adjacent forest and non-forest matrices and includes both vertical and temporal heterogeneity in biogeochemical cycling. While the conceptualization of edges as transition zones is useful to understand forest boundaries as a landscape feature, it fundamentally does not align with how we map the distribution of forest ecosystems or model forest processes at larger scales. For example, many countries rely on national

forest inventories (NFIs) to provide an empirical foundation for national and global forest assessments and greenhouse gas reporting (UNFCCC, 2014). Complementing ground-based inventories, remote sensing is used to create continuous maps of forests and land cover. The opening of the Landsat Archive, proliferation of forest-focused satellite and airborne measurements, and increases in computing power have resulted in the release of multiple land-use and forest-cover products over the last decade (Wulder et al., 2012). Ideally, approaches to combine empirical ground measurements with remotely sensed coverage of a region can improve carbon accounting, mapping of forest structure and function, and parameterization of earth system models. However, to succeed in representing ecosystem processes, the synthesis of these approaches must not neglect the role of the transitions and forest edge.

For forest inventories and maps to characterize fragmentation patterns, they need to accurately quantify total forest cover and capture forest pattern—i.e., the complexity of edge configuration. In the US and other countries, NFIs are structured to be statistically representative samples of the nations' forests. Despite this, the US NFI (the US Forest Service's Forest Inventory and Analysis Database, or FIA) excludes forest fragments beneath a minimum area threshold from its inventory and is only just beginning to account for forests in urban areas (Edgar et al., 2021). Further, it is well known that our ability to estimate forest area scales with spatial resolution (H et al., 1986) and that quantification of forest fragmentation is also affected by resolution (Turner et al., 1989). However, evaluations of forest maps typically focus on their ability to characterize total forest area but rarely interrogate their competency at capturing forest pattern. Both NFIs

and remote sensing-based forest maps *implicitly* represent forest edges, but these data products do not account for forest edges *explicitly* in their sampling designs nor development (Haddad et al., 2015; Morreale et al., 2021).

Underestimations in forest area and forest edge

To assess the consequences of omitting forest edges on the US NFI and widely used land-cover maps, we compared estimates of forest area and forest edge area, leveraging the increasing availability and computational feasibility of very high resolution (1 m pixel size; hereafter VHR) land-cover products to map forest edge area in selected regions. VHR maps have been shown to greatly increase our ability to characterize landscape heterogeneity (Wickham & Riitters, 2019). For our baseline estimation of forest area we used VHR maps of the 260,000 km² Chesapeake Bay Watershed and the 27,000 km² Commonwealth of Massachusetts (Supplementary Figure 3.1), which map tree canopy with up to 98% accuracy (Pallai & Wesson, 2017). This established baseline was then used to quantify bias in forest area and forest edges relative to the other maps.

We define forest edge area as forest within 30 m of a non-forest land cover, consistent with the preponderance of research indicating that the edge influence on forest structure extends up to 30 m (Garvey et al., 2022; Meeussen et al., 2021; Reinmann & Hutyra, 2017). We applied methods described in Morreale et al. 2021 to estimate forest edge prevalence within the US NFI and present our results for the NFI as the percent of stems categorized as forest edge. We used Google Earth Engine (Gorelick et al., 2017) to calculate forest cover and forest edge area across four satellite-based forest maps. In the

US, counties represent a coherent political boundary within which land-use zoning is typically consistent, and they therefore can function as independent samples for the purposes of this analysis. We aggregate forest cover data from the National Land Cover Database (NLCD), the Land Change Monitoring, Assessment, and Projection (LCMAP), and the MODIS Land Cover IGBP annual product to the county level (J. F. Brown et al., 2020b; Sulla-Menashe et al., 2019; Yang et al., 2018). The spatial resolution of these datasets are 30 m, 30 m, and 500 m, respectively, and we condense the legend of available forest classes for comparability (Supplementary Table 3.1). This is a representative sample of products with differing methods for identifying forests that are commonly used in forest area analyses and forest dynamics modeling efforts.

Underestimates of total forest area leads to inaccurate calculations of edge area. In counties with high forest cover (>75%), only the 500 m MODIS land cover dataset has significantly different estimates of percent forest coverage of the county land area ($p < 0.001$) when compared to the VHR products (Fig 2a). However, in areas with lower forest cover (<75%), LCMAP, NLCD, and MODIS all underestimate the percent forest cover relative to the VHR data products, on average, by 14.5%, 7.9%, and 26.0%, respectively ($p < 0.001$). When we compare estimates of the percent of forest area considered an edge, the result is even more pronounced (Fig 2b). Across all counties in the study areas, average forest edge area was 42.1% of total forest area based on the VHR baseline. The other forest monitoring datasets estimate average edge area across our study region as follows: 25.7% in LCMAP, 24.3% in NLCD, 6.8% in the NFI, and 7.2% in MODIS. When compared with the VHR maps, all products significantly underestimate

forest edge area ($p < 0.001$ from Tukey HSD test). Additionally, we find that in counties with less than 75% forest cover, coarser resolution land-cover maps dramatically underestimate forest area ($p < 0.001$). Areas with lower forest cover are frequently more fragmented, with more small fragments and larger proportions of edge forest. Neither the US NFI nor widely used forest maps accurately account for forest edges as visible in VHR imagery. The systematic undercounting of forest area in counties that are less forested and more fragmented further ensures that forest edges are omitted from our evaluation of forest patterns, implicitly and explicitly.

Forest edge area in each region is also controlled by the drivers and patterns of fragmentation, with alternate land use regimes resulting in different configurations of forest patches. In our study area, the dominant non-forest land use can broadly be subdivided into regions of agriculture and development (Smith et al., 2018). In southern New England and the mid-Atlantic metropolitan regions, the pattern of fragmentation is largely driven by residential development set within the dominant forest matrix (Fig 3b). The result is many small forest fragments divided by roads and buildings with high proportions of edge forest. In contrast, forests in agricultural areas are often more consolidated or in longer riparian forests or hedgerows within a matrix of farmland, resulting in a lower ratio of forest edge area to total forest cover (Fig 3a). We found that the relationship between forest edge percent and forest cover differs significantly between forests surrounded by agricultural and urban developed uses (Fig 3c; 3d). In counties dominated by development we find that, on average, 72.0% all forest was categorized as edge, while in agricultural counties the average fell to 37.0%. Two

counties with the same total forest area can have large differences in forest edge area depending on the dominant land-use regimes and consequent forest configuration. Approaches that depend solely on total forest area and do not address landscape heterogeneity will ultimately exclude this distinction and the consequences of fragmentation on ecological processes.

Edges as a distinct class

One reason edges are excluded from forest maps is that they pose a special challenge for categorical land-cover classification. These datasets are produced by relating satellite measurements of spectral reflectance with discrete land cover or land use labels (i.e., forest, development, water). Pixels that intersect a forest edge often include a mixture of both forest and the adjacent non-forest. These are referred to as “mixed pixels” and are not easily classified into a single category (Woodcock & Strahler, 1987). Classifier training data, derived from manually labeled high-resolution imagery, often focuses on examples that are most representative of the chosen classes (i.e., full forest pixels), while the designation of unlabeled mixed pixels in the mapped output is left to the algorithmic classifier. As a result, class labels associated with these pixels often have higher uncertainties and can result in frequent misclassification of forest edges as non-forest, especially when compared to the forest interior.

In an accuracy assessment of a land-cover map created for the Massachusetts Audubon’s 6th Losing Ground Report (Ricci et al., 2020) human interpreters were explicitly directed to identify pixels containing forest edges to assess how the classifier performed on literal edge cases. Analysis of interpreted results indicated that pixels

labeled as forest edge were only classified as forest 44.8 % of the time, compared with a 94.6 % rate for pixels labeled as the forest interior (Supplementary Figure 3.3). The high misclassification rate of mixed pixels contributes to systematic underestimates of forest edges, a bias that increases with pixel size as mixed pixels become more common. To address this problem, we advocate for an exploration of the spectral characteristics of mixed pixels with a goal of creating a new class for forest edges. The creation of a forest edge class in land-cover maps would allow for explicit mapping of edges, more accurate characterizations of fragmentation patterns, and increasing accuracy of maps as a whole.

Making edges count

Our analyses demonstrate a substantial and systematic underrepresentation of forest area and edge forest area in traditional land-cover maps and the US NFI. Consequently, we conclude that temperate forest edges are neither explicitly nor implicitly represented in key national forest assessments, forest carbon budgets, or land system models. While our analysis focuses on the temperate forests of the northeastern and mid-Atlantic US, the underlying causes are expected to apply throughout the temperate forest biome and beyond. Based on our observations, we suggest the following to better represent the fragmented ecological reality of modern temperate forests.

1. National forest inventories need to explicitly account for the prevalence of fragmentation.

The ongoing implementation of the Urban FIA as an expansion of the US NFI may serve as a template for how to augment plot sampling without affecting the existing design. Additionally, the inclusion of more information about abutting

non-forest land uses (as with the Urban FIA) would serve to improve our understanding of the edge forest ecosystem and better align with the forest transition zone framework (Edgar et al., 2021).

2. Increased use of very high resolution forest maps for detailed characterizations of forest patterns.

As we demonstrate, increasingly available VHR forest products reveal large portions of the forest landscape that are invisible with coarser methods. The need for VHR land-cover data is heightened by distinct patterns of forest fragmentation across land use contexts. The complexities of fragmentation patterns that result in significant changes in edge forest area are frequently invisible to the traditional methods of forest area assessment.

3. Forest edges should be included as their own land-cover class in maps derived from coarser-resolution satellite imagery.

A key source of inaccuracies in many coarser remote sensing products derives from challenges in categorizing edges and mixed pixels as either a forest or a non-forest class. Beyond improved area quantification, a distinct forest edge class would improve the spatial accuracy of maps.

4. Explicitly include forest edges in carbon accounting, forest models, and predictions.

The growing literature on forest transition zones can be used to parameterize the distinct ecologies of the forest edge.

Forest edges are dramatically underrepresented in national inventories, land-cover maps, and research. This means that edges are often invisible on the landscape, particularly in

areas where they are most prevalent. Despite this, edges are a ubiquitous feature of modern forests and are the forests that people interact with most. To fully understand modern and future forest ecology, we must first acknowledge the forests that we have, not the ones we imagine to be.

Panel: The consequences of underrepresenting forest area and edges for carbon accounting

Small forest fragments and forest edges are highly prevalent and ecologically distinct from the forest interior. Excluding them from measurements and models has large consequences for calculations of forest ecosystem services, particularly carbon budgets. To illustrate the consequences of underrepresenting forest edges, we made two estimates of aboveground forest carbon in the Chesapeake Bay Watershed. First, we derived county-level values of aboveground forest carbon per hectare from the US NFI, using the *rFIA* package (Stanke et al., 2020). For a baseline estimate, we followed a traditional approach where we used forest area from the NLCD to calculate an aboveground carbon total for each county. We then altered our calculation to correctly account for the fragmented forest landscape by using interior and edge forest area totals from VHR land-cover maps and included observed FIA edge enhancements of aboveground carbon storage (following Morreale et al. 2021). We find that accounting for small forest fragments and edges results in a median 14.8% increase in aboveground carbon estimates per county in our study area and a total increase of 130.4 Tg carbon (Figure 3.4; Supplementary Figure 3.2). In highly fragmented counties where development or agriculture is the dominant land cover we find median increases of 74.2%

and 23.8%, respectively, in estimated county forest carbon storage. These increases in aboveground forest carbon pools are currently unaccounted for in carbon budgets. As states and municipalities increasingly commit to nature-based climate solutions, complete accounting of forest area and edges is imperative to accurately quantify biogenic sequestration.

Acknowledgements

We thank the many colleagues who gave us friendly feedback throughout this research, in particular K. Harper and M. Friedl for their thoughtful suggestions, as well as the members of the Terrestrial Carbon Laboratory at Boston University. We thank Mass Audubon and TerraCorps members J. Collins, S. Kefferstan, and S. Semenza for data collection, analysis and validation of the LosingGround report. Funding: This work was supported, in part, by the United States Department of Agriculture National Institute of Food and Agriculture Award 2017-67003-26487, the Harvard Forest LTER Program (NSF DEB 18-32210), the Rafiki B. Hariri Institute at Boston University and by a National Science Foundation Research Traineeship (NRT) grant to Boston University (DGE 1735087).

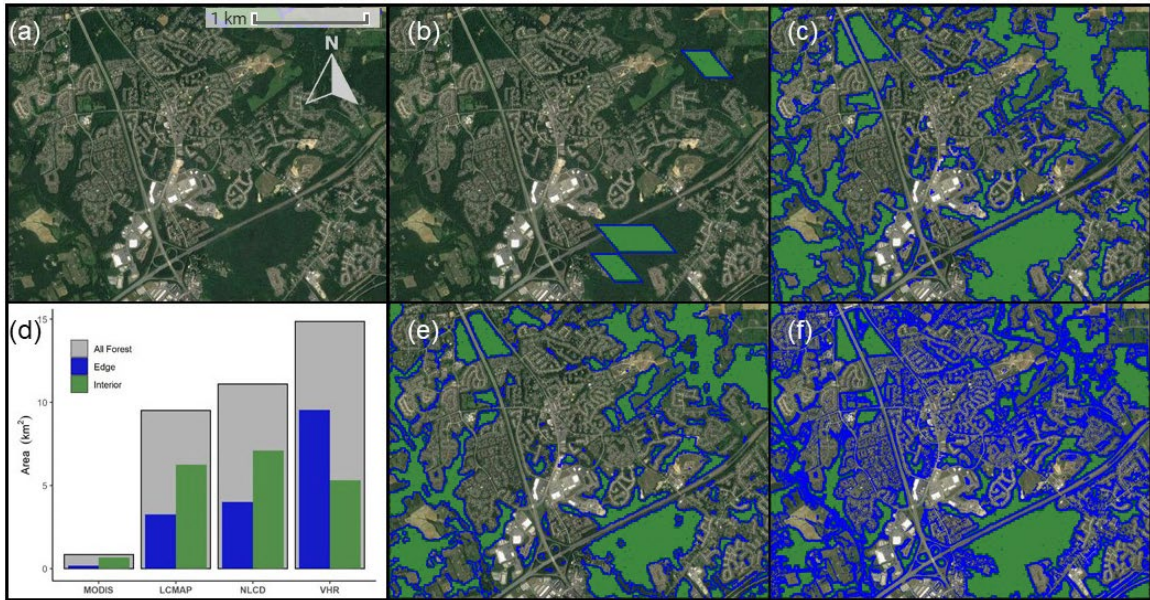


Figure 3.1. Example of resolution effects on estimates of forest area and forest edge area. Interior forest area (> 30 m from a non-forest land cover) is shown in green and forest edge area (≤ 30 m from a non-forest land cover) is displayed in blue. The impact of different characterizations of forest fragmentation is shown based on a) Google Earth Imagery of a suburban area outside of Baltimore, MD b) MODIS Land Cover IGBP - 500m pixel size ($.85 \text{ km}^2$ forest with $.18 \text{ km}^2$ edge), c) LCMAP – 30m pixel size (9.52 km^2 forest with 3.3 km^2 edge), e) NLCD – 30m pixel size (11.1 km^2 forest with 4 km^2 ha edge), and f) Chesapeake Bay Watershed Land Cover – 1m pixel size (14.9 km^2 forest with 9.55 km^2 edge). d) Area of total forest, edge, and interior from each product.

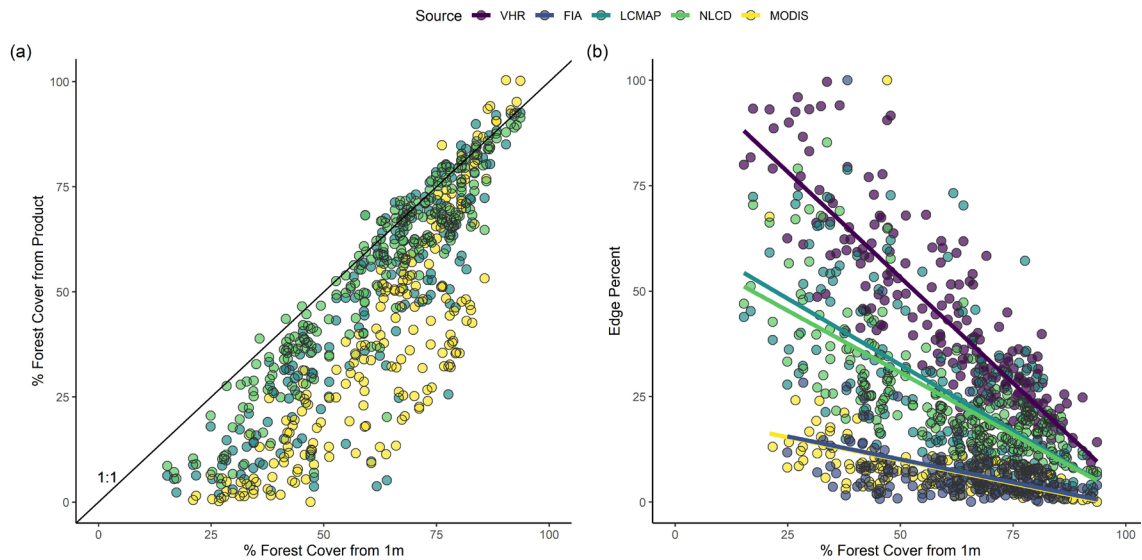


Figure 3.2. Underestimates of forest edge percent increases with decreasing forest cover.

a) The relationship between county-level % forest cover from 1 m products and county-level % forest cover estimates from coarser remote sensing products. b) The relationship between county level % forest cover from 1 m products and county-level % of forest area within 30 m of an edge from all forest monitoring methods. Pixel resolution for LCMAP, NLCD, and MODIS is 30 m, 30 m, and 500 m, respectively.

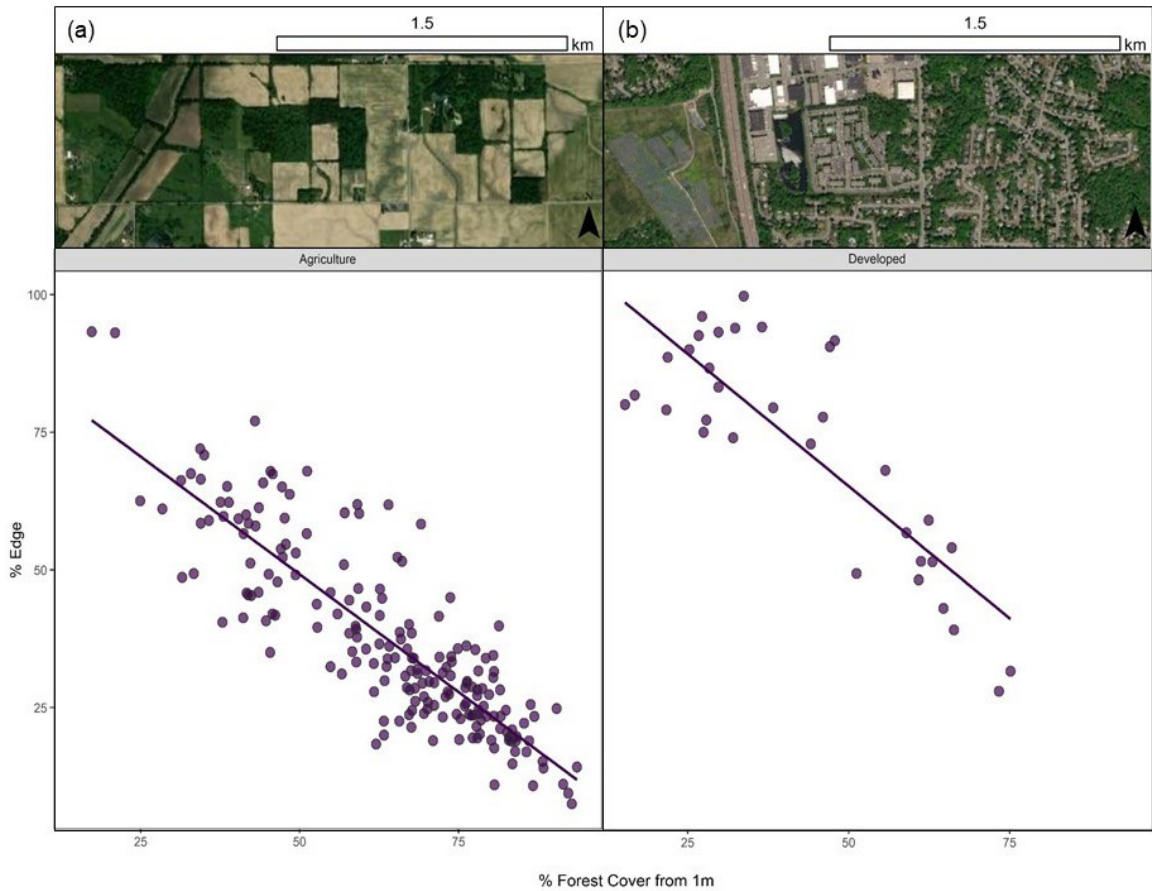


Figure 3.3. Development leads to higher amounts of forest edge than agriculture.
 a) The relationship between percent of forest edge area and % county forest cover in counties where agriculture is the majority non-forest land cover; an example of fragmentation patterns in an agricultural area. b) The relationship between percent of forest edge area and % county forest cover in counties where development is the majority non-forest land cover; an example of fragmentation patterns in a developed region.

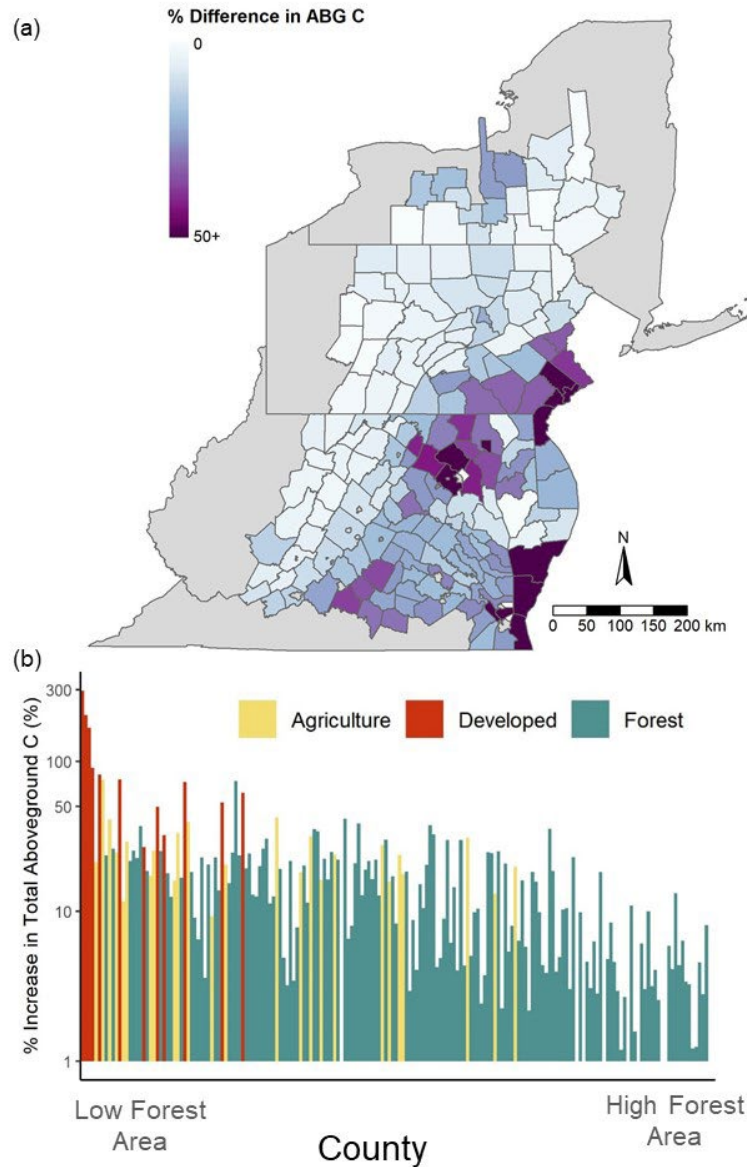


Figure 3.4. Undercounting forest edges significantly changes estimates of aboveground forest carbon.

a) The % increase per county in total aboveground carbon across the Chesapeake Watershed portion of our analysis. b) The % increase per county in total aboveground carbon across the Chesapeake Watershed portion of our analysis. Counties are colored by the dominant land cover in the county (forest, agriculture, or development) and counties are ordered from lowest forest area to highest forest area. The y-axis is log-scaled for readability. In four counties, the 1 m maps have smaller total forest area, resulting in slight negative differences in total aboveground carbon; these counties are not displayed in the figures for visual simplicity.

CHAPTER FOUR: THE ROLE OF FOREST EDGES IN TEMPERATE FOREST CARBON CYCLING

Abstract

Temperate forests are the most heavily fragmented forest biome and contain the largest area of forest affected by a non-forest edge. Despite the ubiquity of temperate forest fragmentation, current forest carbon (C) accounting does not include known differences in forest C cycling that characterize forest edges. Here, we used a novel approach to quantifying aboveground C fluxes by partitioning C fluxes into forest edge and interior categories. This approach explicitly accounts for the extent of forest edge area and differences in edge forest growth to create a forest C budget for the New England region of the United States for 2010 to 2020. We found that in this 10-year period, the prevalence of forest edges increased by 2.7% of total forest area throughout our study area. Despite the increasing proportion of forest area delineated as forest edge, we reported a net loss of > 190,000 ha of forest area across New England and note that forest edge area was significantly more likely to be lost than the forest interior. Our analysis of aboveground C fluxes confirmed that New England forests are a C sink, and we report a net uptake of 55.0 Tg C over the study period. By partitioning C fluxes into forest edge and interior categories, we found that forest edges account for 21.1% (19.1 Tg C) of forest C uptake and 29.7% (10.6 Tg C) of forest C emissions in this region. We compared our results with a more traditional calculation of forest C fluxes that does not account for forest edges and found that inclusion of edges results in a 8.6% (4.36 Tg C)

increase in the estimate of the net forest C sink for New England. Our results demonstrate that forest edges play a critical role in forest C fluxes, contributing disproportionately to the net C balance even compared to their high prevalence on the landscape.

Introduction

Forest ecosystems are the largest component of the terrestrial carbon (C) sink and play a key role mitigating climate warming from anthropogenic greenhouse gas (GHG) emissions (Bonan, 2008; Friedlingstein et al., 2022; Pan et al., 2011). Realizing the full potential of the forest C sink is essential to reaching the emissions targets set in the Paris Climate Agreement, and there is growing political interest in actively managing forests to increase their C uptake to reach larger net C neutrality goals (Anderegg et al., 2020; Bastin et al., 2019; Grassi et al., 2017; Novick et al., 2022). Recent analyses of the forest C cycle estimate that terrestrial forests remove between 0.88 and 2.11 Pg C from the atmosphere each year (Harris et al., 2021; Xu et al., 2021). Temperate forests alone comprise up to 46% of the global forest C sink, removing an estimated 0.31 - 0.97 Pg C from the atmosphere annually (Harris et al., 2021; Xu et al., 2021).

The size of the forest C sink is mediated by historical and ongoing deforestation, as well as persistent land-use change (Foley et al., 2005; Houghton & Nassikas, 2017). In recent decades, tropical deforestation has constituted the majority of emissions of C from land use and land cover change (LULCC), whereas northern non-tropical regions have experienced much lower rates of deforestation and have acted as a net sink since the mid-20th century (Houghton & Nassikas, 2017). While it is critical to quantify ongoing emissions from forest loss, the widespread focus on deforestation has obscured the

importance of LULCC secondary effects on forest C fluxes. In the temperate forests of the northeastern United States (US), European colonialism led to broadscale deforestation in the 19th century (Foster, 1992) which was then followed by rapid reforestation, mirroring global trends found throughout the northern temperate forest biome (Mather, 1992). The legacy of forest transition has large consequences for the pattern, structure and function of modern temperate forests and their C dynamics (Haddad et al., 2015; Morreale et al., In review; Turner, 1989a).

Beyond immediate forest loss, LULCC divides remaining forest into smaller fragments and creates forest edges that are laterally exposed to non-forest land cover (Fischer et al., 2021). Lateral exposure creates large gradients in microclimate from the forest edge to interior, and forest edges experience elevated insolation, summer temperatures, wind exposure and atmospheric deposition compared to closed-canopy, interior forest (Matlack, 1993; Schmidt et al., 2017). Forest edges are further influenced by human management of adjacent non-forest land, intensifying perturbations to nutrient and hydrological cycling at the edge (Caron et al., 2023; Pocewicz et al., 2007a; Weathers et al., 2001).

The generalizable gradients in microclimate and nutrient inputs at the forest edge have wide-ranging consequences for forest structure and productivity (Franklin et al., 2021; Smith et al., 2018). In temperate forests, there is growing evidence that edge forests grow faster, have higher stem density and tree basal area, and have similar tree mortality rates when compared to their interior counterparts. (Meeussen et al., 2020; Morreale et al., 2021; Reinmann & Hutya, 2017). As a consequence, temperate edge forests store

more and uptake C more rapidly than the forest interior, with studies reporting up to a 95% increase in both aboveground biomass (C stock) and woody increment (C uptake) relative to the forest interior (Meeussen et al., 2020; Reinmann et al., 2020). In a previous study, we found that the observed enhancement in growth and biomass at the temperate forest edge is highest in forests adjacent to anthropogenic land cover, suggesting that this enhancement is attributable to LULCC (Morreale et al., 2021). These findings are in stark contrast to those in tropical forests, where forest edges exhibit elevated mortality and suppressed tree growth due to increased drought, fire and wind-throw (Laurance & Ferreira, 1997; Ordway & Asner, 2020). Despite observed differences in forest edge C cycling, current methods of measuring forests at scale (*i.e.*, national forest inventories and land cover maps), significantly underestimate the prevalence of forest edges (Morreale et al., In review).

Significant uncertainties remain in estimates of the C fluxes of forest processes (*i.e.*, mortality and growth) and LULCC, which contribute to large discrepancies in estimates of net forest C fluxes between global C budgets and national GHG accountings (Grassi et al., 2018; *IPCC Special Report on Climate Change, Desertification, Land Degradation, Sustainable Land Management, Food Security, and Greenhouse Gas Fluxes in Terrestrial Ecosystems Summary for Policymakers*, 2019). Advancements in forest observations and ground-based inventories demonstrate that improved spatial and ecological detail can bridge this gap (Harris et al., 2021; Schwingshackl et al., 2022). However, most state-of-the-art approaches to forest C flux inventories fail to *explicitly* account for the legacy of forest fragmentation on the landscape, focusing instead on

direct emissions from forest loss. Due to the exclusion of forest edges and fragments from ground inventories and remote observations, neither do these approaches *implicitly* include fragmentation effects (Morreale et al., In review). Accounting for fragmentation effects on forest C cycling is necessary to quantify the influence of LULCC on C fluxes.

Here, we present a novel approach to aboveground C accounting that explicitly includes the role of temperate forest edges in C cycling. We combine highly-resolved forest growth rates from the US national forest inventory (NFI) with contiguous maps of forest area and land-cover change across a six state region in the northeastern US to quantify aboveground forest C pools and fluxes over the 10-year period from 2010 to 2020. We apply empirically derived differences in rates of C uptake between the forest edge and interior to elucidate the impact of fragmentation on forest C inventories. We find that forest fragmentation significantly impacts estimates of LULCC forest C fluxes with critical implications for understanding of the current and future terrestrial C sink.

Material and methods

Study area

We conducted our study on the New England region in the northeastern United States (Figure 4.1). New England has a land area of 162,716 km² and includes six states: Connecticut (12,509 km²), Maine (80,068 km²), Massachusetts (20,269 km²), New Hampshire (23,247 km²), Rhode Island (2,700 km²), and Vermont (23,923 km²). The area ranges in latitude from 41°N to 47°N and includes a latitudinal gradient of forest compositional types from temperate oak-pine forests in the south to boreal conifer forests in the north (Figure 4.1a; Duveneck & Thompson, 2019). While urbanization and solar

development are the primary drivers of forest loss in southern New England (Duveneck & Thompson, 2019; Thompson, Plisinski, et al., 2017), timber harvest is most prevalent in the north (Thompson, Canham, et al., 2017), reflecting the variability of human land-use across our study region. This study area was selected because: 1) there are multiple studies in this region reporting differences in aboveground productivity at the forest edge relative to forest interior, including variability between forest compositions (Briber et al., 2015; Morreale et al., 2021; Reinmann & Hutrya, 2017); 2) regional history of forest clearing and regrowth has created a matrix of forest that is heavily fragmented by human land use resulting in high overall forest cover and large amounts of forest edge; and 3) gradients of land use result in divergent patterns of fragmentation and allow comparisons of edge C dynamics across differing landscapes.

Mapping forest area and forest change

To map forest area and quantify both forest loss and gain, we used an annual time-series of 30 m resolution land-cover maps from the US Geological Survey's Land Change Monitoring, Assessment, and Projection (LCMAP; J. F. Brown et al., 2020a). The tree-cover class in the LCMAP Collection 1.2 land-cover product has a user's accuracy of 93% ($\pm .5$), supporting our application of it for mapping forest area (Pengra et al., 2021). All forest mapping and subsequent spatial analyses were performed in the Google Earth Engine geospatial platform (Gorelick et al., 2017). We combined information from the primary and secondary land-cover products from the LCMAP Collection 1.2 for each year from 2010 to 2020 to create annual maps of forest area across New England. We categorized as 'forest' any pixel that has a primary land-cover

classification of tree cover or of wetland and with a secondary class of tree cover. The LCMAP land-cover product represents the land cover at the end of each calendar year; thus our analysis produces 11 maps of forest area (one for each year of study period). To map annual change in forest area, we identified pixels that change from forest to any non-forest class as ‘forest loss’, pixels that transition from non-forest to forest as ‘forest gain’, and pixels that remain forest as ‘stable forest’. Resulting maps for each year from 2011 to 2020 reflect changes in forest area that occur during the given calendar year (hereafter, change years). Our approach followed the method for identifying annual land cover change used in LCMAP change products, with non-forest land covers simplified to a single class (J. F. Brown et al., 2020a).

A known limitation of LCMAP is the misidentification of ephemeral land surface disturbances as a categorical, persistent cover change. Changes in spectral reflectance associated with ephemeral disturbances (*i.e.*, insect infestations that cause defoliation but not tree mortality) can be incorrectly identified as forest loss (J. F. Brown et al., 2020a). The southern portion of our study region experienced widespread insect defoliation events from spongy moth (*Lymantria dispar*) between 2015 and 2018 (Pasquarella et al., 2018), and incorrect categorization of spongy moth defoliation as forest loss significantly affected calculations of forest area in southern New England. To mediate overestimates of forest loss, we applied a filter based on published maps of the severity and extent of spongy moth defoliation (Pasquarella et al., 2018): if a forested pixel experienced defoliation of severity considered ‘moderate’ or greater *and* the pixel was then identified as forest loss with a subsequent forest gain, it was reclassified as stable forest.

Timber harvest from commercial forestry also poses a challenge for categorical land-cover change maps. Tree removals associated with harvest events may be identified as forest conversion to a non-forest class despite subsequent forest regrowth and re-identification as tree cover (J. F. Brown et al., 2020a). For our purposes, the categorization of timber harvest as forest loss was acceptable for accounting of aboveground C fluxes. We note that timber harvest is an ephemeral loss of forest area and associated C storage, but over the 10-year time scale of our study period this represents a significant, real loss of C stored in forests.

Creating forest edge and interior classes

We used our annual maps of forest area to differentiate forest into ‘edge’ and ‘interior’ categories. Because accumulating evidence suggests that the distance of edge influence on aboveground forest structure and productivity extends up to 30 meters into the forest interior in temperate forests (Briber et al., 2015; Meeussen et al., 2020; Reinmann et al., 2020; Reinmann & Hutya, 2017), forest area within 30 m of non-forest land cover was classified as forest edge, while the remainder was classified as interior forest. In each change year, forest area was first separated into edge and interior classes based on the initial pixel status at the beginning of the year. We then applied our forest area change-analysis methods to the edge and interior forest classes, resulting in four possible change outcomes for a given forest pixel: stable edge forest, stable interior forest, lost interior forest, and lost edge forest (Figure 4.2). Forest gain was not divided into edge and interior classes as current research does not report differences in initial

regeneration from forest edge to interior. Following the initial gain year, forest was subsequently categorized as interior or edge forest.

County-level forest growth rates

We used data from the US NFI conducted by the US Forest Service's Forest Inventory and Analysis (FIA) program to calculate forest growth rates in our study area. The FIA encompasses a systematic, hexagonal grid of permanent ground plots designed to be a statistically-representative sample of the US's forested lands (Bechtold & Patterson, 2005). An individual plot comprised of four subplots is randomly located within each 2,428 ha hexagon, and if the plot contains forest area, all adult trees (> 12.7 cm diameter at breast height; DBH) that fall within its forested subplots are inventoried. Within each 7.3 m radius subplot is a smaller 2.1 m radius microplot, and live saplings (> 5 cm DBH) within microplots are additionally inventoried. Dead trees and their associated mortality agent are also recorded during each survey, and mortality agents are broadly grouped into natural causes (termed 'mortality') and harvest (termed 'removals'). All plots within our study area are remeasured every 5 – 7 years. The spatial and temporal standardization of the FIA makes it well suited for aboveground biomass and C accounting with statistical power maintained at even the US county level (Tinkham et al., 2018).

We quantified forest net growth rates at the county level using the *rFIA* package (Stanke et al., 2020) in the R computing environment (R Team, 2019). The *rFIA* package implements standard FIA methods of estimating tree volume, biomass and C while accounting for sample design and non-response bias of inventory plots. To calculate the

net change in aboveground C by county across the New England study area, we used the *growMort* function to make estimates of tree growth, recruitment, mortality, and removals, and we used the FIA's temporally-indifferent (TI) estimator to make annual estimates from 2010 to 2020 of each component. TI uses a moving-window average, treating plots as a periodic inventory to reduce variance driven by stochasticity in plot re-measurement cycles (Stanke et al., 2020).

To account for differences in growth and aboveground C storage between forest edge and interior, we first isolated interior forest plots using a filter that excluded all plots that contained both a forest and non-forest condition (*i.e.*, forest edges; *sensu* Morreale et al., 2021). We then summed the median annual estimates of positive growth components (*i.e.*, tree growth and recruitment) and loss components (*i.e.*, mortality and removal) to produce a single net forest growth rate in $\text{Mg C ha}^{-1} \text{ yr}^{-1}$ for each county. Note that we constrained our analysis to counties with > 10 forested FIA plots as a robustness threshold for our net growth estimates; six counties with a total land area of 108,000 ha were omitted from our analysis. We then calculated county-specific net growth rates for edge forests that explicitly account for differential tree growth at the forest edge. To quantify percent differences in aboveground C increment between forest edge and interior, we followed methods detailed in Morreale et al., 2021. We estimated percent increase in forest growth at the edge relative to the interior for eight forest compositional groups. We used these results to create a single growth for modifier for each county using a weighted-average of the forest composition within the county. County-specific growth

modifiers were then included in net change estimates to produce discrete net growth rates for forest edge and forest interior within the county.

We reported uncertainty in our analyses as the Root Mean Squared Error (RMSE) of the net growth in each county. We accounted for potential double-counting of timber harvest (via inclusion in both the removal component of the FIA growth calculation *and* the forest loss class in our LULCC analysis) by setting a threshold of 0.8% of stems removed annually in a county, above which we set the removal component from the county growth calculation to zero.

Forest C accounting

We then calculated an aboveground C budget that explicitly accounts for both forest edge and forest interior in New England from 2010 – 2020 using our LULCC maps and FIA-derived net growth rates by county. We initialized our forest C analysis with an aboveground biomass product for the year 2010 (T_0 ; [Spawn et al., 2020; Figure 4.1b](#)). This 300 m-resolution product reports close agreement ($R^2 = .96$) with state-level estimates of biomass from the FIA. We masked the biomass map to include only area defined as forest by LCMAP in 2010. We then aggregated our forest area and change maps by year and county to quantify stable edge and interior forest area, edge and interior forest loss, and forest gain for each county throughout our study period. We calculated forest C uptake in Mg C yr^{-1} by multiplying county-specific interior and edge net forest growth rates ($\text{Mg C ha}^{-1} \text{ yr}^{-1}$) from the FIA by stable interior and stable edge forest area (ha), respectively. To quantify forest C loss from LULCC, we first calculated the biomass at T_0 for interior and edge forest loss pixels. We accounted for growth between T_0 and the

loss year (T_L) by multiplying net edge and interior growth rates by $(T_L - T_0)$, or years until loss. Forest C uptake associated with forest gain was assigned a value of 0.25 Mg C ha^{-1} based on empirical models of forest regeneration derived from the FIA in our study region (Ma et al., 2018). After the initial year of regrowth, forest gain pixels were grouped into either edge or interior forest classes. Finally, we re-ran our C accounting with only interior forest growth rates to quantify the net difference in C uptake attributable to forest edges.

Results

Using the US NFI and annual land cover maps, we quantified how forest edges influence regional forest C budgets. Accounting for the differential growth rates within the forest edge area resulted in significant increases in aboveground net C uptake. We further characterized changes in forest and forest edge area over a 10-year period, finding that fragmentation is increasing over time.

Change in forest area and pattern

For the New England region over our study period we report 564,262 ha of gross forest loss and 374,041 ha of forest gain, resulting in a net loss of 190,221 ha representing a net decrease of 0.7% in total forest area (Figure 4.3). All states experienced a net loss of forest from 2010 – 2020, with an average decrease of 1.09% of forest. Maine, which constitutes roughly half of the study area, had the largest net forest loss area (121,981 ha), but the lowest net loss on a percentage basis (0.65%). The highest percent loss occurred in New Hampshire, losing 1.45% of forest area. Maine also had the largest gross area of forest gain with 309,607 hectares. We report large inter-annual

variation in the rate of net forest change in New England ranging from 3,891 ha of net forest loss in 2011 to 36,306 ha in 2016. Using linear regression, we find significant trends in gross forest gain and gross forest loss over time across our study region ($p < 0.05$). Forest loss is increasing at a rate of 3033 ha yr^{-1} ($p < 0.02$; Adj. $R^2 = .48$) greatly outpacing forest gain, which is increasing at a rate of 797.7 ha yr^{-1} ($p < .03$; Adj. $R^2 = .40$).

To understand changes in forest edges, we categorized forest area and forest loss into edge and interior classes (Figure 4.4). Forest edge area expanded by 302,024 ha in New England over the 10 years of our study period, an increase from 13.9% to 16.6% of regional forest area. Rhode Island, with 22.2% of forest categorized as edge, and Vermont, with 9.7% edge forest, were the most and least fragmented states, respectively. Both forest edge area and proportion increased in all New England states. Maine exhibited the biggest change in relative abundance of forest edge area, from 14.7% of state forest area in 2010 to 18.3% in 2020. Edge forests were also more likely to be converted to non-forest than the forest interior. If forest loss was distributed randomly, we would expect loss proportionate to the prevalence of edge forests: instead, we found that 34.6% of all forest loss in New England occurred in forest edges. We found this to be true in all individual states, and the disparity between prevalence of edge forests and their relative rate of loss was particularly acute in the more developed states of southern New England (Massachusetts, Rhode Island, and Connecticut).

Forest carbon fluxes

Between 2010 and 2020, New England forests were a net sink for aboveground C with an uptake of 55.0 Tg C ($RMSE = 36.7$) (Figure 4.5). Forest growth C uptake was 90.6 TgC ($RMSE = 35.81$), more than offsetting forest loss emissions of 35.7 Tg C ($RMSE = .93$). Forests in all six New England states were net C sinks, with net C fluxes of 21.5 Tg C ($RMSE = 14.1$) in Maine, 9.20 Tg C ($RMSE = 6.83$) in Vermont, 8.73 Tg C ($RMSE = 6.96$) in New Hampshire, 7.37 Tg C ($RMSE = 4.09$) in Massachusetts, 7.1 Tg C ($RMSE = 4.0$) in Connecticut, and 1.10 Tg C ($RMSE = 0.72$) in Rhode Island.. Moreover, all but two counties in New England were net C sinks over the study period, with the both largest county-level C storage and emissions occurring in northern Maine (Figure 4.6).

Growth in interior forests comprised the largest C flux, totaling 71.5 Tg C ($RMSE = 30.0$) of uptake from the atmosphere, compared to the forest edge growth flux of 19.1 Tg C ($RMSE = 5.81$). We estimated C emissions from interior forest loss as 25.1 Tg C ($RMSE = .622$) and emissions from forest edge loss as 10.6 Tg C ($RMSE = .309$). We report that edge forest contribution to C fluxes is disproportionate to their 13.9% prevalence (at the beginning of the study period) on the landscape as they constituted 21.1% and 29.7% of New England forest C uptake and emissions, respectively. Their relative contribution to forest C fluxes increases with prevalence of fragmentation as forest edges in Connecticut and Massachusetts constitute 41.4% and 38.7% of forest C emissions and 23.9% and 25.4% of forest C uptake, respectively. While we report significant areas of forest gain, the first-year of C uptake that we attributed to gain is dwarfed by growth in stable forests.

We expanded our quantification of the role of forest edges to forest C cycling by reanalyzing our study region treating all forest as interior forest. We find that inclusion of differential forest edge growth results in an increase of 4.36 Tg C, or a 8.6% difference, in our estimate of net C flux for New England (Figure 4.7). At the state level, accounting for forest edges can increase C uptake values by up to 10.1% and 10.4% in Maine and Massachusetts. Even in Vermont, the state with the lowest proportion of forest edges, we found a 5.3% difference in net C flux.

Discussion

A changing forest landscape

Our analyses of LULCC describes an increasingly fragmented forest landscape. Although forest area is decreasing in all states, significant amounts of forest gain currently mediate changes in overall forest area. While rates of forest gain and loss are both increasing, the rate of forest loss is growing at three times that of forest regrowth. In southern New England, some amount of this forest conversion may be attributable to the ongoing expansion of utility-scale solar farms (Tao et al., 2023). In areas where commercial timber harvest is the dominant driver of forest clearing, *e.g.*, Maine and northern New Hampshire, forest loss is likely to be an ephemeral change, a conclusion supported by the corresponding high rates of forest gain in these areas. While not a persistent land cover change, timber harvest is the most common forest disturbance in the northeastern United States and thus necessary to account for in forest C analyses (Thompson, Canham, et al., 2017).

The LCMAP methodology ensures that classification uncertainty of individual pixels does not result in constant toggling between forest and non-forest classes. However, high pixel-level uncertainty, present in all land-cover maps, can produce overestimates of forest loss and gain when aggregated across a region. We acknowledge that there is inherent uncertainty in our estimates of forest area change and aboveground C fluxes that is attributable to our choice of land cover products. While we expect that product-based differences in estimates of forest area have large consequences for the magnitude of C fluxes, we do not expect this to have a meaningful effect on the relative difference between edge and interior C fluxes.

Despite small changes in overall forest area, forest edge area and proportion steadily increase in all states throughout our entire study period. The differing trends in forest edge proportion and total forest area underscore the need to account for pattern in analyses of forest area. While reforestation may moderate losses in forest area it does not guarantee that the resulting patterns of forest area remain the same. Research suggests that forest edges and small fragments are less likely to be correctly classified as forest in moderate-to-coarse resolution land cover maps or to be included in forest inventories (Morreale et al., In review; Wickham & Riitters, 2019). As forest edge area increases, it may become more difficult to accurately quantify forest area with traditional methods. Furthermore, disproportionate conversion of edge forests to non-forest land cover could result in significant forest loss that is excluded from LULCC monitoring.

C fluxes in New England forests

Our results are consistent with other studies concluding that New England forests are a net C sink (Duveneck & Thompson, 2019; Graham MacLean et al., 2021). Even with high rates of timber harvest, northern forests drive a large portion of the region's C uptake. Our findings demonstrate that accounting for forest edges is crucial in estimating aboveground C fluxes. In southern New England, where edge forests make up 18.4% of forest area in 2010, enhanced edge growth increases net C uptake by 9.1%. Throughout the study area the inclusions of forest edges also results in increased estimates of C emissions due, in large part, to the differential rates of conversion of edge forests. Although elevated conversion rates result in an increase in total C emissions, enhanced growth of edge forests increases the net C sink of New England forests. Moreover, forest edge growth offsets 53.5% of total C emissions from forest loss in New England over the 10-year period. We note that while enhanced forest edge growth mediates some amount of C emissions from forest clearing, we emphatically are not advocating for the creation of edge forest to increase forest C uptake. Emissions from forest conversion and foregone C uptake from the lost forest will always outweigh elevated edge growth. Instead, we demonstrate that forest edges represent large proportions of C emissions and uptake, and that accounting for forest edges is necessary to fully quantify the effects on LULCC on forest C dynamics.

Our results are a likely a conservative estimate of forest edge contribution in C accounting. Morreale et al. (in review) found that 30 m – resolution land cover maps significantly underestimate forest edge area and proportion (16.4% in the case of

LCMAP) and the US NFI does not currently measure forests in developed areas, resulting in their exclusion from forest C analyses. The six counties omitted from our analysis include the most populous, urban counties in New England, where the majority of forests are highly fragmented and, consequently, forest edge growth may have the largest relative effects on net forest C fluxes. Furthermore, due to limitations of current biomass maps, we were unable to implement differences between edge and interior initial forest biomass in [Spawn et al., 2020](#), despite strong empirical evidence (Meeussen et al., 2020; Morreale et al., 2021). We expect that this results in an underestimation of C emissions from edge forest loss and is a key area to address in future studies.

Of critical note, our analysis is limited by uncertainties associated with forest cover classification and change detection. Beyond impacts on quantification of forest gain and loss, misclassified forest change will also affect edge delineation and area estimates. Particularly, high-severity timber harvest is often categorized as forest-loss in our study region. This resulted in large estimates of forest loss and increases in forest edge area in counties with commercial timber harvest (*e.g.*, northern Maine). While timber harvest does produce substantial C emissions over a 10-year period it does not constitute a land-cover or land-use change, and therefore should not be classified as a loss of forest. We expect that this also biases the analyses of edge area and prevalence over time, particularly in Maine and northern New Hampshire. Future C accounting of forest edges in New England should better partition between timber harvest and forest conversion.

Conclusions

Our results underscore the need to explicitly consider forest edges in C accounting given the critical role they play in maintaining and increasing the temperate forest C sink both now and into the future. Fragmentation and forest edge are increasing in our study area and in forests globally, increasing the weight of forest edges C dynamics even in areas where total forest area remains relatively stable. Growing interest in forests as a natural climate solution make it imperative for researchers to account for C fluxes associated with forest fragmentation and not focus solely on those from forest gain and loss. Forest C accounting that does not account for the effects of spatial pattern on forest C processes cannot capture the magnitude of forest C fluxes. Beyond differences in aboveground C dynamics, growing evidence suggests large alterations to belowground C cycling from forest edge to interior and underscore the critical importance of forest edges in our understanding of C fluxes from forests and LULCC (Garvey et al., 2022; Meeussen et al., 2020; Reinmann et al., 2020).

Currently, temperate forest edges enhance the terrestrial carbon sink through elevated growth and biomass compared to their interior forest counterparts. However, edge forests are under disproportionate threat from forest conversion, and expanding human populations and increasing urbanization could undermine this increased C sink. Forest edges are also vulnerable to heat and drought, and in warmer, tropical forests increased tree mortality reduces C storage and often results in edges as a net C source (Chaplin-Kramer et al., 2015; Ordway & Asner, 2020). Increasing global temperatures and more variable precipitation in temperate regions may further threaten forest edges. If

a critical threshold is crossed, it may trigger tree mortality at the forest edge that could cascade as previously-interior forests are exposed to edge conditions. Increasing threats to temperate edge forests combined with their disproportionate contribution to the temperate forest carbon sink may indicate the existence of another positive feedback cycle of C emissions that is currently invisible from C cycle models.

Acknowledgements

We thank the colleagues who gave us friendly feedback throughout this research, in particular to M. Friedl, K. Lane and the members of the Hutyra Terrestrial Carbon Lab for their thoughtful suggestions. Funding: This work was supported, in part, by the United States Department of Agriculture National Institute of Food and Agriculture Award 2017-67003-26487, the Harvard Forest LTER Program (NSF DEB 18-32210), the Rafiki B. Hariri Institute at Boston University and by a National Science Foundation Research Traineeship (NRT) grant to Boston University (DGE 1735087).

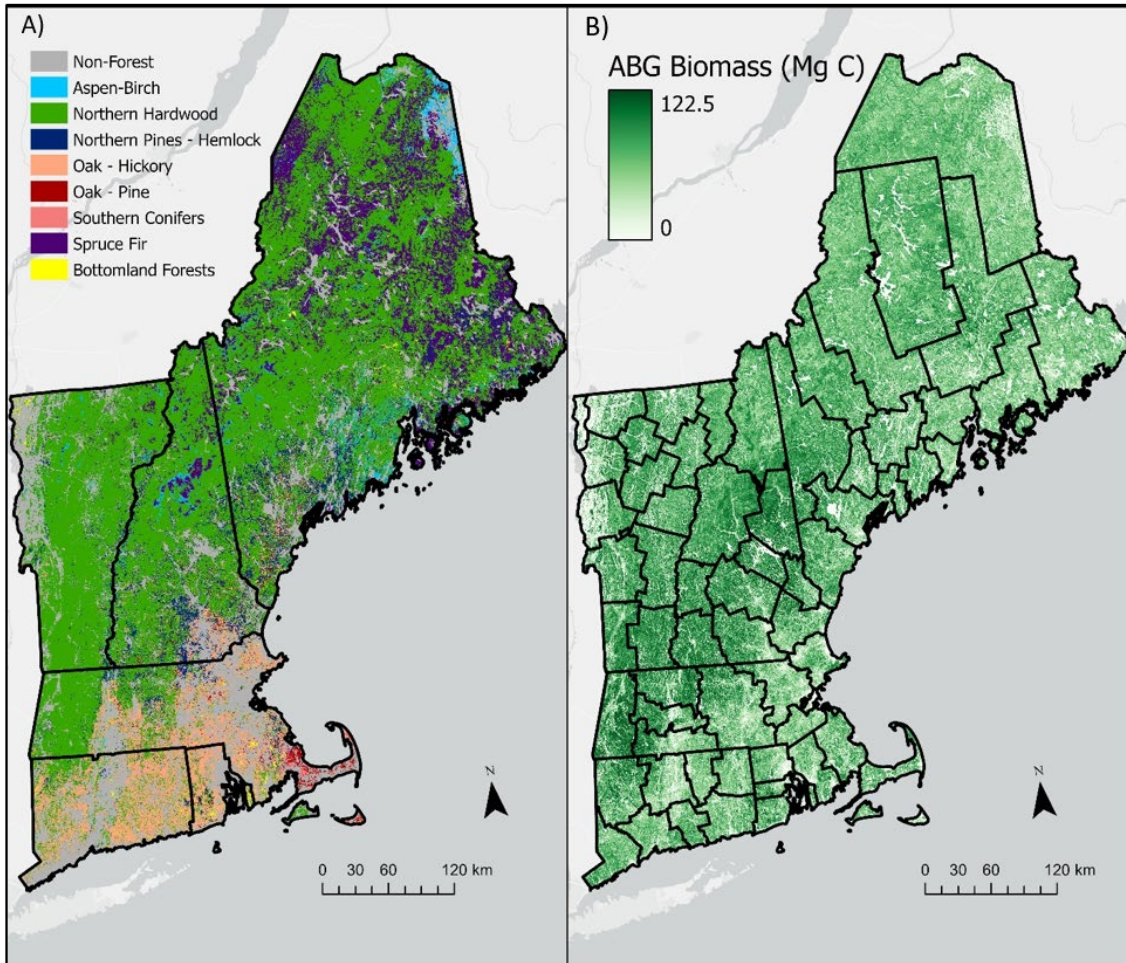


Figure 4.1. Maps of study area — the New England region of the northeastern United States.

A) Map of forest-type compositional groups (*sensu* Morreale et al. 2021) with US State borders in black. B) Map of aboveground biomass (Mg C) in 2010, with US county borders in black.

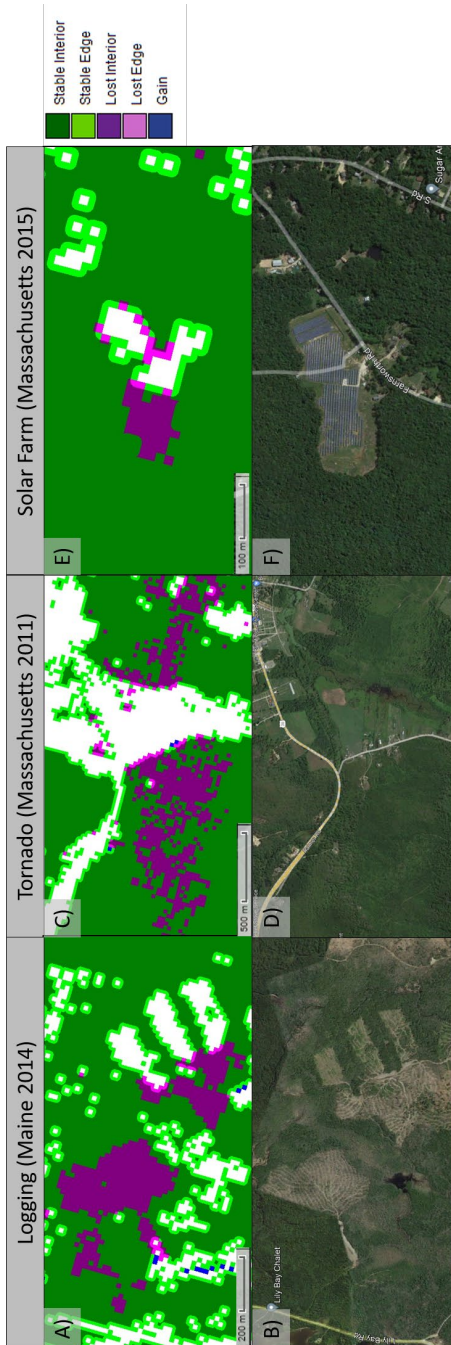


Figure 4.2. Examples of forest disturbance and loss.

Categorical maps of forest loss from disturbance and corresponding GoogleEarth Imagery shown for logging in Maine (A, B), a tornado (C, D) and a solar farm in Massachusetts (E, F). Stable interior forest is shown in dark green and stable edge forest in light green, while lost interior forest is shown in dark purple and lost edge forest in light purple. Forest gain is in blue. Panels B), D), and E) show earliest available leaf-on imagery post-disturbance.

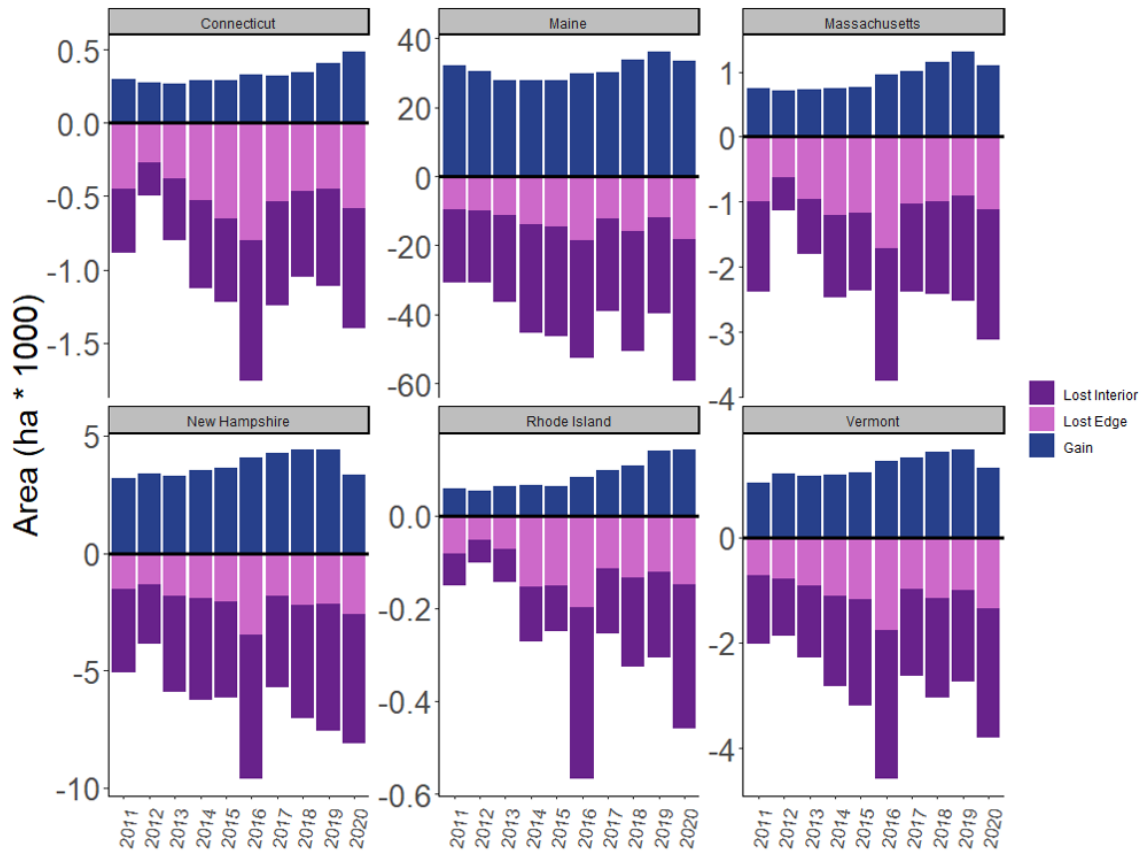


Figure 4.3. Total annual change in forest area by state and year of change.

Forest loss is shown in purple and separated into forest edge and interior category, while forest gain is shown in blue. Year of change refers to change occurring within the listed calendar year.

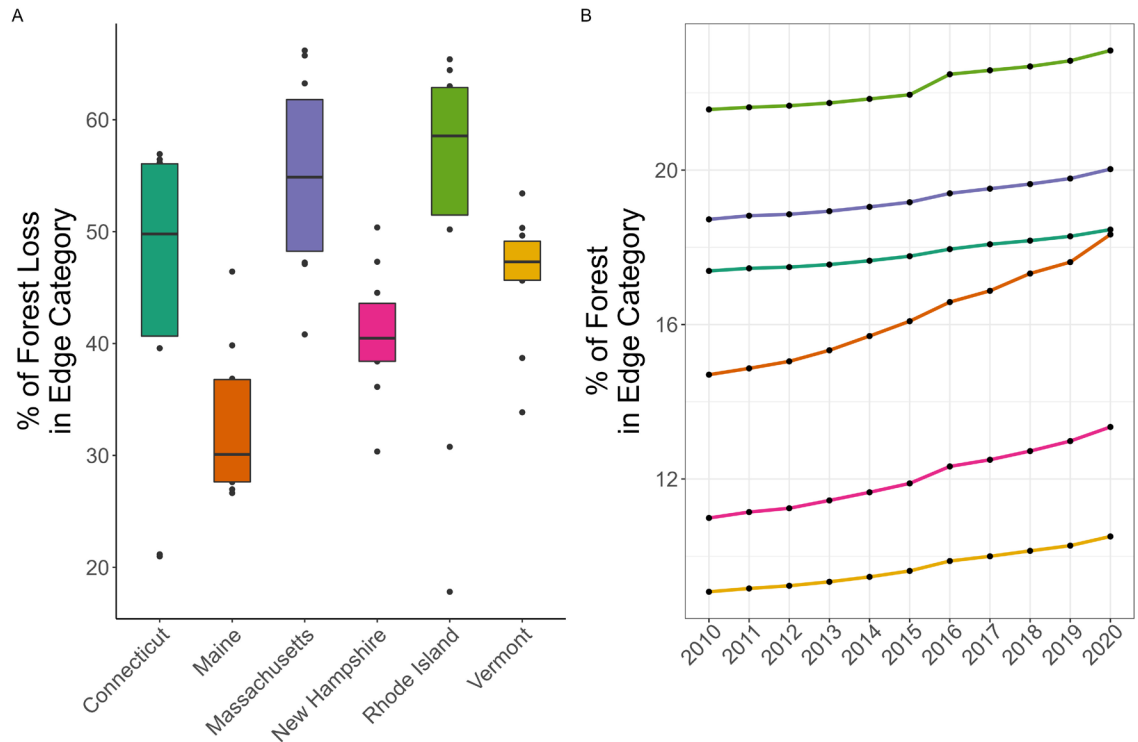


Figure 4.4. Percent (%) of annual forest loss and forest area in forest edge category.

A) Relative amount of forest loss from forest edge category in each state. Boxplots display distributions of annual % forest loss for each change year from 2010 to 2020; midline indicates median value, lower and upper hinges represent the 25th and 75th percentiles, respectively. B) Percentage (%) of forest categorized as edge in each state from 2010 to 2020.

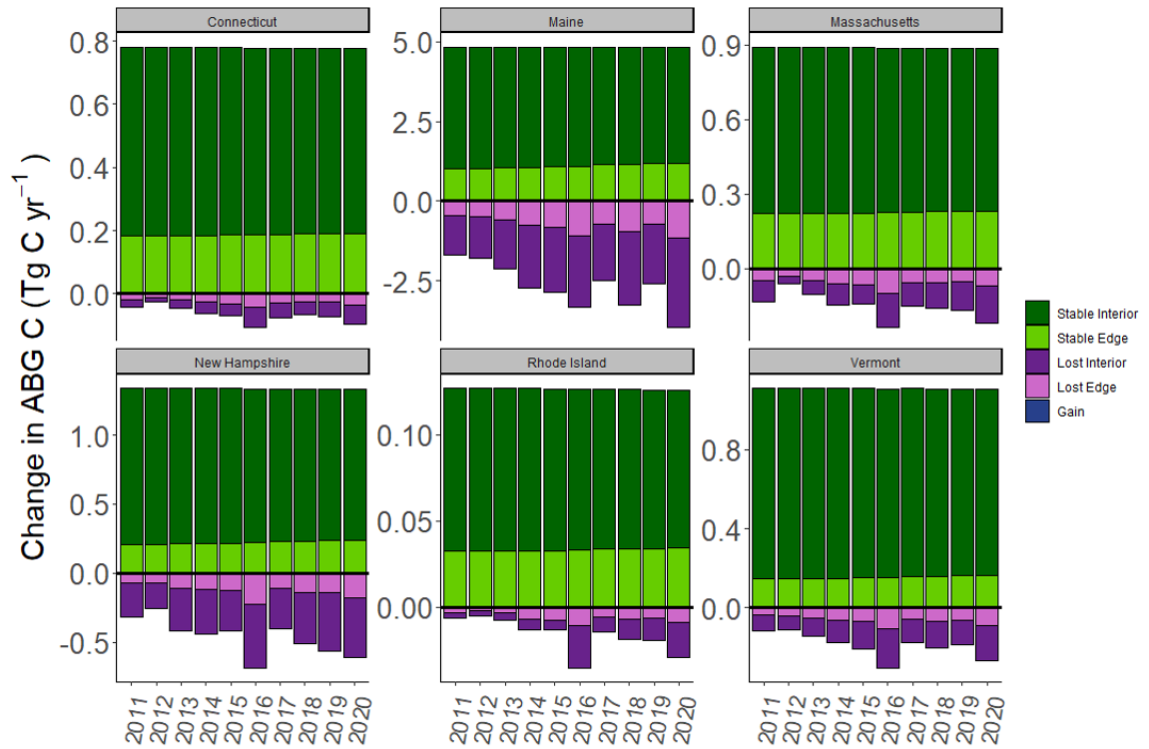


Figure 4.5. C fluxes across our study region from 2010 to 2020.

Total annual change in aboveground C by state. Stable interior forest is shown in dark green and stable edge forest in light green, while lost interior forest is shown in dark purple and lost edge forest in light purple. Forest gain is in blue.

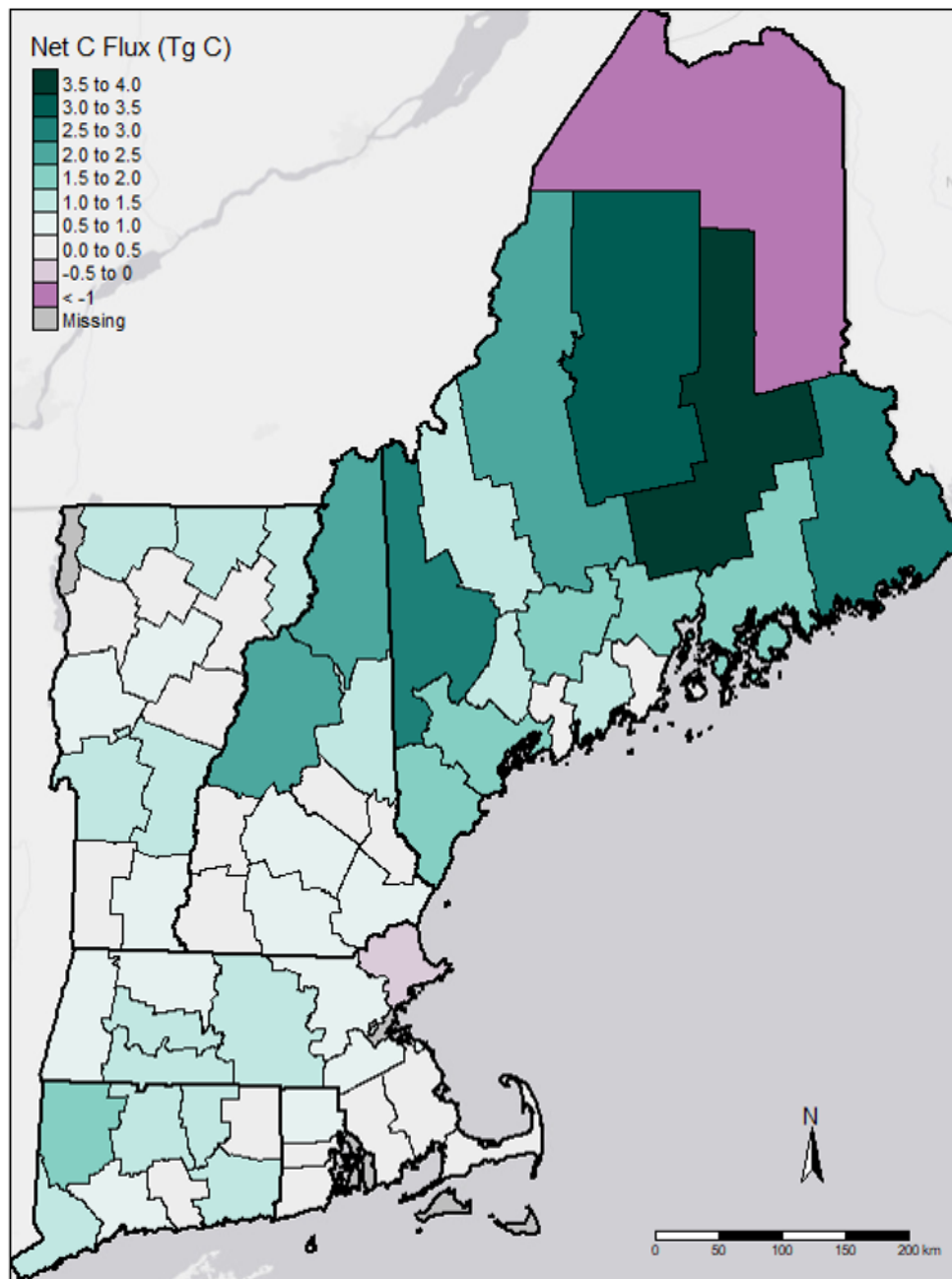


Figure 4.6. Net C flux by county from 2010 to 2020.

Color indicates net aboveground C flux within each county, where teal reflects net C gain and purple reflects C loss. Counties with insufficient forest inventory data are shown in grey.

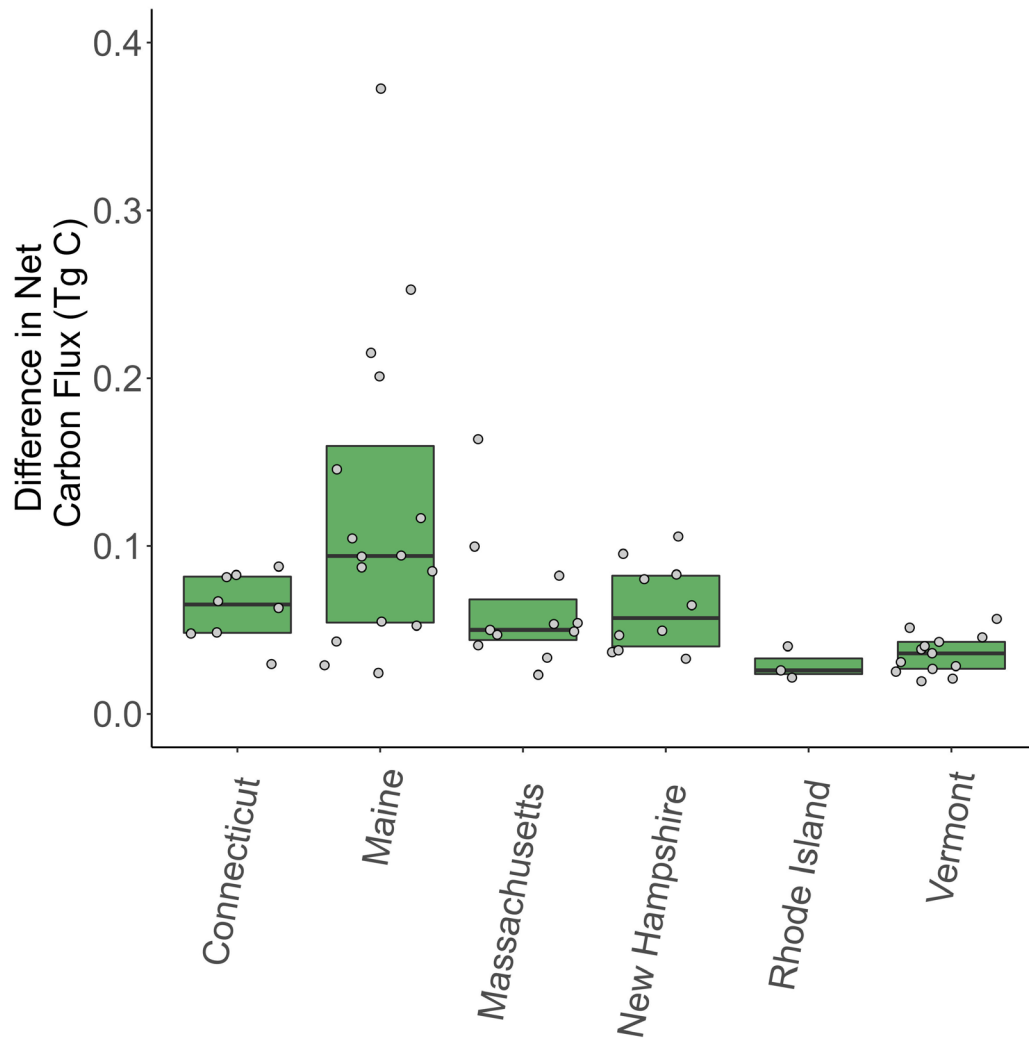


Figure 4.7. Difference in estimates of net C flux for each county when accounting for forest edges.

Y-axis displays the difference in county-level C flux estimates from a carbon accounting including forest edge and interior delineation as compared to accounting without enhanced forest edge growth. Boxplots represent the distribution of county-level differences in C flux estimates within each state from 2010 to 2020. Points indicate individual counties, midline reflects the median, lower and upper hinges represent the 25th and 75th percentiles, respectively.

CHAPTER FIVE: CONCLUSIONS

Fragmented forests are the new reality of forest ecosystems in the Anthropocene, and their prevalence is likely to increase in coming decades (Fischer et al., 2021; Seto et al., 2012). Despite the ubiquity of fragmentation, forest edges are excluded from greenhouse gas accounting and LULCC impact assessments. Furthermore, the consequences of edge exposure on forest processes in temperate forests, which comprise the largest component of the global forest C sink, remain largely unknown. In my second dissertation chapter, I explored differences in forest edge and interior growth and biomass across a 20 state region in the northeastern US (Morreale et al., 2021). I found that temperate forest edges have higher stem density, grow faster and have greater biomass than interior forests, with the greatest increases occurring along anthropogenic edges. I further found no difference in tree mortality between forest edge and interior. Critically, I report that temperate forests are more fragmented than tropical forests on a percent basis and in total area of edge forest. These results are in stark contrast to previous findings from tropical forest edges and add complexity to the understanding of fragmentation effects on forest ecosystems.

Importantly however, we have not yet elucidated the mechanism(s) behind differential responses at the forest edge between tropical and temperate forests. I hypothesize that due to decreased water limitation and cooler climates in temperate compared to tropical regions, increased aridity and temperatures associated with the forest edge do not currently pose the same danger in temperate as tropical forests. Increased light availability at the edge without increased mortality risk likely functions to

release temperate edge forests from their primary growth constraint (Nemani et al., 2003), resulting in observed increases in NPP. I additionally hypothesize that differences in land-use history may account for some portion of observed differences between temperate and tropical edge dynamics. Temperate forests are largely secondary forests that have regrown into an extant matrix of human land covers, resulting in forest edges that have persisted for long periods of time. In contrast, active deforestation in tropical forest ecosystems divides intact forests, exposing formerly interior forest to novel edge conditions. Differences in modes of edge creation and durations of edge persistence could result in specific adaptations to distinct edge environments (*e.g.*, altered rooting behavior or tree growth forms).

Our modern understanding of forest ecosystems over large regions relies upon forest inventories and remotely-sensed forest maps. In using these approaches to characterize forest area and processes in forest models and C accounting, we assume that they accurately represent forest landscapes. However, the majority of such approaches do not explicitly account for forest edges, making it imperative to determine if edges are implicitly included in forest assessments. In the third chapter of my dissertation, I compared forest maps of varying spatial resolutions and the US NFI to very high resolution forest maps and demonstrated that forest edges are systematically excluded from all traditional methods. I found that conventional forest maps and inventories underestimate both the relative proportion and total area of edge forest. I concluded that fragmentation patterns and effects are not implicitly accounted for in current assessments of temperate forests. While we previously lacked the ability to measure forest edges at

very high resolutions across large regions, this is no longer the case. Advances in our ability to quantify forest edge area and characterize edge-to-interior gradients in forest function make it imperative that we update forest assessments to account for edges.

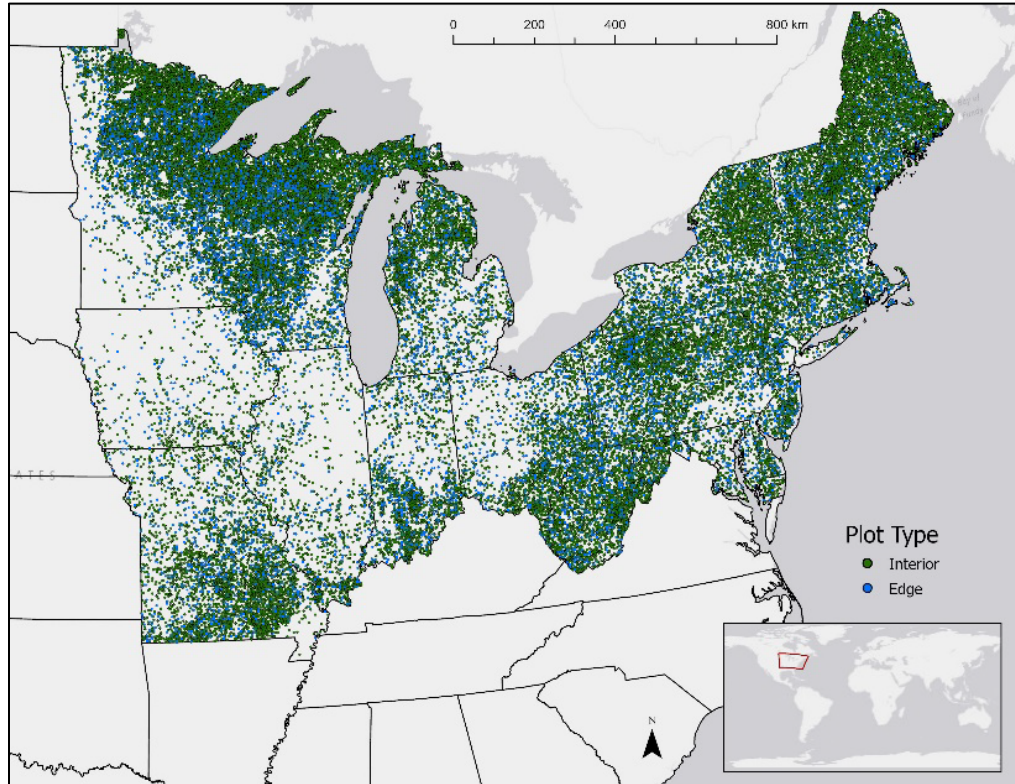
In my fourth and final research chapter, I conducted a novel temperate forest C analysis that quantifies the role of forest edges in aboveground C cycling in New England. I found that edge forests constitute > 21% of C uptake from forest growth and nearly 30% of C emissions from forest conversion. I further demonstrate that forest fragmentation is increasing and that forest edges are disproportionately subjected to land-cover conversion relative to their prevalence on the landscape. The inclusion of edge-specific forest C growth rates ultimately resulted in an 8.6% increase in estimates of the net forest C sink in our study area. This analysis underscores the need to explicitly account for forest edges in forest C assessments and provides a potential path forward.

Collectively, my dissertation research demonstrates that temperate forest edges are distinct from both their interior counterparts and tropical forests edges. I further assert that edges are an integral part of the modern temperate forest landscape that must be better understood. Future research must elucidate the mechanisms behind variability in the structure and function of forest edges globally. We need to improve understandings of edge forest vulnerability to drought and rising temperatures from climate change. Future planetary warming may induce mortality along temperate forest edges, which could trigger these forests to transition from a net C sink to a net C source due to the outsized role of edges in the temperate forest C sink.

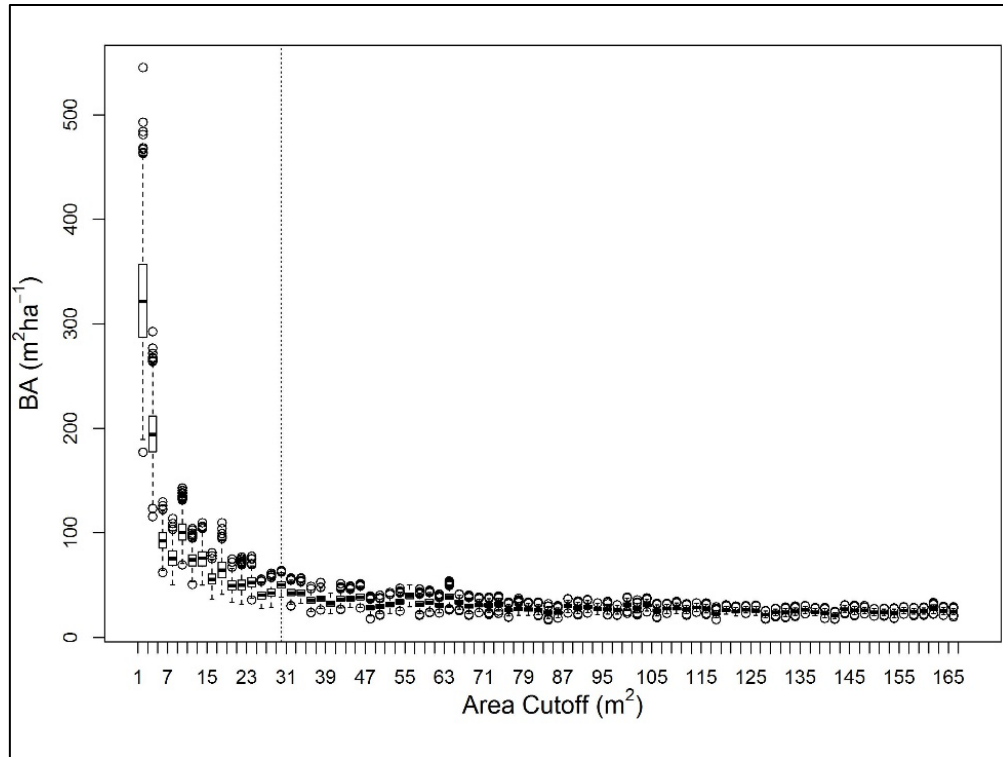
It is also critical to investigate the long-term dynamics of persistent forest edges with regards to forest succession, species composition and biogeochemical cycling. Biophysical gradients associated with edges are often perceived as sustained disturbances to the natural state of interior forests. However, my dissertation reinforces the conception of persistent temperate forest edges as their own ecotone, or even ecosystem, rather than an ephemeral perturbation. Moreover, across sufficiently-long time scales, differential selection of species-specific traits may result in diverging community composition between forest edges and the interior.

Finally, the simplistic perception of forest fragments and forest edges as degraded remnants must be updated. Millennia of human land-use have resulted in persistent alterations to the physical and ecological characteristics of ecosystems at the forest-non-forest interface. Forest edge area continues to grow alongside rising human populations, expanding anthropogenic land use, and ongoing deforestation. Modern temperate forests exist as a mosaic of fragments, distinct from pre-Anthropocene patterns of sprawling, intact forest ecosystems. Through my dissertation I demonstrate that we now have both the tools and the knowledge to conceptualize forest edges as variable, complex ecosystems. It incumbent upon us to understand the forests that we have, not the forests that we imagine.

APPENDIX A: SUPPLEMENTARY FIGURES

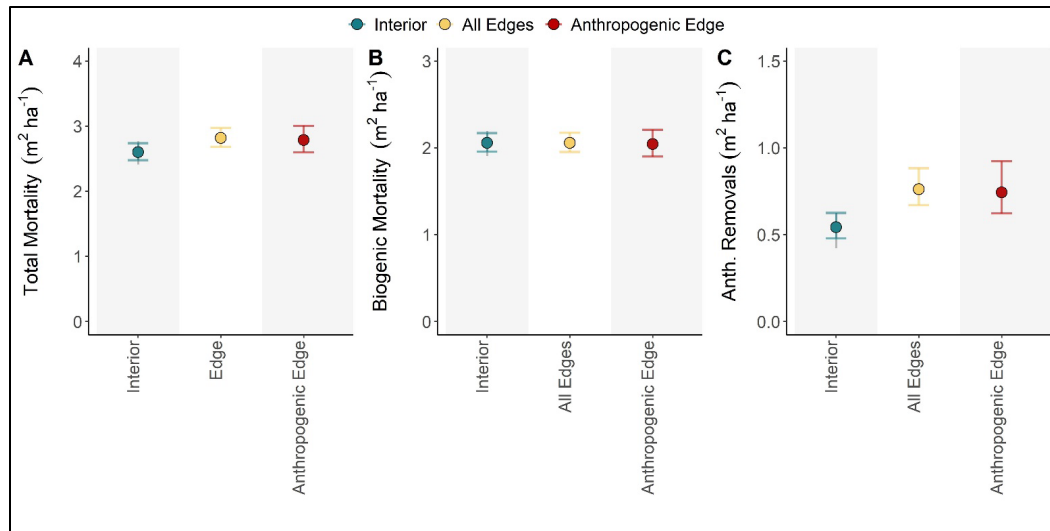


Supplementary Figure 2.1. Study region and approximate locations of edge and interior FIA plots.



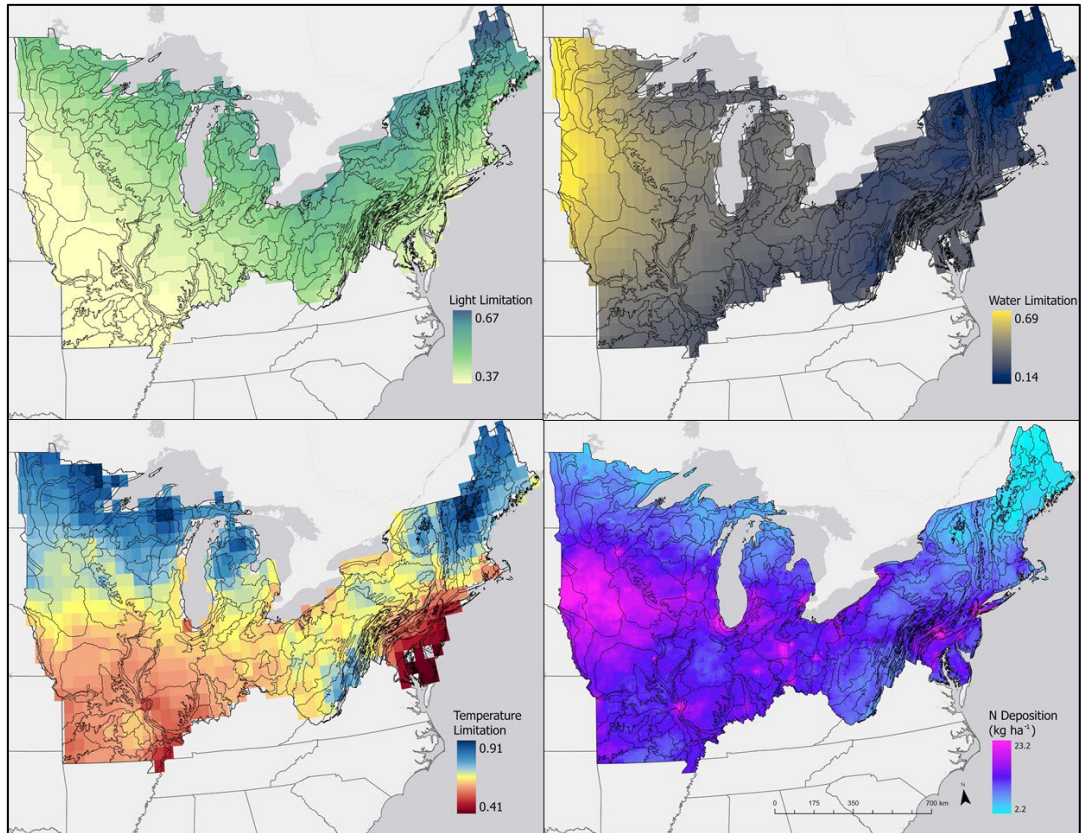
Supplementary Figure 2.1. Sensitivity of basal area estimates to subplot area.

FIA plots with an area of <30m² (vertical line) were excluded from this analysis due to small area biases. $n = 10583$ forest subplots were used for this sensitivity analysis. Boxplots indicate median (center line), 25th and 75th percentile (box) 5th and 95th percentile (whiskers), and outliers (individual points).



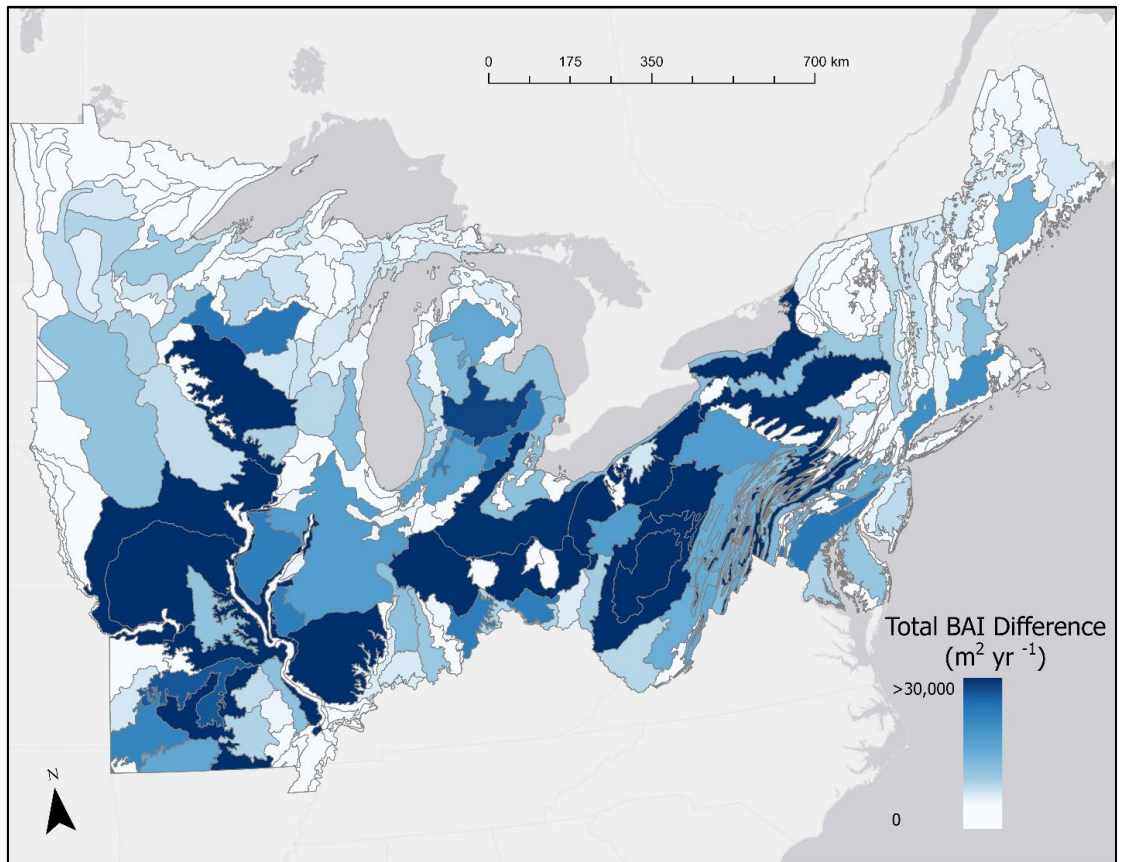
Supplementary Figure 2.3. Mortality differences between edge, interior, and anthropogenic edges.

(A) Combined biogenic mortality and anthropogenic removals. (B) Mortality from biogenic causes, measured in BA of dead trees that remained on the subplot. (C) Mortality from anthropogenic cutting, measured in BA of trees that were cut and removed from the subplot. Error bars show 95% confidence intervals on mean marginal effects. Interior and All Edge groups have $n = 6607$ independent subplots, Anthropogenic Edges have $n = 4327$ independent subplots.

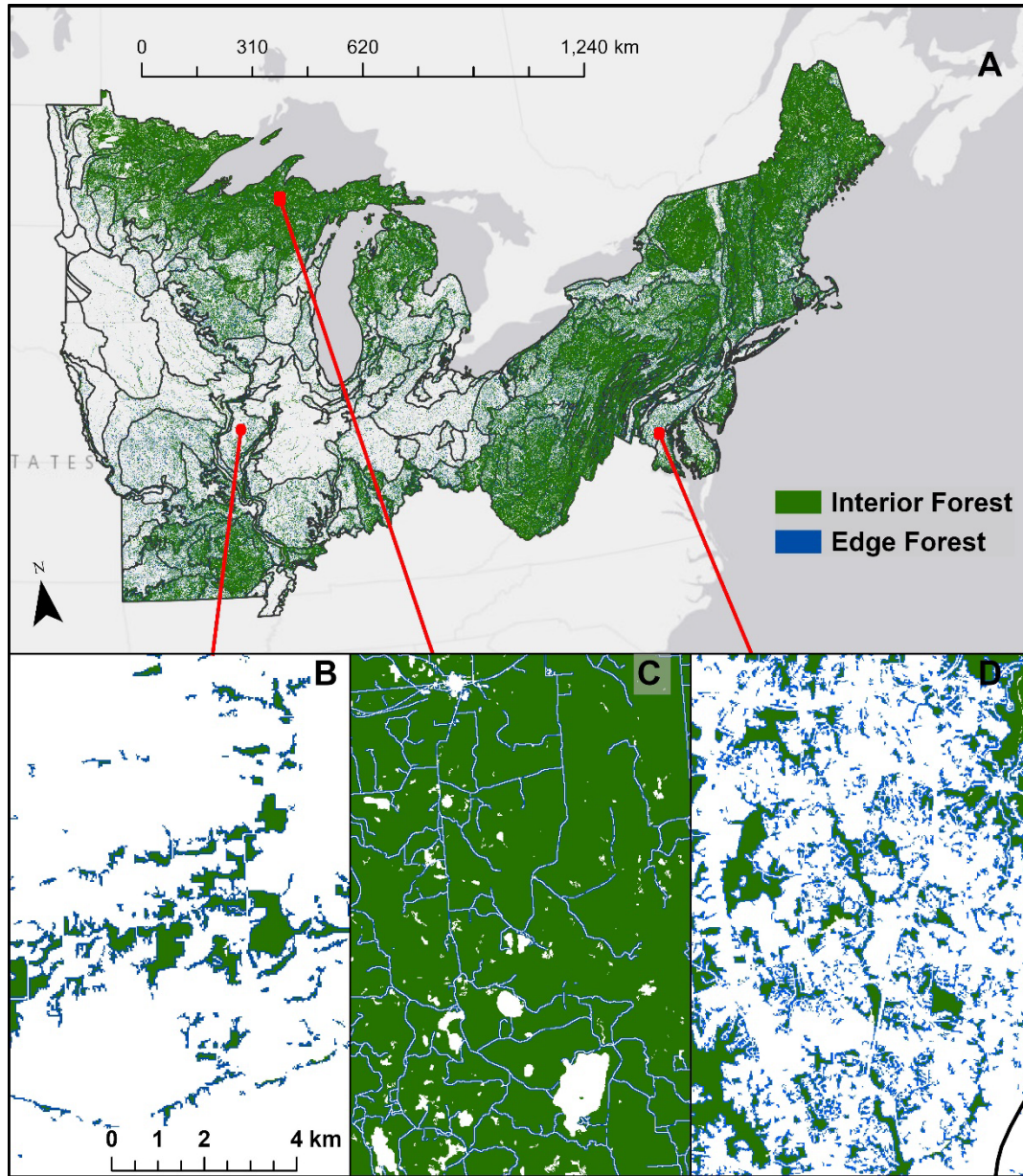


Supplementary Figure 2.4. Gridded abiotic predictors of forest productivity.

(A) Light limitation on vegetation productivity, unit-index ranging from 0 to 1⁶. (B) Water limitation on vegetation productivity, unit-index ranging from 0 to 1⁶. (C) Temperature limitation on vegetation productivity, unit-index ranging from 0 to 1⁶. (D) Atmospheric nitrogen deposition in 2018, kg ha⁻¹⁷.

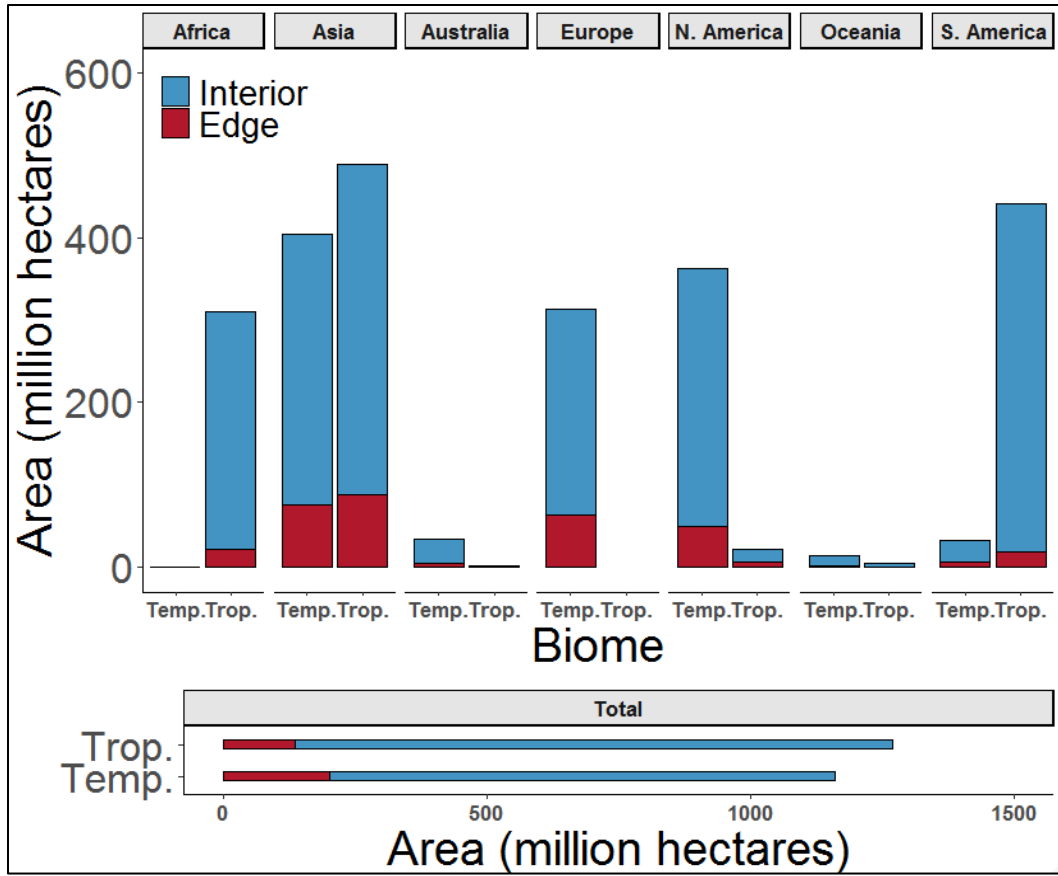


Supplementary Figure 2.5. Increases in total ecoregion BAI ($\text{m}^2 \text{yr}^{-1}$) associated with elevated growth at the forest edge.
BAI difference was calculated from individual ecoregion forest composition and forest edge area.

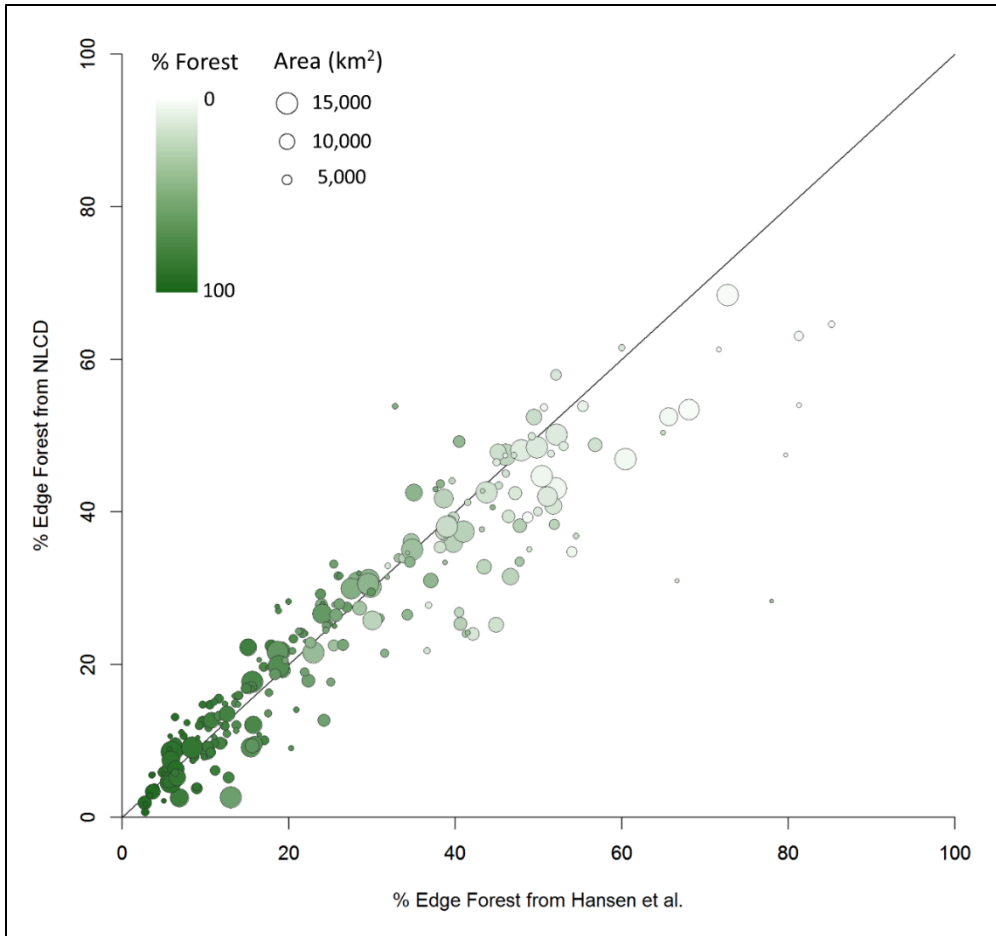


Supplementary Figure 2.6. Edge and interior forest cover designated from the 2016 National Land Cover Database

(A) Edge and interior forest cover designated from the 2016 National Land Cover Database ²⁵. (B) Agricultural areas have a high proportion of edge forest (Illinois). (C) The northern areas in our study region have the smallest amount of fragmentation (Michigan). (D) The metropolitan east coast is both heavily fragmented and moderately forested (Maryland). EPA Level IV ecoregion boundaries are shown in black.

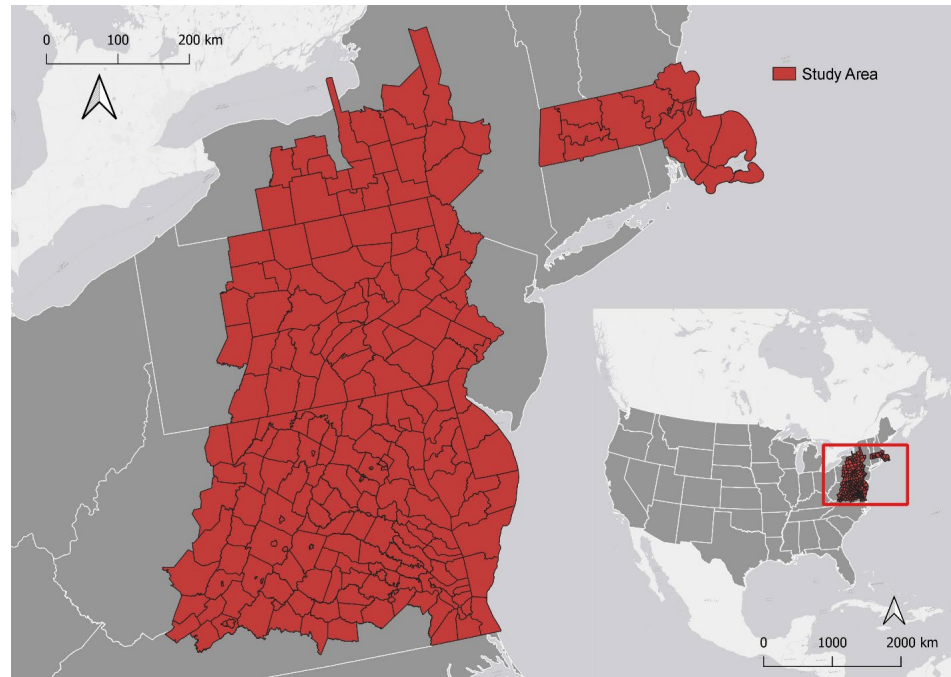


Supplementary Figure 2.7. Results from the robustness test of % forest cover threshold for estimates of temperate and tropical fragmentation using a 30% forest cover minimum definition of forest.

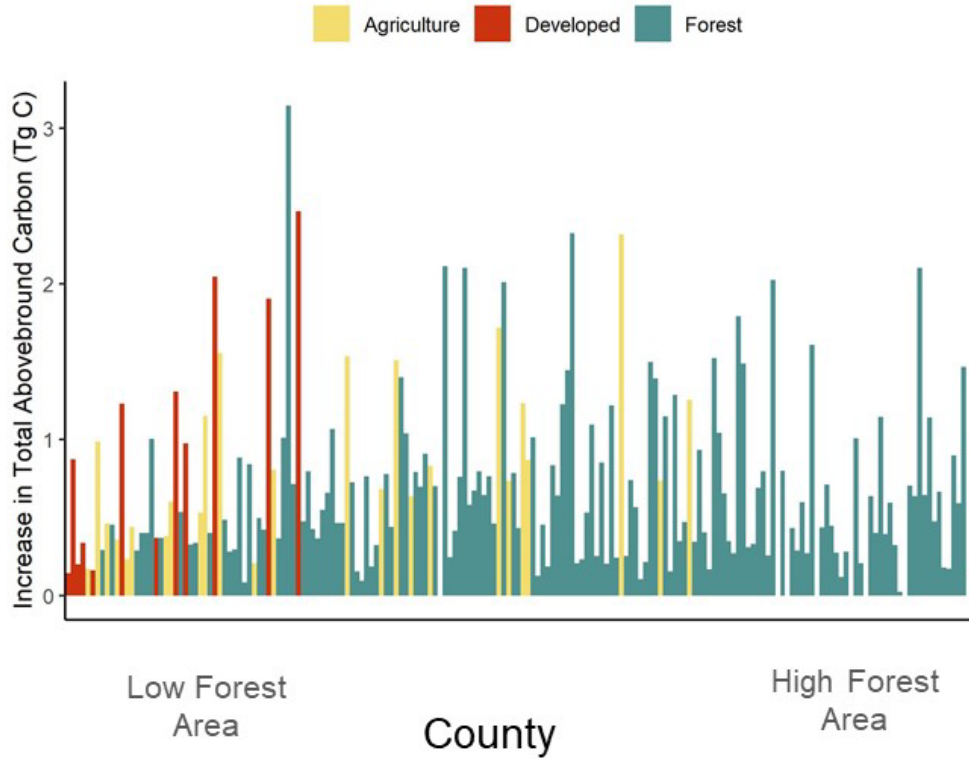


Supplementary Figure 2.8. Percent edge forest of 247 ecoregions located in the Northeast US derived from Hansen Global Forest Change (v1.7) 16 dataset versus from NLCD land cover map 13.

Size of the points corresponds to the size of the ecoregions, color of the points corresponds to percent forest cover within each ecoregion.

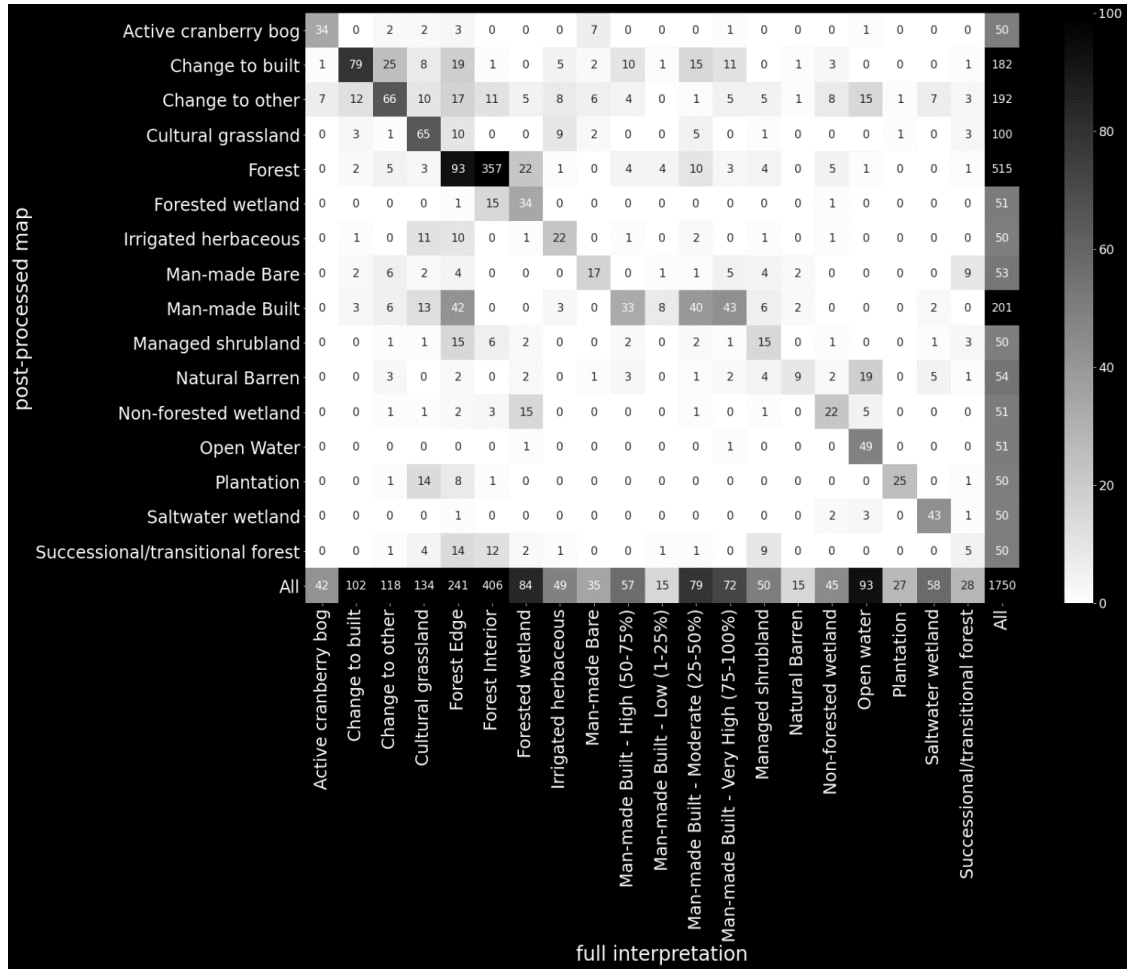


Supplementary Figure 3.1. Study area (in red) spanning the Chesapeake Bay Watershed and the Commonwealth of Massachusetts in the northeastern United States.



Supplementary Figure 3.2. The increase per county in total aboveground carbon across the Chesapeake Watershed portion of our analysis.

Counties are colored by the dominant land cover in the county (forest, agriculture, or development) and counties are ordered from lowest forest area to highest forest area. In four counties, the 1 m maps have smaller total forest area, resulting in slight negative differences in total aboveground carbon; these counties are not displayed in the figures for visual simplicity.



Supplementary Figure 3.3. Accuracy assessment of Mass Audubon’s Losing Ground 6 land cover product.

Mapped land cover classes shown on the vertical axis and human-interpreted classes (including forest edge) on the horizontal axis.

APPENDIX B: SUPPLEMENTARY TABLES**Supplementary Table 2.1. Definition of forest type groups with sample size used in final analyses.**

| Forest Type Name | FIA Forest Type Codes | N - All Edges | N -Anthropogenic Edges |
|--------------------------|------------------------------|----------------------|-------------------------------|
| Northern Pines - Hemlock | 100 - 105 | 491 | 247 |
| Spruce - Fir | 120 - 129 | 402 | 98 |
| Southern Conifers | 140 - 391 | 123 | 75 |
| Oak - Pine | 400 - 409 | 248 | 156 |
| Oak - Hickory | 500 - 520 | 2551 | 1831 |
| Bottomland Forests | 600 - 709 | 693 | 329 |
| Northern Hardwood | 800 - 809 | 1229 | 773 |
| Aspen - Birch | 900 - 905 | 776 | 305 |

Supplementary Table 2.2. Model forms and fits from GLMs with BA and BAI as response variables.

dAIC is the difference in AIC relative to the best model within each model set. Pseudo R^2 = Nagelkerke pseudo R^2 , a goodness of fit metric calculated from model likelihood. Resid. Dev = Residual deviance, a generalization of residual sum of squares. Resid. Df = Residual degrees of freedom used in the calculation of residual deviance.

| | Response Var. | Model Form | Pseudo R^2 | Resid. Dev | Resid. DF | AIC | dAIC |
|---------------|---------------|--|--------------|--------------------|--------------|----------------------|------------|
| All Edges | | | | | | | |
| | BA | EdgeType * ForestType + Light + Water + Temperature + N.Dep | 0.069 | 697 1.6 | 13652 | 1092 73.2 | 0.0 |
| | BA | EdgeType * ForestType + Water | 0.067 | 698 6.6 | 13655 | 1092 99.0 | 25. 7 |
| | BA | EdgeType * ForestType + Temperature | 0.060 | 703 4.7 | 13655 | 1094 00.8 | 12 7.5 |
| | BA | EdgeType * ForestType + Light | 0.057 | 705 4.0 | 13655 | 1094 41.2 | 16 7.9 |
| | BA | EdgeType + ForestType | 0.055 | 706 5.9 | 13664 | 1094 48.3 | 17 5.1 |
| | BA | EdgeType * ForestType + N.Dep | 0.056 | 706 0.5 | 13655 | 1094 54.9 | 18 1.7 |
| | BA | EdgeType * ForestType | 0.056 | 706 2.0 | 13656 | 1094 56.0 | 18 2.8 |
| | BA | ForestType | 0.047 | 712 3.3 | 13665 | 1095 66.2 | 29 3.0 |
| | BA | EdgeType | 0.008 | 738 6.7 | 13672 | 1100 91.4 | 81 8.2 |
| Anthro. Edges | | | | | | | |
| | BA | EdgeType * ForestType + Light + Water + Temperature + N.Dep | 0.059 | 401 5.5 | 8088 | 6563 7.3 | 0.0 |
| | BA | EdgeType * ForestType + Water | 0.058 | 402 2.8 | 8091 | 6564 7.2 | 10. 0 |
| | BA | EdgeType * ForestType + Temperature | 0.053 | 404 1.7 | 8091 | 6568 8.3 | 51. 1 |
| | BA | EdgeType * ForestType + Light | 0.051 | 404 6.8 | 8091 | 6569 9.4 | 62. 1 |
| | BA | EdgeType + ForestType | 0.049 | 405 6.0 | 8100 | 6570 1.2 | 64. 0 |
| | BA | EdgeType * ForestType + N.Dep | 0.051 | 404 9.8 | 8091 | 6570 5.9 | 68. 6 |
| | BA | EdgeType * ForestType | 0.050 | 405 1.2 | 8092 | 6570 6.8 | 69. 6 |
| | BA | ForestType | 0.031 | 412 8.3 | 8101 | 6585 4.4 | 21 7.2 |

| | | | | | | | |
|---------------|------------|--|--------------|--------------------|--------------|--------------------|------------|
| | BA | EdgeType | 0.019 | 417 5.1 | 8108 | 6593 9.3 | 30 2.1 |
| All Edges | | | | | | | |
| | BAI | EdgeType * ForestType + Light + Water + Temperature + N.Dep | 0.153 | 697 7.2 | 13652 | 7718 .4 | 0.0 |
| | BAI | EdgeType * ForestType + Temperature | 0.122 | 707 5.9 | 13655 | 7920 .5 | 20 2.1 |
| | BAI | EdgeType * ForestType + Water | 0.121 | 708 2.0 | 13655 | 7933 .1 | 21 4.7 |
| | BAI | EdgeType * ForestType + N.Dep | 0.118 | 709 1.1 | 13655 | 7952 .3 | 23 4.0 |
| | BAI | EdgeType * ForestType + Light | 0.107 | 712 6.9 | 13655 | 8027 .0 | 30 8.6 |
| | BAI | EdgeType * ForestType | 0.106 | 712 9.9 | 13656 | 8031 .1 | 31 2.7 |
| | BAI | EdgeType + ForestType | 0.102 | 714 2.4 | 13664 | 8041 .2 | 32 2.8 |
| | BAI | ForestType | 0.053 | 730 1.4 | 13665 | 8366 .1 | 64 7.7 |
| | BAI | EdgeType | 0.049 | 731 3.1 | 13672 | 8375 .9 | 65 7.6 |
| Anthro. Edges | | | | | | | |
| | BAI | EdgeType * ForestType + Light + Water + Temperature + N.Dep | 0.149 | 379 2.7 | 8088 | 5409 .1 | 0.0 |
| | BAI | EdgeType * ForestType + N.Dep | 0.131 | 382 7.5 | 8091 | 5483 .0 | 74. 0 |
| | BAI | EdgeType * ForestType + Temperature | 0.130 | 383 0.6 | 8091 | 5490 .0 | 80. 9 |
| | BAI | EdgeType * ForestType + Water | 0.128 | 383 3.4 | 8091 | 5496 .4 | 87. 3 |
| | BAI | EdgeType * ForestType + Light | 0.126 | 383 8.0 | 8091 | 5506 .9 | 97. 8 |
| | BAI | EdgeType * ForestType | 0.124 | 384 1.7 | 8092 | 5513 .2 | 10 4.1 |
| | BAI | EdgeType + ForestType | 0.118 | 385 3.5 | 8100 | 5524 .1 | 11 5.0 |
| | BAI | EdgeType | 0.098 | 389 4.8 | 8108 | 5601 .2 | 19 2.2 |
| | BAI | ForestType | 0.022 | 404 6.1 | 8101 | 5949 .1 | 54 0.0 |

Supplementary Table 2.3. Predicted mean marginal effects for each forest type and edge group.

Upper and lower 95% confidence intervals in parentheses. Marginal effects were calculated with other predictors held at their within-forest type means. All reported values are in the units of BAI and BA ($\text{m}^2 \text{ha}^{-1} \text{yr}^{-1}$ and $\text{m}^2 \text{ha}^{-1}$, respectively).

| Unit | Forest Type | Edge Type | Predicted |
|------|--------------------------|--------------------|---------------------|
| BAI | All Forests | Interior | 0.51 (0.5-0.51) |
| BAI | All Forests | Edge | 0.63 (0.62-0.64) |
| BAI | All Forests | Anthropogenic Edge | 0.71 (0.7-0.72) |
| BAI | Aspen - Birch | All Edges | 0.5 (0.48-0.53) |
| BAI | Aspen - Birch | Interior | 0.46 (0.44-0.48) |
| BAI | Aspen - Birch | Anthropogenic Edge | 0.62 (0.58-0.66) |
| BAI | Bottomland Forests | All Edges | 0.62 (0.59-0.65) |
| BAI | Bottomland Forests | Interior | 0.52 (0.49-0.54) |
| BAI | Bottomland Forests | Anthropogenic Edge | 0.7 (0.66-0.75) |
| BAI | Northern Hardwood | All Edges | 0.64 (0.61-0.66) |
| BAI | Northern Hardwood | Interior | 0.52 (0.5-0.53) |
| BAI | Northern Hardwood | Anthropogenic Edge | 0.69 (0.66-0.72) |
| BAI | Northern Pines - Hemlock | All Edges | 0.72 (0.68-0.76) |
| BAI | Northern Pines - Hemlock | Interior | 0.62 (0.59-0.65) |
| BAI | Northern Pines - Hemlock | Anthropogenic Edge | 0.78 (0.73-0.84) |
| BAI | Oak - Hickory | All Edges | 0.65 (0.64-0.67) |
| BAI | Oak - Hickory | Interior | 0.5 (0.49-0.51) |
| BAI | Oak - Hickory | Anthropogenic Edge | 0.7 (0.68-0.72) |
| BAI | Oak - Pine | All Edges | 0.7 (0.65-0.76) |
| BAI | Oak - Pine | Interior | 0.53 (0.49-0.57) |
| BAI | Oak - Pine | Anthropogenic Edge | 0.77 (0.71-0.85) |
| BAI | Southern Conifers | All Edges | 0.66 (0.59-0.74) |
| BAI | Southern Conifers | Interior | 0.55 (0.5-0.62) |
| BAI | Southern Conifers | Anthropogenic Edge | 0.67 (0.59-0.77) |
| BAI | Spruce - Fir | All Edges | 0.44 (0.42-0.47) |
| BAI | Spruce - Fir | Interior | 0.37 (0.35-0.4) |
| BAI | Spruce - Fir | Anthropogenic Edge | 0.6 (0.54-0.68) |
| BA | All Forests | Interior | 21.69 (21.35-22.05) |
| BA | All Forests | Edge | 24.71 (24.3-25.13) |
| BA | All Forests | Anthropogenic Edge | 26.93 (26.37-27.51) |
| BA | Aspen - Birch | Edge | 16.86 (16.1-17.7) |
| BA | Aspen - Birch | Interior | 16.02 (15.31-16.8) |

| | | | |
|----|--------------------------|--------------------|---------------------|
| BA | Aspen - Birch | Anthropogenic Edge | 19.75 (18.41-21.31) |
| BA | Bottomland Forests | Edge | 22.56 (21.49-23.74) |
| BA | Bottomland Forests | Interior | 20.1 (19.18-21.11) |
| BA | Bottomland Forests | Anthropogenic Edge | 23.14 (21.62-24.89) |
| BA | Northern Hardwood | Edge | 26.95 (25.98-28) |
| BA | Northern Hardwood | Interior | 23.27 (22.46-24.14) |
| BA | Northern Hardwood | Anthropogenic Edge | 27.97 (26.74-29.32) |
| BA | Northern Pines - Hemlock | Edge | 31.8 (30.04-33.77) |
| BA | Northern Pines - Hemlock | Interior | 27.64 (26.14-29.34) |
| BA | Northern Pines - Hemlock | Anthropogenic Edge | 34.29 (31.74-37.29) |
| BA | Oak - Hickory | Edge | 25.69 (25.04-26.37) |
| BA | Oak - Hickory | Interior | 22.08 (21.54-22.65) |
| BA | Oak - Hickory | Anthropogenic Edge | 26.67 (25.89-27.5) |
| BA | Oak - Pine | Edge | 26.69 (24.64-29.1) |
| BA | Oak - Pine | Interior | 22.54 (20.83-24.55) |
| BA | Oak - Pine | Anthropogenic Edge | 29.38 (26.67-32.71) |
| BA | Southern Conifers | Edge | 25.65 (22.94-29.09) |
| BA | Southern Conifers | Interior | 21.93 (19.75-24.65) |
| BA | Southern Conifers | Anthropogenic Edge | 25.94 (22.58-30.48) |
| BA | Spruce - Fir | Edge | 19.14 (17.97-20.47) |
| BA | Spruce - Fir | Interior | 19.11 (17.96-20.41) |
| BA | Spruce - Fir | Anthropogenic Edge | 22.35 (19.87-25.55) |

Supplementary Table 2.4. Pre- and post-matching covariate distributions for all edges.

Mean Edge and Mean Control show the average value of each predictor within Edge and Interior groups, respectively, before and after the matching process. Std. mean difference shows the difference in means.

| Continuous Variables | | Mean Edge | Mean Control | SD Control | Std mean difference | eCDF Median | eCDF Mean | eCDF max |
|--|--------|-----------|--------------|------------|---------------------|-------------|-----------|----------|
| N. Deposition (kg ha-1) | Before | 9.08 | 8.15 | 2.58 | 0.37 | 0.12 | 0.10 | 0.13 |
| | After | 9.08 | 9.06 | 2.49 | 0.01 | 0.00 | 0.00 | 0.01 |
| Light | Before | 0.47 | 0.49 | 0.06 | -0.28 | 0.03 | 0.05 | 0.12 |
| | After | 0.47 | 0.47 | 0.05 | 0.00 | 0.00 | 0.00 | 0.00 |
| Water | Before | 0.38 | 0.35 | 0.11 | 0.30 | 0.05 | 0.05 | 0.12 |
| | After | 0.38 | 0.38 | 0.10 | 0.00 | 0.00 | 0.00 | 0.00 |
| Temperature | Before | 0.68 | 0.70 | 0.09 | -0.21 | 0.02 | 0.04 | 0.10 |
| | After | 0.68 | 0.68 | 0.09 | 0.00 | 0.00 | 0.00 | 0.00 |
| Forest Types | | | | | | | | |
| Northern Hardwood | Before | 0.18 | 0.27 | 0.45 | -0.23 | 0.04 | 0.04 | 0.09 |
| | After | 0.18 | 0.18 | 0.39 | 0.00 | 0.00 | 0.00 | 0.00 |
| Northern Pines - Hemlock | Before | 0.07 | 0.06 | 0.23 | 0.04 | 0.01 | 0.01 | 0.01 |
| | After | 0.07 | 0.07 | 0.25 | 0.00 | 0.00 | 0.00 | 0.00 |
| Oak - Hickory | Before | 0.39 | 0.33 | 0.47 | 0.12 | 0.03 | 0.03 | 0.06 |
| | After | 0.39 | 0.39 | 0.49 | 0.00 | 0.00 | 0.00 | 0.00 |
| Oak - Pine | Before | 0.04 | 0.03 | 0.18 | 0.01 | 0.00 | 0.00 | 0.00 |
| | After | 0.04 | 0.04 | 0.19 | 0.00 | 0.00 | 0.00 | 0.00 |
| Southern Pines - Other Conifers | Before | 0.02 | 0.02 | 0.13 | 0.04 | 0.00 | 0.00 | 0.01 |
| | After | 0.02 | 0.02 | 0.14 | 0.00 | 0.00 | 0.00 | 0.00 |
| Spruce - Fir | Before | 0.06 | 0.11 | 0.31 | -0.21 | 0.02 | 0.02 | 0.05 |
| | After | 0.06 | 0.06 | 0.23 | 0.00 | 0.00 | 0.00 | 0.00 |
| Bottomland Forests | Before | 0.11 | 0.07 | 0.25 | 0.14 | 0.02 | 0.02 | 0.04 |
| | After | 0.11 | 0.11 | 0.31 | 0.00 | 0.00 | 0.00 | 0.00 |

Supplementary Table 2.5. Pre- and post-matching covariate distributions for anthropogenic edges.

Mean Edge and Mean Control show the average value of each predictor within Edge and Interior groups, respectively, before and after the matching process. Std. mean difference shows the difference in means.

| Continuous Variables | | Mean Edge | Mean Control | SD Control | Std mean difference | eCDF Median | eCDF Mean | eCDF max |
|--|--------|-----------|--------------|------------|---------------------|-------------|-----------|----------|
| N. Deposition (kg ha-1) | Before | 9.48 | 8.15 | 2.58 | 0.53 | 0.16 | 0.15 | 0.22 |
| | After | 9.48 | 9.47 | 2.50 | 0.01 | 0.00 | 0.00 | 0.01 |
| Light | Before | 0.47 | 0.49 | 0.06 | -0.38 | 0.04 | 0.06 | 0.16 |
| | After | 0.47 | 0.47 | 0.05 | 0.00 | 0.00 | 0.00 | 0.00 |
| Water | Before | 0.37 | 0.35 | 0.11 | 0.20 | 0.03 | 0.03 | 0.10 |
| | After | 0.37 | 0.37 | 0.10 | 0.00 | 0.00 | 0.00 | 0.00 |
| Temperature | Before | 0.66 | 0.70 | 0.09 | -0.49 | 0.04 | 0.08 | 0.22 |
| | After | 0.66 | 0.66 | 0.08 | -0.01 | 0.00 | 0.00 | 0.00 |
| Forest Types | | | | | | | | |
| Northern Hardwood | Before | 0.20 | 0.27 | 0.45 | -0.19 | 0.04 | 0.04 | 0.07 |
| | After | 0.20 | 0.20 | 0.40 | 0.00 | 0.00 | 0.00 | 0.00 |
| Northern Pines - Hemlock | Before | 0.06 | 0.06 | 0.23 | 0.00 | 0.00 | 0.00 | 0.00 |
| | After | 0.06 | 0.06 | 0.24 | 0.00 | 0.00 | 0.00 | 0.00 |
| Oak - Hickory | Before | 0.47 | 0.33 | 0.47 | 0.28 | 0.07 | 0.07 | 0.14 |
| | After | 0.47 | 0.47 | 0.50 | 0.00 | 0.00 | 0.00 | 0.00 |
| Oak - Pine | Before | 0.04 | 0.03 | 0.18 | 0.02 | 0.00 | 0.00 | 0.00 |
| | After | 0.04 | 0.04 | 0.19 | 0.00 | 0.00 | 0.00 | 0.00 |
| Southern Pines - Other Conifers | Before | 0.02 | 0.02 | 0.13 | 0.04 | 0.00 | 0.00 | 0.01 |
| | After | 0.02 | 0.02 | 0.15 | 0.00 | 0.00 | 0.00 | 0.00 |
| Spruce - Fir | Before | 0.02 | 0.11 | 0.31 | -0.54 | 0.04 | 0.04 | 0.08 |
| | After | 0.02 | 0.02 | 0.15 | 0.00 | 0.00 | 0.00 | 0.00 |
| Bottomland Forests | Before | 0.10 | 0.07 | 0.25 | 0.09 | 0.01 | 0.01 | 0.03 |
| | After | 0.10 | 0.10 | 0.29 | 0.00 | 0.00 | 0.00 | 0.00 |

Supplementary Table 3.1. Condensing individual land cover map legends to a simplified 3-class (Forest, Developed, Agriculture) legend for forest area intercomparison.

| Pixel Size | Product | Classes | | |
|-------------------|---------------------------------|------------------------|------------------|--------------------|
| | | <i>Forest</i> | <i>Developed</i> | <i>Agriculture</i> |
| 1 m | <i>Chesapeake Bay Watershed</i> | 3,4 | 7,8,9,10,11,12 | 5 |
| | <i>MassGIS</i> | 9,10,11,12,13,14,16,17 | 2,5 | 6,7,8 |
| 30 m | <i>LCMAP</i> | 4 | 1 | 2 |
| | <i>NLCD</i> | 41,42,43, 90 | 21, 22,23,24 | 81, 82 |
| 500 m | <i>MODIS IGBP</i> | 1,2,3,4,5 | 13 | 12 |

BIBLIOGRAPHY

- Akaike, H. (1998). *Information Theory and an Extension of the Maximum Likelihood Principle*. https://doi.org/10.1007/978-1-4612-1694-0_15
- Allen, J. A., Setälä, H., & Kotze, D. J. (2020). Dog Urine Has Acute Impacts on Soil Chemistry in Urban Greenspaces. *Frontiers in Ecology and Evolution*, 8. <https://www.frontiersin.org/articles/10.3389/fevo.2020.615979>
- Anderegg, W. R. L., Trugman, A. T., Badgley, G., Anderson, C. M., Bartuska, A., Ciais, P., Cullenward, D., Field, C. B., Freeman, J., Goetz, S. J., Hicke, J. A., Huntzinger, D., Jackson, R. B., Nickerson, J., Pacala, S., & Randerson, J. T. (2020). Climate-driven risks to the climate mitigation potential of forests. *Science*, 368(6497), eaaz7005. <https://doi.org/10.1126/science.aaz7005>
- Anderson-Teixeira, K. J., Miller, A. D., Mohan, J. E., Hudiburg, T. W., Duval, B. D., & DeLucia, E. H. (2013). Altered dynamics of forest recovery under a changing climate. *Global Change Biology*, 19(7), 2001–2021. <https://doi.org/10.1111/gcb.12194>
- Bastin, J. F., Finegold, Y., Garcia, C., Mollicone, D., Rezende, M., Routh, D., Zohner, C. M., & Crowther, T. W. (2019). The global tree restoration potential. *Science*, 364(6448), 76–79. <https://doi.org/10.1126/science.aax0848>
- Bechtold, W. A., & Patterson, P. L. (2005). The Enhanced Forest Inventory and Analysis Program—National Sampling Design and Estimation Procedures. *USDA General Technical Report, SRS-80*, 85. <https://doi.org/10.2737/SRS-GTR-80>
- Bierregaard, R. O., Lovejoy, T. E., Kapos, V., & Hutchings, R. W. (1992). The Biological Dynamics of Tropical Rainforest Fragments. *BioScience*, 42(11), 859–866. <https://doi.org/10.2307/1312085>
- Bonan, G. B. (2008). Forests and Climate Change: Forcings, Feedbacks, and the Climate Benefits of Forests. *Science*, 320(5882), 1444–1449. <https://doi.org/10.1126/science.1155121>
- Bormann, F. H., & Likens, G. E. (1979). *Pattern and Process In a Forested Ecosystem*.
- Briber, B. M., Hutyrá, L. R., Reinmann, A. B., Raciti, S. M., Dearborn, V. K., Holden, C. E., & Dunn, A. L. (2015). Tree productivity enhanced with conversion from forest to urban land covers. *PLoS ONE*, 10(8), 1–19. <https://doi.org/10.1371/journal.pone.0136237>

- Brinck, K., Fischer, R., Groeneveld, J., Lehmann, S., Dantas De Paula, M., Pütz, S., Sexton, J. O., Song, D., & Huth, A. (2017). High resolution analysis of tropical forest fragmentation and its impact on the global carbon cycle. *Nature Communications*, 8. <https://doi.org/10.1038/ncomms14855>
- Brown, J. F., Tollerud, H. J., Barber, C. P., Zhou, Q., Dwyer, J. L., Vogelmann, J. E., Loveland, T. R., Woodcock, C. E., Stehman, S. V., Zhu, Z., Pengra, B. W., Smith, K., Horton, J. A., Xian, G., Auch, R. F., Sohl, T. L., Saylor, K. L., Gallant, A. L., Zelenak, D., ... Rover, J. (2020a). Lessons learned implementing an operational continuous United States national land change monitoring capability: The Land Change Monitoring, Assessment, and Projection (LCMAP) approach. *Remote Sensing of Environment*, 238, 111356. <https://doi.org/10.1016/j.rse.2019.111356>
- Brown, J. F., Tollerud, H. J., Barber, C. P., Zhou, Q., Dwyer, J. L., Vogelmann, J. E., Loveland, T. R., Woodcock, C. E., Stehman, S. V., Zhu, Z., Pengra, B. W., Smith, K., Horton, J. A., Xian, G., Auch, R. F., Sohl, T. L., Saylor, K. L., Gallant, A. L., Zelenak, D., ... Rover, J. (2020b). Lessons learned implementing an operational continuous United States national land change monitoring capability: The Land Change Monitoring, Assessment, and Projection (LCMAP) approach. *Remote Sensing of Environment*, 238(September 2018), 111356. <https://doi.org/10.1016/j.rse.2019.111356>
- Brown, M. L., Canham, C. D., Murphy, L., & Donovan, T. M. (2018). Timber harvest as the predominant disturbance regime in northeastern U.S. forests: Effects of harvest intensification. *Ecosphere*, 9(3), e02062. <https://doi.org/10.1002/ecs2.2062>
- Bryson, G. M., & Barker, A. V. (2002). Sodium accumulation in soils and plants along Massachusetts roadsides. *Communications in Soil Science and Plant Analysis*, 33(1–2), 67–78. <https://doi.org/10.1081/CSS-120002378>
- Cadenasso, M. L., Pickett, S. T. A., Weathers, K. C., & Jones, C. G. (2003). A framework for a theory of ecological boundaries. *BioScience*, 53(8), 750–758. [https://doi.org/10.1641/0006-3568\(2003\)053\[0750:AFFATO\]2.0.CO;2](https://doi.org/10.1641/0006-3568(2003)053[0750:AFFATO]2.0.CO;2)
- Canham, C., Rogers, N., & Bucholtz, T. (2013). Regional variation in forest harvest regimes in the northeastern United States. *Ecological Applications*. <https://doi.org/10.1890/07-1650.1>
- Caron, S., Garvey, S. M., Gewirtzman, J., Schultz, K., Bhatnagar, J. M., Driscoll, C., Hutya, L. R., & Templer, P. H. (2023). Urbanization and fragmentation have opposing effects on soil nitrogen availability in temperate forest ecosystems. *Global Change Biology*, 29(8), 2156–2171. <https://doi.org/10.1111/gcb.16611>

- Chambers, J., Hastie, T., & Pregibon, D. (1990). Statistical Models in S. In *Compstat*. https://doi.org/10.1007/978-3-642-50096-1_48
- Chaplin-Kramer, R., Ramler, I., Sharp, R., Haddad, N. M., Gerber, J. S., West, P. C., Mandle, L., Engstrom, P., Baccini, A., Sim, S., Mueller, C., & King, H. (2015). Degradation in carbon stocks near tropical forest edges. *Nature Communications*, 6, 1–6. <https://doi.org/10.1038/ncomms10158>
- Chen, J., Franklin, J. F., & Spies, T. A. (1992). Vegetation Responses to Edge Environments in Old-Growth Douglas-Fir Forests. *Ecological Applications*, 2(4), 387–396. <https://doi.org/10.2307/1941873>
- Dantas de Paula, M., Groeneveld, J., & Huth, A. (2015). Tropical forest degradation and recovery in fragmented landscapes—Simulating changes in tree community, forest hydrology and carbon balance. *Global Ecology and Conservation*, 3, 664–677. <https://doi.org/10.1016/j.gecco.2015.03.004>
- Decina, S. M., Templer, P. H., Hutyrá, L. R., Gately, C. K., & Rao, P. (2017). Variability, drivers, and effects of atmospheric nitrogen inputs across an urban area: Emerging patterns among human activities, the atmosphere, and soils. *Science of the Total Environment*, 609, 1524–1534. <https://doi.org/10.1016/j.scitotenv.2017.07.166>
- Duveneck, M. J., & Thompson, J. R. (2019). Social and biophysical determinants of future forest conditions in New England: Effects of a modern land-use regime. *Global Environmental Change*, 55, 115–129. <https://doi.org/10.1016/j.gloenvcha.2019.01.009>
- Edgar, C. B., Nowak, D. J., Majewsky, M. A., Lister, T. W., Westfall, J. A., & Sonti, N. F. (2021). Strategic National Urban Forest Inventory for the United States. *Journal of Forestry*, 119(1), 86–95. <https://doi.org/10.1093/jofore/fvaa047>
- Enderlein, G. (1987). McCullagh, P., J. A. Nelder: Generalized linear models. Chapman and Hall London – New York 1983, 261 S., £ 16,-. *Biometrical Journal*, 29(2), 206–206. <https://doi.org/10.1002/bimj.4710290217>
- Erdős, L., Zalatnai, M., Morschhauser, T., Bátori, Z., & Körmöczi, L. (2011). *Erdos et al. 2011.pdf*. 55(2), 279–287.
- Esseen, P.-A., Hedström Ringvall, A., Harper, K. A., Christensen, P., & Svensson, J. (2016). Factors driving structure of natural and anthropogenic forest edges from temperate to boreal ecosystems. *Journal of Vegetation Science*, 27(3), 482–492. <https://doi.org/10.1111/jvs.12387>

- Eyre, F. H. (1980). Forest cover types. *National Atlas of the United States*.
<http://nationalatlas.gov>
- F. Dormann, C., M. McPherson, J., B. Araújo, M., Bivand, R., Bolliger, J., Carl, G., G. Davies, R., Hirzel, A., Jetz, W., Daniel Kissling, W., Kühn, I., Ohlemüller, R., R. Peres-Neto, P., Reineking, B., Schröder, B., M. Schurr, F., & Wilson, R. (2007). Methods to account for spatial autocorrelation in the analysis of species distributional data: A review. *Ecography*, *30*(5), 609–628.
<https://doi.org/10.1111/j.2007.0906-7590.05171.x>
- Fischer, R., Taubert, F., Müller, M. S., Groeneveld, J., Lehmann, S., Wiegand, T., & Huth, A. (2021). Accelerated forest fragmentation leads to critical increase in tropical forest edge area. *Science Advances*, *7*(37), eabg7012.
<https://doi.org/10.1126/sciadv.abg7012>
- Foley, J. A., DeFries, R., Asner, G. P., Barford, C., Bonan, G., Carpenter, S. R., Chapin, F. S., Coe, M. T., Daily, G. C., Gibbs, H. K., Helkowski, J. H., Holloway, T., Howard, E. A., Kucharik, C. J., Monfreda, C., Patz, J. A., Prentice, I. C., Ramankutty, N., & Snyder, P. K. (2005). Global Consequences of Land Use. *Science*, *309*(5734), 570–574. <https://doi.org/10.1126/science.1111772>
- Foster, D. R. (1992). Land-Use History (1730-1990) and Vegetation Dynamics in Central New England , USA. *Journal of Ecology*, *80*(4), 753–771.
- Franklin, C. M. A., Harper, K. A., & Clarke, M. J. (2021). Trends in studies of edge influence on vegetation at human-created and natural forest edges across time and space. *Canadian Journal of Forest Research*, *51*(2), 274–282.
<https://doi.org/10.1139/cjfr-2020-0308>
- Friedlingstein, P., O’Sullivan, M., Jones, M. W., Andrew, R. M., Gregor, L., Hauck, J., Le Quéré, C., Luijkx, I. T., Olsen, A., Peters, G. P., Peters, W., Pongratz, J., Schwingshackl, C., Sitch, S., Canadell, J. G., Ciais, P., Jackson, R. B., Alin, S. R., Alkama, R., ... Zheng, B. (2022). Global Carbon Budget 2022. *Earth System Science Data*, *14*(11), 4811–4900. <https://doi.org/10.5194/essd-14-4811-2022>
- Garvey, S. M., Templer, P. H., Pierce, E. A., Reinmann, A. B., & Hutrya, L. R. (2022). Diverging patterns at the forest edge: Soil respiration dynamics of fragmented forests in urban and rural areas. *Global Change Biology*, *28*(9), 3094–3109.
<https://doi.org/10.1111/gcb.16099>
- Gorelick, N., Hancher, M., Dixon, M., Ilyushchenko, S., Thau, D., & Moore, R. (2017). Google Earth Engine: Planetary-scale geospatial analysis for everyone. *Remote Sensing of Environment*, *202*, 18–27. <https://doi.org/10.1016/j.rse.2017.06.031>

- Graham MacLean, M., Duveneck, M. J., Plisinski, J., Morreale, L. L., Laflower, D., & Thompson, J. R. (2021). Forest carbon trajectories: Consequences of alternative land-use scenarios in New England. *Global Environmental Change*, *69*, 102310. <https://doi.org/10.1016/j.gloenvcha.2021.102310>
- Grassi, G., House, J., Dentener, F., Federici, S., den Elzen, M., & Penman, J. (2017). The key role of forests in meeting climate targets requires science for credible mitigation. *Nature Climate Change*, *7*(3), Article 3. <https://doi.org/10.1038/nclimate3227>
- Grassi, G., House, J., Kurz, W. A., Cescatti, A., Houghton, R. A., Peters, G. P., Sanz, M. J., Viñas, R. A., Alkama, R., Arneth, A., Bondeau, A., Dentener, F., Fader, M., Federici, S., Friedlingstein, P., Jain, A. K., Kato, E., Koven, C. D., Lee, D., ... Zaehle, S. (2018). Reconciling global-model estimates and country reporting of anthropogenic forest CO₂ sinks. *Nature Climate Change*, *8*(10), Article 10. <https://doi.org/10.1038/s41558-018-0283-x>
- Guisan, A., Edward, T. C., Jr, & Hastie, T. (2016). Generalized linear and generalized additive models in studies of species distributions: Setting the scene. *Ecological Modelling*, *157*(157), 89–100.
- H, S. A., E, W. C., & A, S. J. (1986). On the Nature of Models in Remote Sensing. *Remote Sensing of Environment*, *20*, 121.
- Haddad, N. M., Brudvig, L. A., Clobert, J., Davies, K. F., Gonzalez, A., Holt, R. D., Lovejoy, T. E., Sexton, J. O., Austin, M. P., Collins, C. D., Cook, W. M., Damschen, E. I., Ewers, R. M., Foster, B. L., Jenkins, C. N., King, A. J., Laurance, W. F., Levey, D. J., Margules, C. R., ... Townshend, J. R. (2015). Habitat fragmentation and its lasting impact on Earth's ecosystems. *Science Advances*, *1*(2), e1500052–e1500052. <https://doi.org/10.1126/sciadv.1500052>
- Hansen, M. C., Potapov, P. V., Moore, R., Hancher, M., Turubanova, S. a, Tyukavina, A., Thau, D., Stehman, S. V., Goetz, S. J., Loveland, T. R., Kommareddy, A., Egorov, A., Chini, L., Justice, C. O., & Townshend, J. R. G. (2013a). High-Resolution Global Maps of 21st-Century Forest Cover Change. *Science (New York, N.Y.)*, *850*(November), 2011–2014. <https://doi.org/10.1126/science.1244693>
- Hansen, M. C., Potapov, P. V., Moore, R., Hancher, M., Turubanova, S. A., Tyukavina, A., Thau, D., Stehman, S. V., Goetz, S. J., Loveland, T. R., Kommareddy, A., Egorov, A., Chini, L., Justice, C. O., & Townshend, J. R. G. (2013b). High-resolution global maps of 21st-century forest cover change. *Science*, *342*(6160), 850–853. <https://doi.org/10.1126/science.1244693>

- Harper, K. A., & Macdonald, S. E. (2011). Quantifying distance of edge influence: A comparison of methods and a new randomization method. *Ecosphere*, 2(8), art94. <https://doi.org/10.1890/es11-00146.1>
- Harper, K. A., Macdonald, S. E., Burton, P. J., Chen, J., Brosnokske, K. D., Saunders, S. C., Euskirchen, E. S., Roberts, D., Jaiteh, M. S., & Esseen, P. A. (2005). Edge influence on forest structure and composition in fragmented landscapes. *Conservation Biology*, 19(3), 768–782. <https://doi.org/10.1111/j.1523-1739.2005.00045.x>
- Harris, N. L., Gibbs, D. A., Baccini, A., Birdsey, R. A., de Bruin, S., Farina, M., Fatoyinbo, L., Hansen, M. C., Herold, M., Houghton, R. A., Potapov, P. V., Suarez, D. R., Roman-Cuesta, R. M., Saatchi, S. S., Slay, C. M., Turubanova, S. A., & Tyukavina, A. (2021). Global maps of twenty-first century forest carbon fluxes. *Nature Climate Change*, 11(3), 234–240. <https://doi.org/10.1038/s41558-020-00976-6>
- Ho, D. E., Imai, K., King, G., & Stuart, E. A. (2011). MatchIt: Nonparametric preprocessing for parametric causal inference. *Journal of Statistical Software*, 42(8), 1–28. <https://doi.org/10.18637/jss.v042.i08>
- Houghton, R. A., & Nassikas, A. A. (2017). Global and regional fluxes of carbon from land use and land cover change 1850–2015. *Global Biogeochemical Cycles*, 31(3), 456–472. <https://doi.org/10.1002/2016GB005546>
- IPCC Special Report on Climate Change, Desertification, Land Degradation, Sustainable Land Management, Food Security, and Greenhouse Gas Fluxes in Terrestrial Ecosystems Summary for Policymakers*. (2019). <http://hdl.handle.net/10044/1/76614>
- Jin, S., Homer, C., Yang, L., Danielson, P., Dewitz, J., Li, C., Zhu, Z., Xian, G., & Howard, D. (2019). Overall Methodology Design for the United States National Land Cover Database 2016 Products. *Remote Sensing*, 11(24), 2971. <https://doi.org/10.3390/rs11242971>
- Laurance, W. F., Camargo, J. L. C., Luizão, R. C. C., Laurance, S. G., Pimm, S. L., Bruna, E. M., Stouffer, P. C., Bruce Williamson, G., Benítez-Malvido, J., Vasconcelos, H. L., Van Houtan, K. S., Zartman, C. E., Boyle, S. A., Didham, R. K., Andrade, A., & Lovejoy, T. E. (2011a). The fate of Amazonian forest fragments: A 32-year investigation. *Biological Conservation*, 144(1), 56–67. <https://doi.org/10.1016/j.biocon.2010.09.021>
- Laurance, W. F., Camargo, J. L. C., Luizão, R. C. C., Laurance, S. G., Pimm, S. L., Bruna, E. M., Stouffer, P. C., Bruce Williamson, G., Benítez-Malvido, J.,

- Vasconcelos, H. L., Van Houtan, K. S., Zartman, C. E., Boyle, S. A., Didham, R. K., Andrade, A., & Lovejoy, T. E. (2011b). The fate of Amazonian forest fragments: A 32-year investigation. *Biological Conservation*, *144*(1), 56–67. <https://doi.org/10.1016/j.biocon.2010.09.021>
- Laurance, W. F., & Curran, T. J. (2008). Impacts of wind disturbance on fragmented tropical forests: A review and synthesis. *Austral Ecology*, *33*(4), 399–408. <https://doi.org/10.1111/j.1442-9993.2008.01895.x>
- Laurance, W. F., & Ferreira, L. V. (1997). Effects of Forest Fragmentation on Mortality and Damage of Selected Trees in Central Amazonia. *Conservation Biology*, *11*(3), 797–801.
- Laurance, W. F., Ferreira, L. V., Merona, J. M. R., & Laurance, S. G. (1998). Rain Forest Fragmentation and the Dynamics of Amazonian Tree. *Ecology*, *79*(6), 2032–2040.
- Laurance, W. F., Nascimento, H. E. M., Laurance, S. G., Andrade, A. C., Fearnside, P. M., Ribeiro, J. E. L., & Capretz, R. L. (2006). Rain forest fragmentation and the proliferation of successional trees. *Ecology*, *87*(2), 469–482. <https://doi.org/10.1890/05-0064>
- Laurance, W. F., Nascimento, H. E. M., Laurance, S. G., Andrade, A., Ewers, R. M., Harms, K. E., Luizão, R. C. C., & Ribeiro, J. E. (2007). Habitat fragmentation, variable edge effects, and the landscape-divergence hypothesis. *PLoS ONE*, *2*(10). <https://doi.org/10.1371/journal.pone.0001017>
- Laurance, W. F., & Yensen, E. (1991). Predicting the impacts of edge effects in fragmented habitats. *Biological Conservation*, *55*(1), 77–92. [https://doi.org/10.1016/0006-3207\(91\)90006-U](https://doi.org/10.1016/0006-3207(91)90006-U)
- Lüdecke, D. (2018). ggeffects: Tidy Data Frames of Marginal Effects from Regression Models. *Journal of Open Source Software*, *3*(26), 772. <https://doi.org/10.21105/joss.00772>
- Ma, W., Woodall, C. W., Domke, G. M., D'Amato, A. W., & Walters, B. F. (2018). Stand age versus tree diameter as a driver of forest carbon inventory simulations in the northeastern U.S. *Canadian Journal of Forest Research*, *48*(10), 1135–1147. <https://doi.org/10.1139/cjfr-2018-0019>
- Mather, A. S. (1992). The forest transition. *The Royal Geographical Society*, *24*(4), 367–379. https://doi.org/10.1057/978-1-349-96042-2_5134

- Matlack, G. R. (1993). Microenvironment variation within and among forest edge sites in the eastern United States. *Biological Conservation*, 66(3), 185–194. [https://doi.org/10.1016/0006-3207\(93\)90004-K](https://doi.org/10.1016/0006-3207(93)90004-K)
- McDowell, N. G., Allen, C. D., Anderson-Teixeira, K., Aukema, B. H., Bond-Lamberty, B., Chini, L., Clark, J. S., Dietze, M., Grossiord, C., Hanbury-Brown, A., Hurtt, G. C., Jackson, R. B., Johnson, D. J., Kueppers, L., Lichstein, J. W., Ogle, K., Poulter, B., Pugh, T. A. M., Seidl, R., ... Xu, C. (2020). Pervasive shifts in forest dynamics in a changing world. *Science*, 368(6494).
- Meeussen, C., Govaert, S., Vanneste, T., Bollmann, K., Brunet, J., Calders, K., Cousins, S. A. O., De Pauw, K., Diekmann, M., Gasperini, C., Hedwall, P.-O., Hylander, K., Iacopetti, G., Lenoir, J., Lindmo, S., Orczewska, A., Ponette, Q., Plue, J., Sanczuk, P., ... De Frenne, P. (2021). Microclimatic edge-to-interior gradients of European deciduous forests. *Agricultural and Forest Meteorology*, 311(May), 108699. <https://doi.org/10.1016/j.agrformet.2021.108699>
- Meeussen, C., Govaert, S., Vanneste, T., Haesen, S., Van Meerbeek, K., Bollmann, K., Brunet, J., Calders, K., Cousins, S. A. O., Diekmann, M., Graae, B. J., Iacopetti, G., Lenoir, J., Orczewska, A., Ponette, Q., Plue, J., Selvi, F., Spicher, F., Sørensen, M. V., ... De Frenne, P. (2020). Drivers of carbon stocks in forest edges across Europe. *Science of The Total Environment*, xxx, 143497. <https://doi.org/10.1016/j.scitotenv.2020.143497>
- Morreale, L. L., Thompson, J. R., Pasquarella, V. J., & Hutyra, L. R. (In review). Edge cases: Fragmentation in temperate forest landscapes. *Frontiers in Ecology and the Environment*.
- Morreale, L. L., Thompson, J. R., Tang, X., Reinmann, A. B., & Hutyra, L. R. (2021). Elevated growth and biomass along temperate forest edges. *Nature Communications*, 12(1), 7181. <https://doi.org/10.1038/s41467-021-27373-7>
- Mourelle, C., Kellman, M., & Kwon, L. (2001). Light occlusion at forest edges: An analysis of tree architectural characteristics. *Forest Ecology and Management*, 154(1–2), 179–192. [https://doi.org/10.1016/S0378-1127\(00\)00624-1](https://doi.org/10.1016/S0378-1127(00)00624-1)
- Nagelkerke, N. J. D. (1991). A note on a general definition of the coefficient of determination. *Biometrika*. <https://doi.org/10.1093/biomet/78.3.691>
- Nelder, J. A., & Wedderburn, R. W. M. (1972). Generalized Linear Models. *Journal of the Royal Statistical Society. Series A (General)*, 135(3), 370–384. <https://doi.org/10.2307/2344614>

- Nemani, R. R., Keeling, C. D., Hashimoto, H., Jolly, W. M., Piper, S. C., Tucker, C. J., Myneni, R. B., & Running, S. W. (2003). Climate-driven increases in global terrestrial net primary production from 1982 to 1999. *Science*, *300*(5625), 1560–1563. <https://doi.org/10.1126/science.1082750>
- Novick, K. A., Metzger, S., Anderegg, W. R. L., Barnes, M., Cala, D. S., Guan, K., Hemes, K. S., Hollinger, D. Y., Kumar, J., Litvak, M., Lombardozzi, D., Normile, C. P., Oikawa, P., Runkle, B. R. K., Torn, M., & Wiesner, S. (2022). Informing Nature-based Climate Solutions for the United States with the best-available science. *Global Change Biology*, *28*(12), 3778–3794. <https://doi.org/10.1111/gcb.16156>
- Office, N. P. (2020). *National Atmospheric Deposition Program (NRSP-3)*. Wisconsin State Laboratory of Hygiene.
- Olson, D. M., Dinerstein, E., Wikramanayake, E. D., Burgess, N. D., Powell, G. V. N., Underwood, E. C., D’Amico, J. A., Itoua, I., Strand, H. E., Morrison, J. C., Loucks, C. J., Allnutt, T. F., Ricketts, T. H., Kura, Y., Lamoreux, J. F., Wettengel, W. W., Hedao, P., & Kassem, K. R. (2001). Terrestrial ecoregions of the world: A new map of life on Earth. *BioScience*, *51*(11), 933–938. [https://doi.org/10.1641/0006-3568\(2001\)051](https://doi.org/10.1641/0006-3568(2001)051)
- Omernik, J. M., & Griffith, G. E. (2014). Ecoregions of the Conterminous United States: Evolution of a Hierarchical Spatial Framework. *Environmental Management*, *54*(6), 1249–1266. <https://doi.org/10.1007/s00267-014-0364-1>
- Ordway, E. M., & Asner, G. P. (2020). Carbon declines along tropical forest edges correspond to heterogeneous effects on canopy structure and function. *Proceedings of the National Academy of Sciences of the United States of America*, *117*(14), 7863–7870. <https://doi.org/10.1073/pnas.1914420117>
- Pallai, C., & Wesson, K. (2017). *Chesapeake Bay Program Partnership High-Resolution Land Cover Classification Accuracy Assessment Methodology*.
- Pan, Y., Birdsey, R. A., Fang, J., Houghton, R., Kauppi, P. E., Kurz, W. A., Phillips, O. L., Shvidenko, A., Lewis, S. L., Canadell, J. G., Ciais, P., Jackson, R. B., Pacala, S. W., McGuire, A. D., Piao, S., Rautiainen, A., Sitch, S., & Hayes, D. (2011). A Large and Persistent Carbon Sink in the World’s Forests. *Science*, *333*(6045), 988–993. <https://doi.org/10.1126/science.1201609>
- Pan, Y., Birdsey, R. A., Phillips, O. L., & Jackson, R. B. (2013). The Structure, Distribution, and Biomass of the World’s Forests. *Annual Review of Ecology, Evolution, and Systematics*, *44*(1), 593–622. <https://doi.org/10.1146/annurev-ecolsys-110512-135914>

- Pasquarella, V. J., Elkinton, J. S., & Bradley, B. A. (2018). Extensive gypsy moth defoliation in Southern New England characterized using Landsat satellite observations. *Biological Invasions*, *20*(11), 3047–3053. <https://doi.org/10.1007/s10530-018-1778-0>
- Pengra, B. W., Stehman, S. V., Horton, J. A., & Wellington, D. F. (2021). *Land Change Monitoring, Assessment, and Projection (LCMAP) Collection 1.2 Annual Land Cover and Land Cover Change Validation Tables (1985–2018) for the Conterminous United States: U.S. Geological Survey data release*. <https://doi.org/10.5066/P9M6T45Z>
- Pocewicz, A., Morgan, P., & Kavanagh, K. (2007a). The effects of adjacent land use on nitrogen dynamics at forest edges in northern Idaho. *Ecosystems*, *10*(2), 226–238. <https://doi.org/10.1007/s10021-007-9015-1>
- Pocewicz, A., Morgan, P., & Kavanagh, K. (2007b). The Effects of Adjacent Land Use on Nitrogen Dynamics at Forest Edges in Northern Idaho. *Ecosystems*, *10*(2), 226–238. <https://doi.org/10.1007/s10021-007-9015-1>
- Pöppel, F., & Seidl, R. (2021). Effects of stand edges on the structure, functioning, and diversity of a temperate mountain forest landscape. *Ecosphere*, *12*(8). <https://doi.org/10.1002/ecs2.3692>
- Právělie, R. (2018). Major perturbations in the Earth's forest ecosystems. Possible implications for global warming. *Earth-Science Reviews*, *185*, 544–571. <https://doi.org/10.1016/j.earscirev.2018.06.010>
- Pütz, S., Groeneveld, J., Henle, K., Knogge, C., Martensen, A. C., Metz, M., Metzger, J. P., Ribeiro, M. C., De Paula, M. D., & Huth, A. (2014). Long-term carbon loss in fragmented Neotropical forests. *Nature Communications*, *5*(iDiv), 1–8. <https://doi.org/10.1038/ncomms6037>
- R Team, C. (2019). R Core Team (2017). R: A language and environment for statistical computing. *R Found. Stat. Comput. Vienna, Austria*. URL [Http://Www. R-Project. Org/](http://www.R-Project.Org/), Page R Foundation for Statistical Computing.
- Reinmann, A. B., & Hutrya, L. R. (2017). Edge effects enhance carbon uptake and its vulnerability to climate change in temperate broadleaf forests. *Proceedings of the National Academy of Sciences*, *114*(1), 107–112. <https://doi.org/10.1073/pnas.1612369114>
- Reinmann, A. B., Smith, I. A., Thompson, J. R., & Hutrya, L. R. (2020). Urbanization and fragmentation mediate temperate forest carbon cycle response to climate.

Environmental Research Letters, 15(11), 114036. <https://doi.org/10.1088/1748-9326/abbf16>

- Remy, E., Wuyts, K., Boeckx, P., Ginzburg, S., Gundersen, P., Demey, A., Van Den Bulcke, J., Van Acker, J., & Verheyen, K. (2016). Strong gradients in nitrogen and carbon stocks at temperate forest edges. *Forest Ecology and Management*, 376, 45–58. <https://doi.org/10.1016/j.foreco.2016.05.040>
- Remy, E., Wuyts, K., Boeckx, P., Gundersen, P., & Verheyen, K. (2017). Edge effects in temperate forests subjected to high nitrogen deposition. *Proceedings of the National Academy of Sciences*, 114(34), E7032–E7032. <https://doi.org/10.1073/pnas.1709099114>
- Ricci, E. H., Collins, J., Clarke, J., Dolci, P., & de la Parra, L. (2020). *Losing Ground: Nature's Value in a Changing Climate*.
- Ruefenacht, B., Finco, M. V., Nelson, M. D., Czaplowski, R., Helmer, E. H., Blackard, J. A., Holden, G. R., Lister, A. J., Salajanu, D., Weyermann, D., & Winterberger, K. (2008). Conterminous U.S. and Alaska forest type mapping using forest inventory and analysis data. *Photogrammetric Engineering and Remote Sensing*, 74(11), 1379–1388. <https://doi.org/10.14358/PERS.74.11.1379>
- Schleicher, J., Peres, C. A., Amano, T., Llacayo, W., & Leader-Williams, N. (2017). Conservation performance of different conservation governance regimes in the Peruvian Amazon. *Scientific Reports*, 7(1), 1–10. <https://doi.org/10.1038/s41598-017-10736-w>
- Schmidt, M., Jochheim, H., Kersebaum, K. C., Lischeid, G., & Nendel, C. (2017). Gradients of microclimate, carbon and nitrogen in transition zones of fragmented landscapes – a review. *Agricultural and Forest Meteorology*, 232, 659–671. <https://doi.org/10.1016/j.agrformet.2016.10.022>
- Schwingshackl, C., Obermeier, W. A., Bultan, S., Grassi, G., Canadell, J. G., Friedlingstein, P., Gasser, T., Houghton, R. A., Kurz, W. A., Sitch, S., & Pongratz, J. (2022). Differences in land-based mitigation estimates reconciled by separating natural and land-use CO₂ fluxes at the country level. *One Earth*, 5(12), 1367–1376. <https://doi.org/10.1016/j.oneear.2022.11.009>
- Seto, K. C., Güneralp, B., & Hutya, L. R. (2012). Global forecasts of urban expansion to 2030 and direct impacts on biodiversity and carbon pools. *Proceedings of the National Academy of Sciences*, 109(40), 16083–16088. <https://doi.org/10.1073/pnas.1211658109>

- Smith, I. A., Hutyra, L. R., Reinmann, A. B., Marrs, J. K., & Thompson, J. R. (2018). Piecing together the fragments: Elucidating edge effects on forest carbon dynamics. *Frontiers in Ecology and the Environment*, 16(4), 213–221. <https://doi.org/10.1002/fee.1793>
- Spawn, S. A., Sullivan, C. C., Lark, T. J., & Gibbs, H. K. (2020). Harmonized global maps of above and belowground biomass carbon density in the year 2010. *Scientific Data*, 7(1), Article 1. <https://doi.org/10.1038/s41597-020-0444-4>
- Stanke, H., Finley, A. O., Weed, A. S., Walters, B. F., & Domke, G. M. (2020). RFIA: An R package for estimation of forest attributes with the US Forest Inventory and Analysis database. *Environmental Modelling & Software*, 104664. <https://doi.org/10.1016/j.envsoft.2020.104664>
- Stuart, E. A. (2010). Matching Methods for Causal Inference: A Review and a Look Forward. *Statistical Science*, 25(1), 1–21. <https://doi.org/10.1214/09-STS313>
- Sulla-Menashe, D., Gray, J. M., Abercrombie, S. P., & Friedl, M. A. (2019). Hierarchical mapping of annual global land cover 2001 to present: The MODIS Collection 6 Land Cover product. *Remote Sensing of Environment*, 222(January), 183–194. <https://doi.org/10.1016/j.rse.2018.12.013>
- Tao, S., Rogan, J., Ye, S., & Geron, N. (2023). Mapping photovoltaic power stations and assessing their environmental impacts from multi-sensor datasets in Massachusetts, United States. *Remote Sensing Applications: Society and Environment*, 30, 100937. <https://doi.org/10.1016/j.rsase.2023.100937>
- The State of the World's Forests 2022*. (2022). FAO. <https://doi.org/10.4060/cb9360en>
- Thompson, J. R., Canham, C. D., Morreale, L., Kittredge, D. B., & Butler, B. (2017). Social and biophysical variation in regional timber harvest regimes. *Ecological Applications*, 27(3), 942–955. <https://doi.org/10.1002/eap.1497>
- Thompson, J. R., Plisinski, J. S., Olofsson, P., Holden, C. E., & Duveneck, M. J. (2017). Forest loss in New England: A projection of recent trends. *PLOS ONE*, 12(12), e0189636. <https://doi.org/10.1371/journal.pone.0189636>
- Tinkham, W. T., Mahoney, P. R., Hudak, A. T., Domke, G. M., Falkowski, M. J., Woodall, C. W., & Smith, A. M. S. (2018). Applications of the United States Forest Inventory and Analysis dataset: A review and future directions. *Canadian Journal of Forest Research*, 48(11), 1251–1268. <https://doi.org/10.1139/cjfr-2018-0196>

- Trumbore, S., Brando, P., & Hartmann, H. (2015). Forest health and global change. *Science*, 349(6250), 814–818. <https://doi.org/10.1126/science.aac6759>
- Turner, M. G. (1989a). Landscape Ecology: The Effect of Pattern on Process. *Annual Review of Ecology and Systematics*, 20, 171–197. JSTOR.
- Turner, M. G. (1989b). Landscape Ecology: The Effect of Pattern on Process. *Annual Review of Ecology and Systematics*, 20, 171–197.
- Turner, M. G., O'Neill, R. V., Gardner, R. H., & Milne, B. T. (1989). Effects of changing spatial scale on the analysis of landscape pattern. *Landscape Ecology*, 3(3), 153–162. <https://doi.org/10.1007/BF00131534>
- UNFCCC. (2014). *Handbook on Measurement, Reporting And Verification For Developing Country Parties*.
- Walter, S. T., & Maguire, C. C. (2004). Conifer response to three silvicultural treatments in the Oregon Coast Range foothills. *Canadian Journal of Forest Research*. <https://doi.org/10.1139/X04-068>
- Wang, Y.-P., & Houlton, B. Z. (2009). Nitrogen constraints on terrestrial carbon uptake: Implications for the global carbon-climate feedback. *Geophysical Research Letters*, 36(24), L24403. <https://doi.org/10.1029/2009GL041009>
- Weathers, K. C., Cadenasso, M. L., & Pickett, S. T. A. (2001). Forest edges as nutrient and pollutant concentrators: Potential synergisms between fragmentation, forest canopies, and the atmosphere. *Conservation Biology*, 15(6), 1506–1514. <https://doi.org/10.1046/j.1523-1739.2001.01090.x>
- Wickham, J., & Riitters, K. H. (2019). Influence of high-resolution data on the assessment of forest fragmentation. *Landscape Ecology*, 34(9), 2169–2182. <https://doi.org/10.1007/s10980-019-00820-z>
- Woodcock, C. E., & Strahler, A. H. (1987). The factor of scale in remote sensing. *Remote Sensing of Environment*, 21(3), 311–332. [https://doi.org/10.1016/0034-4257\(87\)90015-0](https://doi.org/10.1016/0034-4257(87)90015-0)
- World Resources Institute. (2022). Forest Loss. *Global Forest Review*.
- Wulder, M. A., Masek, J. G., Cohen, W. B., Loveland, T. R., & Woodcock, C. E. (2012). Opening the archive: How free data has enabled the science and monitoring promise of Landsat. *Remote Sensing of Environment*. <https://doi.org/10.1016/j.rse.2012.01.010>

- Wuyts, K., De Schrijver, A., Staelens, J., Gielis, M., Geudens, G., & Verheyen, K. (2008). Patterns of throughfall deposition along a transect in forest edges of silver birch and Corsican pine. *Canadian Journal of Forest Research*, 38(3), 449–461. <https://doi.org/10.1139/X07-181>
- Xu, L., Saatchi, S. S., Yang, Y., Yu, Y., Pongratz, J., Bloom, A. A., Bowman, K., Worden, J., Liu, J., Yin, Y., Domke, G., McRoberts, R. E., Woodall, C., Nabuurs, G.-J., de-Miguel, S., Keller, M., Harris, N., Maxwell, S., & Schimel, D. (2021). Changes in global terrestrial live biomass over the 21st century. *Science Advances*, 7(27), eabe9829.
- Yang, L., Jin, S., Danielson, P., Homer, C., Gass, L., Bender, S. M., Case, A., Costello, C., Dewitz, J., Fry, J., Funk, M., Granneman, B., Liknes, G. C., Rigge, M., & Xian, G. (2018). A new generation of the United States National Land Cover Database: Requirements, research priorities, design, and implementation strategies. *ISPRS Journal of Photogrammetry and Remote Sensing*, 146(September), 108–123. <https://doi.org/10.1016/j.isprsjprs.2018.09.006>
- Zehetner, F., Rosenfellner, U., Mentler, A., & Gerzabek, M. H. (2009). Distribution of Road Salt Residues, Heavy Metals and Polycyclic Aromatic Hydrocarbons across a Highway-Forest Interface. *Water, Air, and Soil Pollution*, 198(1), 125–132. <https://doi.org/10.1007/s11270-008-9831-8>
- Ziter, C., Bennett, E. M., & Gonzalez, A. (2014). Temperate forest fragments maintain aboveground carbon stocks out to the forest edge despite changes in community composition. *Oecologia*, 176(3), 893–902. <https://doi.org/10.1007/s00442-014-3061-0>

CURRICULUM VITAE

